

DECADAL VARIABILITY ANALYSIS OF EXTREME PRECIPITATION IN
TURKEY AND ITS RELATIONSHIP WITH TELECONNECTION PATTERNS

A THESIS SUBMITTED TO
THE GRADUATE SCHOOL OF NATURAL AND APPLIED SCIENCES
OF
MIDDLE EAST TECHNICAL UNIVERSITY

BY

EREN DÜZENLİ

IN PARTIAL FULFILLMENT OF THE REQUIREMENTS
FOR
THE DEGREE OF MASTER OF SCIENCE
IN
CIVIL ENGINEERING

AUGUST 2017

Approval of the thesis:

**DECADAL VARIABILITY ANALYSIS OF EXTREME PRECIPITATION IN
TURKEY AND ITS RELATIONSHIP WITH TELECONNECTION
PATTERNS**

submitted by **EREN DÜZENLİ** in partial fulfillment of the requirements for the degree of **Master of Science in Civil Engineering Department, Middle East Technical University** by,

Prof. Dr. Gülbin Dural Ünver
Dean, Graduate School of **Natural and Applied Sciences**

Prof. Dr. İsmail Özgür Yaman
Head of Department, **Civil Engineering**

Assist. Prof. Dr. Mustafa Tuğrul Yılmaz
Supervisor, **Civil Engineering Department, METU**

Examining Committee Members:

Prof. Dr. Melih Yanmaz
Civil Engineering Department, METU

Assist. Prof. Dr. Mustafa Tuğrul Yılmaz
Civil Engineering Department, METU

Assoc. Prof. Dr. İsmail Yücel
Civil Engineering Department, METU

Assoc. Prof. Dr. Koray Yılmaz
Civil Engineering Department, METU

Assist. Prof. Dr. Melih Çalamak
Civil Engineering Department, TED University

DATE: 25.08.2017

I hereby declare that all information in this document has been obtained and presented in accordance with academic rules and ethical conduct. I also declare that, as required by these rules and conduct, I have fully cited and referenced all material and results that are not original to this work.

Name, Last name: Eren, Düzenli

Signature :

ABSTRACT

DECADAL VARIABILITY ANALYSIS OF EXTREME PRECIPITATION IN TURKEY AND ITS RELATIONSHIP WITH TELECONNECTION PATTERNS

Düzenli, Eren

MS., Department of Civil Engineering

Supervisor: Assist. Prof. Dr. Mustafa Tuğrul Yılmaz

Co-supervisor: Prof. Dr. Ir. Patrick Willems

August 2017, 150 pages

Natural disasters as droughts and floods originate as a consequence of excessive decrease or increase in precipitation amount and/or frequency, while the variability in the climate significantly impacts the expected change in precipitation. Given that many global ocean-atmosphere teleconnection patterns (AO, WeMO, NAO, SOI, etc.) are tightly related with the climate variability and show decadal/multi-decadal oscillations, it is important to analyze precipitation variability at the decadal time-scale to understand the (expected) variability in the climate more effectively. In this study, decadal oscillations of extreme precipitation in Turkey are investigated using Quantile Perturbation Method (QPM). Daily precipitation data observed over 67 stations in Turkey between 1955 and 2014 are utilized in the analyses. AO, WeMO, NAO, and SOI teleconnection patterns are examined for their relation with the extreme precipitation variability to understand the potential drivers of extreme precipitation in Turkey. According to the analysis based on single drivers, NAO is identified as the most effective driver of Turkey's extreme precipitation among 4 climate indices, while AO has a similar effect. When the teleconnection patterns are investigated in pairs, combination of NAO and SOI results in the highest response to the winter extremes in Turkey.

Keywords: precipitation, extreme, climate variability, decadal oscillation

ÖZ

TÜRKİYE AŞIRI YAĞIŞLARININ ONYILSAK DEĞİŞKENLİK ANALİZİ VE BU DEĞİŞKENLİĞİN UZAK MESAFELİ BAĞLANTI MODELLERİYLE İLİŞKİSİ

Düzenli, Eren

Yüksek Lisans, İnşaat Mühendisliği Bölümü

Tez Yöneticisi: Yar. Doç. Dr. Mustafa Tuğrul Yılmaz

Co-supervisor: Prof. Dr. Ir. Patrick Willems

Ağustos 2017, 150 sayfa

Sel ve kuraklık gibi doğal afetler, yağış oranındaki aşırı artış ya da düşüş sonucunda oluşan ve iklim değışkenliğinden önemli oranda etkilenen olaylardır. Bir çok küresel uzak mesafeli bağlantı modelleri (AO, WeMO, NAO, SOI vb) iklim değışkenliğiyle doğrudan ilişkilidir. Buna bağlı olarak, ilişkilerinde on/onlarca yıllık salınımlar görmek mümkündür. Yağış değışkenliğini on yıllık zaman aralıklarında incelemek, iklim değışkenliğini daha iyi anlamak için büyük önem taşımaktadır. Bu çalışmada Türkiye'deki yağış aşırılıklarının 10 yıllık dalgalanmaları QPM metodu kullanılarak incelenmiştir. Çalışmada, 1955-2014 yıllarını kapsayan 67 farklı istasyonun günlük yağış verileri kullanılmıştır. Türkiye'deki yağış aşırılıklarının olası sebeplerini tayin etmek amacıyla, yağışların AO, NAO, WeMO ve SOI iklim indeksleriyle olan ilişkileri incelenmiştir. Her bir iklim indeksi tekil olarak incelendiğinde NAO, Türkiye'de yağış aşırılıklarına sebep olan en güçlü faktör olarak bulunmuştur. Aynı şekilde AO da bölgesel olarak benzer etkilere sahiptir. İklim indeksleri çiftler halinde incelendiğinde, NAO ve SOI çiftinin kış mevsimindeki aşırı yağışlar üzerindeki en önemli faktör olduğu söylenebilir.

Anahtar kelimeler: yağış, aşırı, iklim değışkenliği, on yıllık salınım

To the pale blue dot of Carl Sagan;

ACKNOWLEDGEMENTS

This thesis is a product of a collaborative work supported by many people in their own ways. First of all I would like to thank my supervisor Assist. Prof. Dr. Mustafa Tuğrul Yılmaz who never gave up on me even when I was in another country and answered all my questions with patience. I am deeply grateful for his generous support.

Dr. Hossein Tabari sincerely shared his knowledge all along my research period. He has been an excellent advisor and a very good friend. I am also very grateful for his visit to Turkey to participate my thesis defense.

I am very thankful to Prof. Dr. Patrick Willems who accepted to conduct my thesis research during my Erasmus stay in KU Leuven. His guidance was very important in the decision of my research topic and my interest on this field.

The other committee members: Prof. Dr. Melih Yanmaz, Asist. Prof. Dr. Melih Çalamak, Assoc. Prof. Dr. Koray K. Yılmaz greatly assisted me through their insightful comments in shaping the final draft of this study. I am very thankful to them for spending their time and efforts.

I have greatly benefited from the feedbacks and comments of Prof. Dr. Murat Türkeş. I would like to express my gratitude for sharing his knowledge.

I would also like to express my respect for Prof. Dr. Elçin Kentel for her constructive comments and suggestions on my study.

I would like to share my deepest gratitude to Assoc. Prof. Dr. İsmail Yücel. He helped me all along my masters study and strengthened my relation to this department by his valuable guidance and encouragement. I will be appreciating this in my whole life.

I would like to thank my group members: Burak Bulut, Mehdi Hesami Afshar, Nuri Erhan Ersoy, Alper Önen and İpek Gül Karasu for all their help and support. I would especially thank my roommate İpek Gül Karasu for her friendship.

Not only my friends from the academic circle but also my friends with whom I share the burden of our lives were always with me through their endless love, joy and support. For this, I would like to thank: Mert Alperden, Udit Baliga, Özge Arman, Ruken Dilara Zaf, Özgür Balkılıç and Ecem Seçkin. Besides, I would like to open a parenthesis for the scientific contribution of Ecem Seçkin during my study.

I would like to thank both my former teacher and lovely friend Zeynep Tufan and my cousin Alper Nakkaş for their encouragement. They have always been inspiring me both in perception of science and my seek to understand the essence of the universe.

My precious friends: Gamze Karaca and Emre Gökyer, will always be significant and unforgettable. Even their presence is enough for me to have hope on life. Their smiles will always warm the colors of my sight.

In every decision I make, my brother Emre Düzenli and my sister Deniz Düzenli have always been backing me. I would like to thank them both. I know that I will always become stronger when I have them beside me.

I would like to express my deepest gratitude to my two lovely mothers and home mates Asya Düzenli and Yıldız Nakkaş for their unconditional and endless love.

I would like to thank Perihan Öztürk who has as much contribution as I have in this dissertation as well as every single step I moved forward for the passing 3 years. I feel her breath in my soul.

I would like to thank the loving memory of Ahmet Nakkaş.

I would like to thank my father Ali Düzenli with all my respect and longing.

TABLE OF CONTENTS

ABSTRACT	v
ÖZ	vi
ACKNOWLEDGEMENTS	viii
TABLE OF CONTENTS	x
LIST OF FIGURES.....	xii
LIST OF TABLES	xv
TABLE OF ABBREVIATIONS.....	xviii
CHAPTERS	
1 INTRODUCTION.....	1
2 METHODS.....	9
3 STUDY AREA AND DATA.....	19
3.1 Study area	19
3.2 Data.....	22
4 RESULTS AND DISCUSSION	29
4.1 Analyses of total precipitation.....	29
4.2 Analyses of decadal precipitation anomaly in the high extremes	34
4.2.1 The summary of all regions.....	34
4.2.2 Black Sea Region (BLS)	42
4.2.3 Continental Central Anatolia (CCAN).....	46
4.2.4 Continental Eastern Anatolia (CEAN).....	49

4.2.5	Continental Mediterranean (CMED).....	52
4.2.6	Mediterranean (MED).....	54
4.2.7	Mediterranean Transition (MEDT).....	57
4.2.8	Marmara Transition (MRT).....	60
4.3	Analyses of Decadal Precipitation Anomaly In The Low Extremes.....	61
4.4	Relationship Between The Teleconnection Patterns And The Decadal High Extreme Precipitation Variability	68
4.4.1	The single relationship analysis	69
4.4.2	The multiple relationship analysis	95
4.5	Relationship Between The Teleconnection Patterns And The Decadal Low Extreme Precipitation Variability	123
4.5.1	The single relationship analysis	123
4.6	5-years block responses.....	138
5	CONCLUSION, SUMMARY AND RECOMMENDATIONS.....	143
	REFERENCES.....	147

LIST OF FIGURES

Figure 1.1 Climate Indices	6
Figure 2.1 Decadal anomaly fluctuations of Kütahya in winter season with 10 years block	13
Figure 3.1 Digital Elevation Model (DEM) of Turkey	21
Figure 3.2 Effective pressure systems over Turkey	22
Figure 3.3 Locations of Selected Stations (Red Points= BLS, Black points= CCAN, Pink Points= CEAN, Light Blue Points= CMED, Blue points= MED, Yellow Points=MEDT, Green Points=MRT)	27
Figure 3.4 Time series of climate indices for the study period	28
Figure 4.1 Total precipitation variation of Turkey	31
Figure 4.2 Standardized total precipitation variation of Turkey	33
Figure 4.3 Comparison of the region anomalies with respect to sesason	36
Figure 4.4 The Areas of the anomaly variability in the region anomalies with respect to all seasons.....	38
Figure 4.5 The number of floods occurred in Turkey between 1940 and 2010 (Retrieved from https://www.mgm.gov.tr/arastirma/dogal-afetler.aspx?s=taskinlar)	41
Figure 4.6 Decadal precipitation variation of the declared stations for the autumn season	43
Figure 4.7 The comparison of the winter anomalies of Sakarya and Bolu with İnebolu and Kireçburnu.....	45
Figure 4.8 Decadal extreme precipitation fluctuation of Kayseri	48
Figure 4.9 Comparison of the mean and the median of long-term average annual precipitation of the stations in BLS and CEAN with Artvin.....	51
Figure 4.10 The Areas of the anomaly variability in the CMED stations with respect to all seasons.....	54

Figure 4.11 Comparison of the median anomalies in the Mediterranean with respect to seasons	57
Figure 4.12 Decadal anomaly fluctuations of the stations in the MEDT region.....	59
Figure 4.13 Decadal low extreme oscillations of the regions with respect to seasons	63
Figure 4.14 The continuous map of spearman's rank order correlation coefficient between NAO and extreme precipitation with respect to seasons	71
Figure 4.15 The continuous map of non-linear power law regression coefficient (R) between NAO and extreme precipitation with respect to seasons	73
Figure 4.16 The continuous map of spearman rank order correlation coefficient between AO and extreme precipitation with respect to seasons	78
Figure 4.17 The continuous map of non-linear power law regression coefficient (R) between AO and extreme precipitation with respect to seasons	80
Figure 4.18 The continuous map of spearman rank order correlation coefficient between SOI and extreme precipitation with respect to seasons	84
Figure 4.19 The continuous map of non-linear power law regression coefficient (R) between SOI and extreme precipitation with respect to seasons	85
Figure 4.20 The continuous map of spearman rank order correlation coefficient between SOI and extreme precipitation with respect to seasons	90
Figure 4.21 The continuous map of non-linear power law regression coefficient (R) between WeMO and extreme precipitation with respect to seasons.....	91
Figure 4.22 The continuous map of multiple linear regression coefficient between NAO and SOI pair and extreme precipitation with respect to seasons	96
Figure 4.23 The continuous map of multivariate adaptive regression splines coefficient between NAO and SOI pair and extreme precipitation with respect to seasons.....	99
Figure 4.24 The continuous map of multiple linear regression coefficient between AO and SOI pair and extreme precipitation with respect to seasons.....	103
Figure 4.25 The continuous map of multivariate adaptive regression splines coefficient between AO and SOI pair and extreme precipitation with respect to seasons	105

Figure 4.26 The continuous map of multiple linear regression coefficient between NAO and WeMO pair and extreme precipitation with respect to seasons.....	109
Figure 4.27 The continuous map of multivariate adaptive regression splines coefficient between NAO and WeMO pair and extreme precipitation with respect to seasons.....	111
Figure 4.28 The continuous map of multiple linear regression coefficient between AO and WeMO pair and extreme precipitation with respect to seasons	115
Figure 4.29 The continuous map of multivariate adaptive regression splines coefficient between AO and WeMO pair and extreme precipitation with respect to seasons.....	117
Figure 4.30 The continuous map of MLR and MARS coefficients between SOI and WeMO pair and summer extremes.....	121
Figure 4.31 The continuous map of SROC coefficient between dry day numbers and NAO with respect to seasons	125
Figure 4.32 The continuous map of SROC coefficient between dry day numbers and NAO with respect to seasons	128
Figure 4.33 The continuous map of SROC coefficient between dry day numbers and SOI with respect to seasons.....	133
Figure 4.34 The continuous map of SROC coefficient between dry day numbers and SOI with respect to seasons.....	136
Figure 4.35 Winter anomalies of the regions for block lengths of 5 and 10 years ..	141

LIST OF TABLES

Table 2.1 Relation Analysis Methods	14
Table 3.1 The rainfall characteristics of the regions	20
Table 3.2 Characteristics of the stations	24
Table 3.3 Station names with respect to their rainfall regions.....	26
Table 4.1 Correlation between decadal high extreme precipitation anomalies and decadal dry day number anomalies	65
Table 4.2 Average dry day numbers and average standard deviations of the stations according to seasons.....	67
Table 4.3 Threshold values with respect to actual and effective sample size.....	68
Table 4.4 The number of station having significant correlation with NAO in winter with regard to actual sample size threshold	72
Table 4.5 The relationship between anomaly of extreme precipitation and NAO anomaly (<i>Bold black numbers= The significant relationship for the effective sample size and the actual sample size, Red Numbers: The significant relationship for the actual sample size, Black Numbers= The insignificant relationship</i>)	75
Table 4.6 The comparison of the number of station having significant correlation with AO and NAO in winter with regard to actual sample size threshold.....	78
Table 4.7 The relationship between anomaly of extreme precipitation and AO anomaly (<i>Bold black numbers= The significant relationship for the effective sample size and the actual sample size, Red Numbers: The significant relationship for the actual sample size, Black Numbers= The insignificant relationship</i>).....	81
Table 4.8 The relationship between anomaly of extreme precipitation and SOI anomaly (<i>Bold black numbers= The significant relationship for the effective sample size and the actual sample size, Red Numbers: The significant relationship for the actual sample size, Black Numbers= The insignificant relationship</i>).....	87
Table 4.9 The relationship between anomaly of extreme precipitation and WeMO anomaly (<i>Bold black numbers= The significant relationship for the effective sample</i>	

size and the actual sample size, Red Numbers: The significant relationship for the actual sample size, Black Numbers= The insignificant relationship)..... 93

Table 4.10 The number of the station having the significant relationship with NAO and SOI pair based on the effective sample size threshold with respect to the rainfall regions and seasons 98

Table 4.11 The relationship between anomaly of extreme precipitation and the pair of NAO and SOI anomaly (**Black numbers= The significant relationship for the effective sample size and the actual sample size, Red Numbers: The significant relationship for the a**..... 100

Table 4.12 The number of the stations with significant relationship for AO and SOI pair based on the effective sample size threshold with respect to the rainfall regions and seasons 104

Table 4.13 The relationship between anomaly of extreme precipitation and the pair of AO and SOI anomaly (**Black numbers= The significant relationship for the effective sample size and the actual sample size, Red Numbers: The significant relationship for the actual sample size, Black Numbers= The insignificant relationship)** 106

Table 4.14 The number of the stations with significant relationship with NAO and WeMO pair based on the effective sample size threshold with respect to the rainfall regions and seasons 110

Table 4.15 The relationship between anomaly of extreme precipitation and the pair of NAO and WeMO anomaly (**Black numbers= The significant relationship for the effective sample size and the actual sample size, Red Numbers: The significant relationship for the actual sample size, Black Numbers= The insignificant relationship)** 112

Table 4.16 The number of the station with significant relationship with AO and WeMO pair based on the effective sample size threshold with respect to the rainfall regions and seasons 116

Table 4.17 The relationship between anomaly of extreme precipitation and the pair of AO and WeMO anomaly (**Black numbers= The significant relationship for the effective sample size and the actual sample size, Red Numbers: The significant**

<i>relationship for the actual sample size, Black Numbers= The insignificant relationship)</i>	118
Table 4.18 The number of the station having the significant relationship with SOI and WeMO pair in summer based on the effective sample size threshold with respect to the rainfall regions	120
Table 4.19 The relationship between anomaly of extreme precipitation and the pair of SOI and WeMO anomaly for summer (<i>Bold black numbers= The significant relationship for the effective sample size and the actual sample size, Red Numbers: The significant relationship for the actual sample size, Black Numbers= The insignificant relationship)</i>	121
Table 4.20 The number of the station having the significant relationship between NAO and its dry day number in winter.....	124
Table 4.21 The correlation between anomaly of dry day number and NAO anomaly (<i>Red numbers= The significant relationship for the effective sample size, Black Numbers= The insignificant relationship)</i>	126
Table 4.22 The number of the station having the significant relationship between AO and its dry day number in winter.....	128
Table 4.23 The comparison of the correlation values of dry day number with NAO and AO	129
Table 4.24 The correlation between anomaly of dry day number and AO anomaly (<i>Red numbers= The significant relationship for the effective sample size, Black Numbers= The insignificant relationship)</i>	131
Table 4.25 The number of the station having the significant relationship between SOI and its dry day number in winter.....	134
Table 4.26 The number of the station having the significant relationship between WeMO and its dry day number in winter.....	137
Table 4.27 The standard deviation increment for different block lengths	140

TABLE OF ABBREVIATIONS

AO	Arctic Oscillation
CCAN	Continental Central Anatolia
CEAN	Continental Eastern Anatolia
CMED	Continental Mediterranean
DEM	Digital Elevation Model
GCV	Generalized Cross Validation
IDW	Inverse-distance weighting
MARS	Multiple Adaptive Regression Splines
MED	Mediterranean
MEDT	Mediterranean Transition
MLR	Multiple Linear Regression
MRT	Marmara Transition
NAO	North Atlantic Oscillation
NDVI	Normalized Difference Vegetation Index
PF	Perturbation factor
PLR	Power Law Regression
QPM	Quantile Perturbation Method
RC	Relative changes
SLP	Sea level pressure
SOI	Southern Oscillation Index
SPI	Standardized Precipitation Index
SROC	Spearman's Rank-Order Correlation
SST	Sea surface temperature
WeMO	Western Mediterranean Oscillation

CHAPTER 1

INTRODUCTION

Droughts and floods occur as a consequence of excessive decrease and increase in precipitation amount and/or frequency, respectively. Hence, precipitation is arguably the most significant driver of these events. A drought is a natural event, which results from receiving less precipitation than the long-term average for an extended period of time (Smakhtin, 2001). On the other hand, flood is a rather short duration phenomenon (Taye and Willems, 2011) that originates from an extremely high amount of precipitation in short time. Given the occurrence of these natural hazards are closely interconnected with the amount and frequency of precipitation, analysis of variability gains in importance.

The variability of a climatic event can be described as the anomaly from the mean state and the changes in the occurred extremes within the climatic event. Thus, climate variability measures the deviations called anomalies. Climatic variability is caused by naturally occurring internal processes and has various modes of variability involving components of the climate systems such as the atmosphere and the oceans. The variations in the mentioned components cause the rise of spatially coherent anomalies in large-scale and/or geographically spatial patterns like sea surface temperature (SST) and sea level pressure (SLP) (Hurrell, 1995).

The climate variability occurs especially over seasonal or longer time-scales. The spatially large-scale components of the climate system such as oceans are prone to vary over longer time-scales. The anomalous behavior of these components may persist throughout long time periods. Thus, the decadal analysis of the variability in the spatially large-scale atmosphere-ocean interaction pattern is essential since the

anomalies associated with these components achieve consistent levels over inter annual or decadal time-scales.

As stated before, precipitation variability analysis is crucial for taking necessary precautions for extreme events such as droughts and floods. Moreover, since precipitation is highly related to both ecological and economic issues, it becomes critical not only in extreme cases but also in everyday life. To address these needs, Türkeş and Erlat (2003) performed a study on the spatial and temporal precipitation variability in Turkey and the correlation between precipitation variability and NAO (Türkeş and Erlat, 2003). Their results showed a decreasing trend in annual precipitation starting from 1970. Besides, a strong relation was figured out between NAO and precipitation anomalies especially in winter season. Precipitation in autumn season was also highly correlated with NAO. Yet there was relatively less correlation between NAO and spring precipitation. Finally, in general, the insignificant correlation was obtained for summer precipitation. When annual responses are considered, most of the stations in which statistically significant correlation was seen, are located in Marmara Transition, Mediterranean Transition and Continental Central Anatolia rainfall regions. In general, negative correlations were attained between NAO and precipitation anomalies except Mid-Eastern Black Sea and North-Anatolia Sub regions.

The constant increase in urbanization and population density and correspondingly the rise in water demand in Turkey make the investigation of the anomaly in the low extremes necessary (Baltacı et al., 2014). Additionally this constant increase results in unplanned land use which may cause hydrological and climatic degradation (Maktav et al., 2005). The increased water demand and mentioned degradations make Turkey a drought-prone country along with other climatic vulnerabilities. It is highly possible to face water shortage if proper water usage terms are not planned. Thus, the analysis of droughts become more imperative. Accordingly, the spatial and temporal dimensions of droughts in Turkey were investigated by Sönmez et al (2005). They used Standardized Precipitation Index (SPI) method to represent drought vulnerability which was assessed at different time steps starting from 3

months to 24 months. The results revealed that severe droughts at shorter time periods happen in the non-coastal parts of Turkey. In addition, the rainfall needed to overcome the drought condition was calculated with respect to these time steps. It was seen that the rainfall amount to provide non-drought condition rises from coastal part towards the interior part of the country with increasing time steps.

Drought analysis are performed over shorter time scale rather than decadal time period by Sönmez et al (2005). In addition to this, Türkeş and Erlat (2003) utilized annual or seasonal normalized precipitation anomaly series obtained from annual or seasonal mean values while checking the precipitation variability. On the contrary, according to Tabari and Willems (2016), investigating the change in extreme climatic events is more important than that in mean values. Because small changes in mean values can be associated with large changes in the frequency of extremes due to changes in variability (Tabari and Willems, 2016). In their study, decadal anomalies were investigated in Iran between 1961 and 2005 as well as their possible drivers. They assigned the decadal anomalies with the help of Quantile Perturbation Method (QPM) which determines anomalies from precipitation extremes instead of mean values. They could define relatively wet and dry decadal periods by analyzing clustering of positive and negative anomalies in precipitation extremes by means of QPM. Similarly, the significance of the anomalies was tested by using Monte Carlo Confidence Interval. Also, they selected eight different climate indices related to sea surface temperature (SST) and sea level pressure (SLP) to figure out the relation between precipitation anomalies and climate indices.

Based on the outcomes of above mentioned studies, two fundamental questions arise:

- a) Are there significant variabilities in decadal precipitation anomalies when QPM is applied to precipitation extremes of different stations in Turkey?
- b) Is there a relation between teleconnection patterns and extreme precipitation behaviors in Turkey? If so, which teleconnection patterns are the drivers of these behaviors?

To further expand the argument, in this study, decadal extreme precipitation variability and possible significant anomalies in the precipitation of Turkey are investigated. Accordingly, this study is comprised of two distinct parts. In the first part, daily extreme precipitation data are analyzed in order to investigate high extreme precipitation variability in Turkey. The intent is to detect whether significant anomalies in the high extremes exist. Furthermore, drought analysis is performed by the help of QPM. Unlike the investigation of high extremes, when investigating low extremes by means of QPM, the anomalies in the number of dry days per year is used instead of the anomaly values in the daily high extreme precipitation. In the second part, relation analysis will be carried out between extreme precipitation and global teleconnection patterns to have an understanding on probable drivers of precipitation extremes. For this study, Western Mediterranean Oscillation (WeMO) and Arctic Oscillation (AO) teleconnection patterns are selected to examine their influence on precipitation variability in Turkey. AO has not been reported in the studies of precipitation variability in Turkey. Still, the negative relation between AO index and winter temperature (DJF) at 70 different stations of Turkey is noted (Türkeş and Erlat, 2008). Based on this study, it is considered valuable to investigate the potential effect of AO index on extreme precipitation variability in Turkey. Besides, WeMO is tested because WeMO has recently been determined as highly related with precipitation amount in the Eastern Mediterranean, especially in Turkey (Mathbout et al, 2016). Also, the influence of North Atlantic Oscillation (NAO), which was reported to have significant effects on precipitations in Turkey, is also analyzed (e.g. Türkeş, 2003). In addition, the relation between precipitation extremes in Turkey and Southern Oscillation Index (SOI) is examined in this study. The large-scale fluctuations of SOI is very influential on precipitation behavior of the regions between western and eastern tropical Pacific. The relation analyses with SOI are tested to see if it has the similar influence on Turkey's extreme precipitation attitude. The regions in which the mentioned climate indices arises are shown on the world map in Figure 1.1. Four climate indices taken into consideration in this study are explained below.

- i) **North Atlantic Oscillation (NAO):** A large-scale fluctuation in SLP difference between the Azores high and the Icelandic low pressure (<https://www.ncdc.noaa.gov/teleconnections/nao>). The index may change from year to year as well as it may persist to resume in one phase along several years or decade. It can be two different phase of the index: the positive and negative. In the former phase, the high pressure gets higher and the low pressure gets lower and the difference between SLP values increases. During the positive case, in general, Europe faces wet and warm winter whereas Turkey faces dry and cold winter. In the negative case, the reduced SLP gradient causes wet and warm winter in Turkey and dry and col winter in Europe.
- ii) **Arctic Oscillation (AO):** A global climatic variability index that is estimated by determining daily SLP anomalies over the region the north of 20°N latitude (<https://www.ncdc.noaa.gov/teleconnections/ao>). Like NAO, it has two different phase. These are positive and negative phases. In the positive phase, high pressure forces at the midlatitudes push moist air to the northern part of the world. Consequently, Alaska and Scandinavia encounter with wet weather conditions while United States and Mediterranean region face dry weather condition. Turkey, one of the country which is under the effect of Mediterranean climate, also has dry winter. The negative phase is the opposite phenomenon of the positive phase. AO index is strongly interacted with NAO index. Even though the effect of AO on Turkey's precipitation has not been investigated before, it is expected to have similar results with NAO index.
- iii) **Southern Oscillation Index (SOI):** The oscillations of measured SLP difference between Tahiti and Darwin (<https://www.ncdc.noaa.gov/teleconnections/enso/indicators/soi>). Simply, under normal circumstances, trade winds flow from the eastern side of Pasific Ocean towards the western side of it. This causes the moist warm water to be transported to the western side of the Pacific. The moist warm water evaporates there, creating cloud and/or precipitation. However,

there are two different extreme cases of the index. In the case of El Nino, the trade winds lose their power or even opposite effects are observed. Because of this, the warm water is not carried on the western part and consequently, while the west Pasific region gets drier, the east Pasific gets wetter. The second case, La Nina, is reverse of El Nino. The high pressure zone in the eastern Pasific gets higher and the low pressure zone in the western Pasific gets lower. This condition causes stronger storms than normal condition in western side of the Pasific. The corresponding temporary perturbations caused by the regional SST change may also affect the precipitation behavior of other regions (James et al., 2010).

- iv) **Western Mediterranean Oscillation (WeMO):** The climate index resulting from SLP difference between Cadiz-San Fernando (Spain) and Padua (Italy) (<http://www.ub.edu/gc/en/2016/06/08/wemo/>). The positive phase of WeMO index creates anticyclone (high pressure zone) in the Gulf of Cadiz and cyclone (low pressure zone) over Central Europe. It is precious to check its effect on Turkey since WeMO index is mostly influential on the countries in the Mediterranean region.



Figure 1.1 Climate Indices

Retrieved from: <https://www2.ucar.edu/news/backgrounders/weather-maker-patterns-map>

The recurrence of extreme conditions can be vastly affected by climate variability, which is generated by large-scale atmospheric circulations as well as anthropogenic activities such as land use (Taye and Willems, 2012). In parallel with this, the major objective of this study is to represent precipitation variability in precipitation extremes in Turkey and to explore potential causes and effects of this variability. The incidental objectives that point the fundamental intent of this study can be detailed as below:

- To find out negative and positive anomalies in daily precipitation extremes and to check whether there are clusterings that indicate decadal periods or not.
- To test the significance of the anomalies by using Monte Carlo Confidence Interval in daily precipitation extremes for decadal periods.
- To inspect whether, for the given time interval, observed flood events correspond to positive or negative QPM anomalies.
- To evaluate results with respect to different rainfall regions and to represent extreme precipitation variation for each rainfall region separately.
- To make seasonal interpretation of change in precipitation extremes along decadal periods.
- To reflect the connection between precipitation anomalies and selected teleconnection patterns. Also, to show whether a negative or positive relation exists between climate indices anomalies and precipitation anomalies in each station.
- To find the influences of the multiple teleconnection patterns on the change of precipitation extremes along with single influence via multiple relation analyses.
- To investigate non-linear and linear relationships between drivers and precipitation anomaly and compare them to see if the relationship is linear or non-linear.

CHAPTER 2

METHODS

As stated before, essentially two different analyses are performed in this study. First, decadal changes in frequency and magnitude of precipitation extremes are examined. The QPM is used to represent decadal extreme precipitation variability. It manipulates short-scale data (e.g. daily) to reach decadal oscillations. This method was firstly used by Ntegeka and Willems (2008) to investigate variabilities in hydrological extremes. Besides, they specified the existing significant anomalies in extremes by the help of Monte Carlo Confidence Interval. The QPM approach aims to extract the changes of quantiles between a reference (*i.e.* baseline) period and a subseries of interest (Tabari and Willems, 2016). In QPM, full-time series of a specific site is taken as baseline. After that, sub-series are derived from the full-time series with respect to their block period. The block periods of 5 and 10 years are selected for this study. Also, moving step is chosen as one year. Performing processes with a moving step provides the opportunity of testing any period against baseline period. Hereafter, daily precipitation values are sorted in descending order for each block (*i.e.* each subseries or quantile) and return periods of each data in a block are calculated with respect to ranks. The same processes are also carried out for full-time series. A return period is determined as a specific threshold and precipitation values above the threshold are assumed as precipitation extremes. The threshold may be a specific return period or it can be selected with respect to a specific rank. For this study, the highest 15 precipitation values in a year are accepted as extreme precipitations for each individual station. For instance, 150 precipitation values are assumed as extreme precipitation for 10-years block whereas 900 values are accepted as extreme precipitation for the baseline. This threshold is chosen since the precipitation values above this threshold are quite constant. Then, relative changes are calculated. Relative change is the ratio that is obtained by

dividing extreme value in a block to extreme value in the baseline having the same return period. Nevertheless, it is worthy to note that the return periods of subseries and baseline are not the same due to having different lengths of data. Hence, extreme values for same return periods are gained by means of linear interpolation from values with the closest return periods. Lastly, perturbation factor, which is the average of all relative changes is calculated. Perturbation factor indicates anomaly for a chosen block period and time. The work mechanism of QPM can be followed step by step below;

- First, X_{ij} is defined.
 i: start year of the block
 j: end year of the block
 X_{ij} : a matrix including all daily data between the years i and j
- Sort the data in X_{ij} in a descending order (*i.e.* $X_{ij1} > X_{ij2} > X_{ij3} \dots \dots \dots > X_{ijm}$).
 m: data length of X_{ij}
- Find the empirical return periods of each data by using the formula below.

$$t_n = \frac{2*n-1}{2*m} \tag{1}$$
 n=rank of the sorted data
 t_n =return period of n^{th} data
- Determine extreme values. If $t_n < T$, then X_{ijn} is defined as extreme value.
 T: a threshold return period
 X_{ijn} = data at n^{th} order
- Collect all extreme values (*i.e.* where $t_n < T$) in a matrix X'_{ij}
- Apply the same procedure to the baseline, obtain Y'_{ij} . For baseline, i is the start year of the full-time series and j is the end year of the full-time series. In other words, i is always 1955 and j is always 2014 for this study.
- Relative changes (RC) are taken.

$$RC = \left\{ \frac{X'_{ij1}}{Y'_{ij1}}, \frac{X'_{ij2}}{Y'_{ij2}}, \frac{X'_{ij3}}{Y'_{ij3}}, \dots \dots \dots, \frac{X'_{ijk}}{Y'_{ijk}} \right\} \tag{2}$$

k: the new data length of the block and baseline after interpolation

- Finally, calculate the perturbation factor (PF).

$$PF = \text{mean}(RC) \quad (3)$$

For example, if the block period is 10 years covering the quantile between 1978-1987, the perturbation factor is found as 1.2. This perturbation factor indicates 20% positive anomaly from the baseline for the years between 1978 and 1987. In other words, perturbation factor shows the average deviation of the quantile period from the long term study period. When showing the results on a figure, 1.2 corresponds to the year at the middle of the quantile (*i.e.* 1982).

Low anomalies are also calculated by the help of QPM when performing drought analyses. Albeit the main path is the same with high anomaly calculation, there is a small difference in usage of the method when calculating low anomalies. The low anomaly value is calculated by using dry day number in a year instead of 15 high precipitation values. In other words, the yearly data is utilized instead of daily precipitation data. Thus, low anomaly calculation does not require to selection of a specific threshold. Like high anomaly calculation, the yearly dry day number in a block are ranked in descending order and the return periods are calculated for each dry day number. The same process is conducted for baseline. The relative changes are calculated by dividing each dry day number in block to the baseline. For instance, there are 10 dry day numbers for 10-years block and there are 60 dry day numbers for the baseline. To produce 60 dry day numbers for 10-years block, the values are interpolated with respect to the return periods. Terminally, the values in block are divided to the values in the baseline, which have the same return period. At the end, the perturbation factor are calculated by taking mean of all relative changes.

After computing anomalies via QPM, the significance of the results is tested by Monte Carlo Confidence Interval under the null hypothesis of no significant difference exist in precipitation extremes in time at 5% significance level. As a consequence, an anomaly may be assigned as significant by Monte Carlo Confidence

Interval test with a probability of 5% even if it is not significant. The application of Monte Carlo Confidence Interval can be followed step by step as written below.

- i) The original series of extreme values for baseline are randomly mixed to obtain a new series with the same length but with interchanged values.
- ii) Subseries are derived from new series obtained for each block period and time interval.
- iii) The QPM method is applied to obtain new series and new anomaly values are computed.
- iv) First three steps are repeated 1000 times, and 1000 perturbation factors (*i.e.* anomalies) are gained for each quantile.
- v) Since 5% significance interval is selected for this study, if the anomaly obtained by QPM is not in between 25th and 975th ranked anomalies, then it is accepted as significant anomaly.

To make the Monte Carlo steps clear, one of the results is shown in Figure 2.1. Decadal anomaly fluctuations of Kütahya station for winter season can be seen in this figure. The figure demonstrates that the significantly high anomalies are detected in the early 1960s and 1980s, while the significantly low anomalies are found starting from early 1990s to 2000s. Meanwhile, the significantly low/high anomaly for a block means that it is encountered with the significantly lower/higher extreme precipitation at given block in comparison to the extreme precipitation of whole study period (*i.e.* baseline). A crucial point is that it is conceivable to have some significant anomalies as an output of Monte Carlo Method since there is already 5% chance for each anomaly value to be significant. However, if the distribution of the significant anomalies is focused on, it can be seen that clustering at the distribution of the significant anomalies occur. On this basis, it is evident that these clustering do not occur due to random reasons, some grounded drivers that cause this clustering should exist.

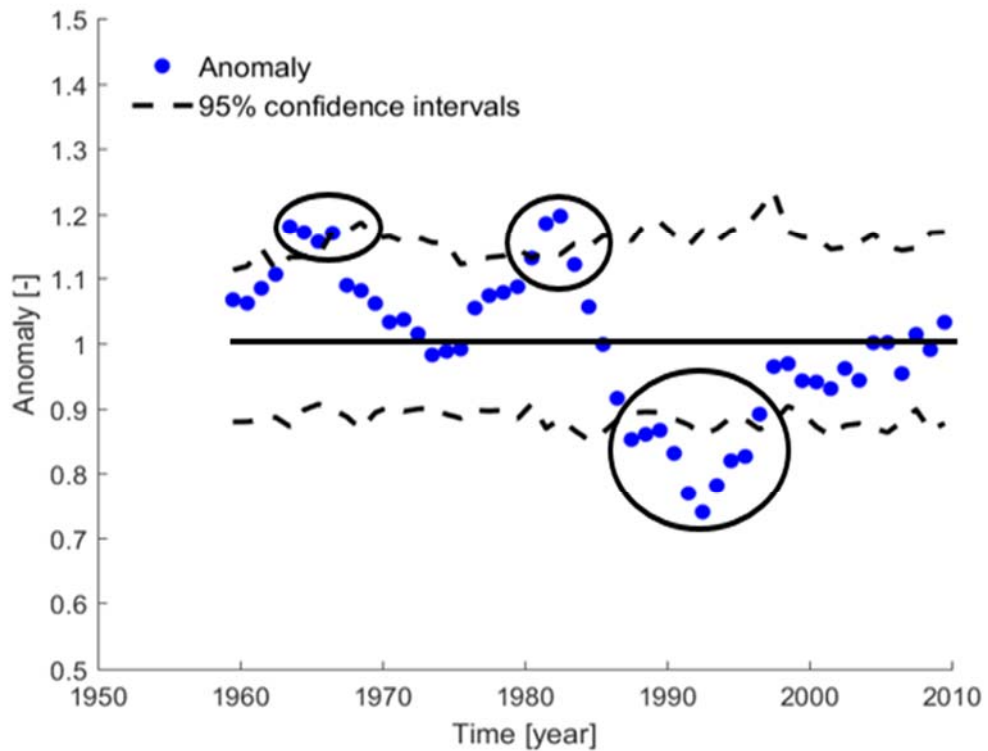


Figure 2.1 Decadal anomaly fluctuations of Kütahya in winter season with 10 years block

In parallel with previous interpretations, to understand probable drivers of general behavior of precipitation extremes, the relation analyses are carried out between extreme precipitation and climate indices extremes. Four different methods shown in Table 2.1, are used to represent relations. The performance of the non-linear methods in the highly variable hydrological components such as precipitation and soil moisture in comparison to linear methods is not still completely explored (Afshar and Yilmaz, 2017). Therefore, both linear and non-linear analyses are performed for each single and multiple relation analyses in order to test if linear or non-linear relation exist between precipitation extremes and climate indices. Namely, the main intent is to show which method gives the best prediction (cor)relation.

Table 2.1 Relation Analysis Methods

	Single Relation Analyses	Multiple Relation Analyses
Linear Methods	Spearman's Rank-Order Correlation	Multiple Linear Regression
Non-Linear Methods	Power Law Regression	Multiple Adaptive Regression Splines

On part of these, Multiple Adaptive Regression Splines (MARS) is not a non-linear method. However, it aims to express nonlinearities between variables. MARS is chosen to carry out relation analyses since it is useful in defining the relations in extreme cases of randomly generated events.

i) Spearman's Rank-Order Correlation (SROC) : It is chosen since it is a non-parametric method that works well with high-variable precipitation behavior. The main purpose here is to reflect the correlation between precipitation anomalies and climate indices anomalies and to measure its significance.

ii) Power Law Regression (PLR): Power law regression is one of the fitting methods which demonstrates the non-linear single relation between two variables. It is used for single relation analyses in this study and its results are compared with Spearman's Rank-Order Correlation's results. The function of the fitting method is,

$$\hat{y} = Ax^B \quad (4)$$

Where;

y=Predictand

x=Predictor

A & B = Regression parameters

iii) Multiple Linear Regression (MLR): Multiple regression is used to show the linkages of one dependent variable with two or more regressors in the model. In our case, the dependent variable is precipitation anomalies whereas regressors are

climate indices anomalies. Different combinations of the chosen teleconnection patterns can be used as regressors with respect to results of single relation analyses. To find out how variables will be used in the test, simple formulation of estimated multiple linear equation can be followed below.

$$E(\hat{y})=b_0+b_1x_1+b_2x_2+\dots+b_kx_k+\epsilon \quad (5)$$

Where;

y= Predictand (precipitation anomalies for this study)

x_k=Regressors (climate indices anomalies for this study)

k=Number of regressors (smallest 2, largest 4 for this study)

b_k=Parameters

ϵ= Error term

To avoid overfitting and artificial regression skill, leave-one-out cross validation method is used in this study. In this validation method, one sample is retained and the remaining samples are used to form the regression model. Then, retained sample is predicted by using formed model. This procedure is applied for each sample once. Finally, a mean square error is calculated from squared errors.

Multiple Adaptive Regression Splines (MARS): It is a non-parametric regression approach which was firstly proposed by Friedman (Friedman, 1991). It is an adaptive linear method still it provides the nonlinearities between predictand and predictors. MARS applies adaptive separated linear regressions to sub regions in order to express changing relation between dependent and independent variables (Felicísimo et al., 2013). Each of these separated linear regression splines are called as basis function. The MARS function form is,

$$\hat{y} = a_i + \sum_{i=1}^k b_i B_i(x) \quad (6)$$

where the a_i is the intercept term and the b_i are the constant coefficients for each basis function B_i(x). Also, the basis function is obtained from the set of reflected pairs;

where,

$$\text{If } x_m > t_i; \text{ then } B_i(x) = \max(0, (x_m - t_i)) \quad (7)$$

$$\text{If } x_m < t_i, \text{ then } B_i(x) = \max(0, (t_i - x_m))$$

x_m = observed value for m^{th} variable

t_i = constants called knot. Knots are the points where slope of the function changes.

The MARS uses two phases to optimize the model. The first phase is the forward pass. At each step in the forward pass, the new basis function pairs are added to model to minimize the residual errors. The basis functions are added to both sides of the selected knots in pairs. All variables are utilized to form basis functions and all observed values of all these variables are tested as knot values. The insertion of the new basis function pairs stop either when the residual errors are sufficiently reduced or when the maximum number of basis functions is reached. In general, the forward-pass overfits the model. The goal of the backward pass section is to remove overfitting from the model. To achieve this, Generalized Cross Validation (GCV) function is put into use. The backward pass deletes one of the basis functions that has the least ability for the sake of the model at each step. It stops when the optimum number of the basis functions are gathered. In this study, the MARS is tested to figure non-linear relationship between precipitation extremes and climate indices. The results of it are compared with MLR to understand if linear or non-linear methods explain the relationship better with respect to our data. Like MLR, to avoid overfitting and artificial regression skill, leave-one-out cross validation method is utilized in MARS analyses.

In total, there are 67 stations and 4 different climate indices in hand. When performing the single analyses, each of the station is tested with each of the climate indices by the help of two different methods (i.e. SROC and PLR). In addition, for multiple analyses, the reasonable pairs of available climate indices are used as input values to predict the extreme precipitation of each station by favor of MLR and

MARS. After, the (cor)relations between the predicted extreme precipitation and the actual extreme precipitation are defined for each station. All analyses are done for 4 different climate seasons.

CHAPTER 3

STUDY AREA AND DATA

3.1 Study area

Turkey is one of the countries which serves as a bridge between Asia and Europe. It is located between 26°-45° E longitude and between 36°-42° N latitude. It is surrounded on three sides by the sea. The Black Sea is located in the northern part of the country and is connected to the Mediterranean Sea that is located in the southern part along the Marmara and the Aegean Sea. In addition, Turkey occupies a large continental place with an approximate area of 770,000 km². Because of having such a large region, it incorporates various geographical features such as mountain chains, deep river valleys, and major river deltas. As Turkey includes variety in its nature, its climate varies from region to region with respect to meteorological and geographical factors. For example, due to the mountain ranges of the northern and southern coasts - the North Anatolian Mountains and the Taurus Mountains - the reaching of coastal effects to Central Anatolia is hindered (Raja et al., 2016). Furthermore, the variety of elevation across Turkey are represented by Digital Elevation Model (DEM) of Turkey (Figure 3.1). Consequently, Turkey has different climate types with respect to zones as a result of being affected by different meteorological factors and climate control elements. By considering these variables, seven different rainfall regions are defined by Türkeş (1996). These are:

- i) **BLS:** Black Sea Region
- ii) **CCAN:** Continental Central Anatolia
- iii) **CEAN:** Continental Eastern Anatolia
- iv) **CMED:** Continental Mediterranean
- v) **MED:** Mediterranean
- vi) **MEDT:** Mediterranean Transition

vii) **MRT: Marmara Transition**

In this study, regional interpretations will be performed with respect to this classification. The rainfall characteristics of these regions can be seen in Table 3.1.

Table 3.1 The rainfall characteristics of the regions

Rainfall region	Basic characteristics
BLS	Temperate, uniform rainy with maximum in autumn
CCAN	Cool rainy in spring, cold rainy in winter, warm and light rainy in summer
CEAN	Cool rainy in spring and early summer, cold rainy in winter
CMED	Rainy in winter and spring, dry in summer
MED	Heavy rainy in winter, dry in summer
MEDT	Moderate rainy in winter and spring, dry in summer
MRT	Uniform rainy, warm and light rainy in summer

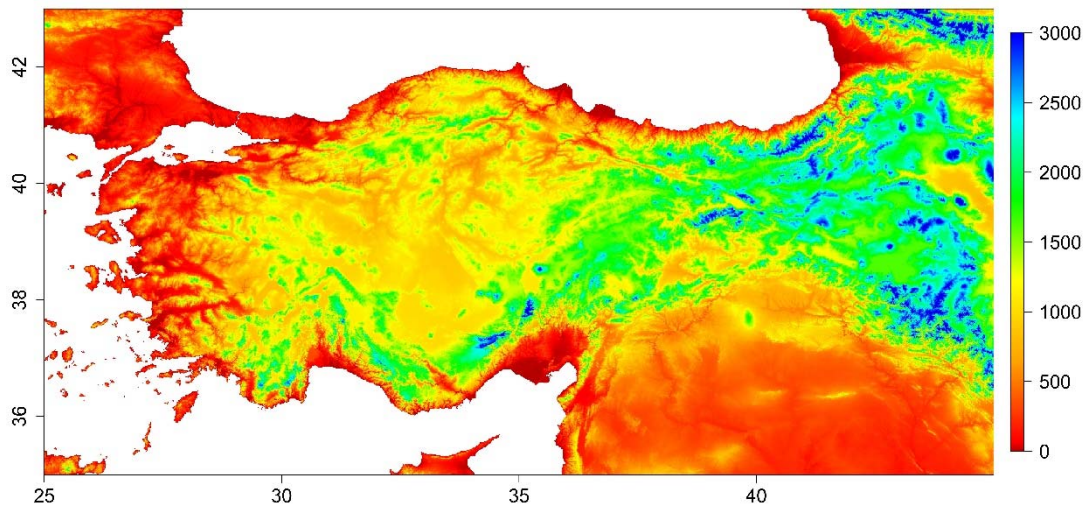


Figure 3.1 Digital Elevation Model (DEM) of Turkey

According to Türkeş (1996), there are 3 main geographical reasons governing precipitation behavior in Turkey : i) Black sea and Mediterranean basins ii) The high mountains which lie in parallel to west-east coast iii) The Anatolian plateau with average altitude of 1130 meters. The main sources of moist air masses for Turkey's precipitation are the Atlantic Ocean and Mediterranean Sea. In general, the precipitation amount decreases from the coastal regions to the interior parts due to the adiabatic process (i.e. orographic). The moist air starts to rise when it encounter with mountain. After, it cools with increasing height and the water vapor condenses as rainfall or snow. The air which has lost its moisture maintains its movement and descends on the other side. This situation makes wetter windward side of the mountain and drier leeward side of it. The process is called as adiabatic process. For instance, the central and eastern parts of the country are arid or semi-arid areas since high mountains (Northern Anatolia and Taurus) prevent the moist air to get there while Black Sea and Mediterranean coasts are quite humid regions. In addition, four different large scale pressure systems govern Turkey's precipitation behavior. As it is seen in Figure 3.2, the impact of Icelandic cyclone comes from Balkan Region. The Icelandic low pressure system is formed by dynamic reasons at 60° N latitude. In general, it is effective all along the year but the main effects are observed during winter. Stronger Icelandic low pressure causes warmer and wetter winter. Moreover,

if it encounters with the mass of cold air, it produces snowfall. The other cyclone influential over the country is Persian cyclone that is generated by thermal forces and it is dominant in summer. It drives dry and hot air masses from Arabian Peninsula to southeastern Anatolia. Besides, two large-scale high pressure systems have noteworthy influence: Azores and Siberian. The former one is a dynamic pressure system which arises at 30° N latitude. It provokes cold and dry winter along with hot and dry summer. The latter is thermal pressure system which is created by extreme cooling of Siberian continent in winter. Thus, it is effective only in winter. The essential domain of the pressure is eastern Anatolia. It pushes cold and dry air masses from Siberian region to the country. If these air masses face moist air masses, they generate snowfall. Winters under influence of this pressure system often pass colder than average.

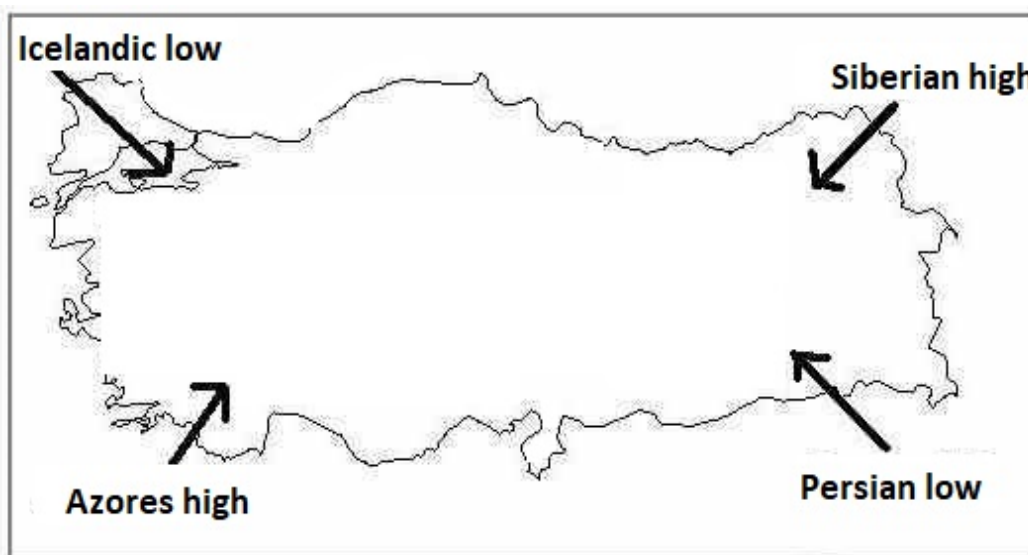


Figure 3.2 Effective pressure systems over Turkey

3.2 Data

Daily precipitation data are provided by Turkish General Directorate of Meteorology (MGM) for this study. Daily precipitation records are of importance to investigate extremely high precipitation events using QPM method. By using small scale data,

short and heavy thunderstorms which may result in severe floods can be evaluated. For example, Vaes *et al.* (2002) found a small negative tendency in high precipitation extremes for small time-scale data (less than 1 day) after analyzing data series of 100 years at Uccle station (Vaes *et al.*, 2002). Even though MGM provided 417 stations with daily precipitation data, some of the stations have very short records which are not sufficiently long for decadal analyses. The usage of records that are long enough to account for the underlying natural variability and that include both dry and wet years is surely a necessity (Taye and Willems, 2012). In addition, some of the stations which have long-term data records are eliminated since they have lots of missing data. It is very important to state that the longer the time series mean the better representation of decadal variability. In parallel with that requirement, there are also stations with records as much as to 90 years length. Here, a trade off between the temporal and spatial coverage exists. Although 90 year records are present for some stations, the number of them is only a few. Hence their spatial coverage is not extensive. Therefore, 60 years time period is used in this study not to miss spatial distribution over rainfall regions. Besides, in order to check credibility of the records for each station, annual average total precipitation of the available data are compared with the annual average precipitation values over long years which are published by MGM in their website. As a consequence of these, 65 stations are selected to examine. The selected station records include the data in the period between 1 January 1955 and 31 December 2014. The detailed characteristics of the stations are summarized in Table 3.2.

Table 3.2 Characteristics of the stations

Station ID	The location of the station	Region that station belongs	Longitudde	Latitude
17351	Adana	MED	35.344	37.004
17190	Afyon	CCAN	30.560	38.738
17099	Ağrı	CEAN	43.052	39.725
17184	Akhisar	MED	27.823	38.912
17310	Alanya	MED	31.980	36.551
17320	Anamur	MED	32.865	36.069
17130	Ankara	CCAN	32.864	39.973
17372	Antakya	MED	36.151	36.205
17300	Antalya	MED	30.799	36.906
17045	Artvin	BLS	41.819	41.175
17234	Aydın	MED	27.838	37.840
17114	Bandırma	MED	27.997	40.332
17120	Bilecik	MRT	29.977	40.141
17290	Bodrum	MED	27.440	37.033
17070	Bolu	BLS	31.602	40.733
17238	Burdur	MEDT	30.294	37.722
17116	Bursa	MRT	29.013	40.231
17968	Ceylanpınar	CMED	40.031	36.841
17112	Çanakkale	MED	26.399	40.141
17080	Çankırı	CCAN	33.610	40.608
17084	Çorum	CCAN	34.936	40.546
17237	Denizli	MED	29.092	37.762
17180	Dikili	MED	26.888	39.074
17280	Diyarbakır	CMED	40.203	37.897
17962	Dört Yol	MED	36.198	36.824
17050	Edirne	MRT	26.551	41.677
17201	Elazığ	CMED	39.256	38.644
17094	Erzincan	CEAN	39.487	39.752
17096	Erzurum	CEAN	41.190	39.953
17296	Fethiye	MED	29.124	36.627
17636	Florya	MRT	28.787	40.976
17261	Gaziantep	CMED	37.351	37.059
17034	Giresun	BLS	38.388	40.923
17100	Iğdır	CEAN	44.052	39.923
17024	Inebolu	BLS	33.764	41.979
17240	Isparta	MEDT	30.568	37.785
17370	İskenderun	MED	36.158	36.592
17220	İzmir	MED	27.082	38.395
17074	Kastamonu	CCAN	33.776	41.371

Table 3.2. Continued

17196	Kayseri	CCAN	35.500	38.687
17160	Kırşehir	CCAN	34.156	39.164
17061	Kireçburnu	MRT	29.050	41.146
17244	Konya	CCAN	32.574	37.984
17059	Kumköy	MRT	29.038	41.251
17155	Kütahya	MEDT	29.989	39.417
17631	Lüleburgaz	MRT	27.311	41.351
17199	Malatya	CMED	38.217	38.337
17186	Manisa	MED	27.405	38.615
17275	Mardin	CMED	40.728	37.310
17340	Mersin	MED	34.603	36.781
17292	Muğla	MED	28.367	37.210
17250	Niğde	CCAN	34.680	37.959
17040	Rize	BLS	40.501	41.040
17069	Sakarya	BLS	30.393	40.768
17030	Samsun	BLS	36.256	41.344
17210	Siirt	CMED	41.935	37.932
17026	Sinop	BLS	35.155	42.030
17090	Sivas	CCAN	37.002	39.744
17270	Şanlıurfa	CMED	38.786	37.161
17610	Şile	MRT	29.601	41.169
17056	Tekirdağ	MRT	27.497	40.959
17188	Uşak	MEDT	29.404	38.671
17172	Van	CEAN	43.346	38.469
17140	Yozgat	CCAN	34.816	39.824
17022	Zonguldak	BLS	31.778	41.449

The names of the stations located in each region are presented in Table 3.3. Accordingly, within the scope of this study, there are 8, 11, 6, 8, 19, 4 and 9 stations located in BLS, CCAN, CEAN, CMED, MED, MEDT and MRT regions respectively to analyze decadal extreme precipitation behavior. Also, the locations of stations are figured on the map of Turkey (Figure 3.3). The background of the figure is based on the Normalized Difference Vegetation Index (NDVI) data between the years 2000 and 2014. The NDVI data are obtained from MODIS satellite. Higher NDVI values indicate more green-fields and photosynthetic plants while lower ones

point the areas that are less green (Bulut and Yılmaz, 2016). In the view of that information, Figure 3.3 shows that the greenest area is BLS in Turkey.

Table 3.3 Station names with respect to their rainfall regions

	BLS	CCAN	CEAN	CMED	MED	MEDT	MRT
Station	Bolu	Afyon	Ağrı	Ceylanpınar	Adana	Burdur	Bilecik
	Giresun	Ankara	Artvin	Diyarbakır	Akhisar	Isparta	Bursa
	İnebolu	Çankırı	Erzincan	Elazığ	Alanya	Kütahya	Edirne
	Rize	Çorum	Erzurum	Gaziantep	Anamur	Uşak	Florya
	Sakarya	Kastamonu	Iğdır	Malatya	Antakya		Kireçburnu
	Samsun	Kayseri	Van	Mardin	Antalya		Kumköy
	Sinop	Kırşehir		Şanlıurfa	Aydın		Lüleburgaz
	Zonguldak	Konya		Siirt	Bandırma		Şile
		Niğde			Bodrum		Tekirdağ
		Sivas			Çanakkale		
		Yozgat			Denizli		
					Dikili		
					Dört Yol		
					Fethiye		
					İskenderun		
					İzmir		
				Manisa			
				Mersin			
				Muğla			

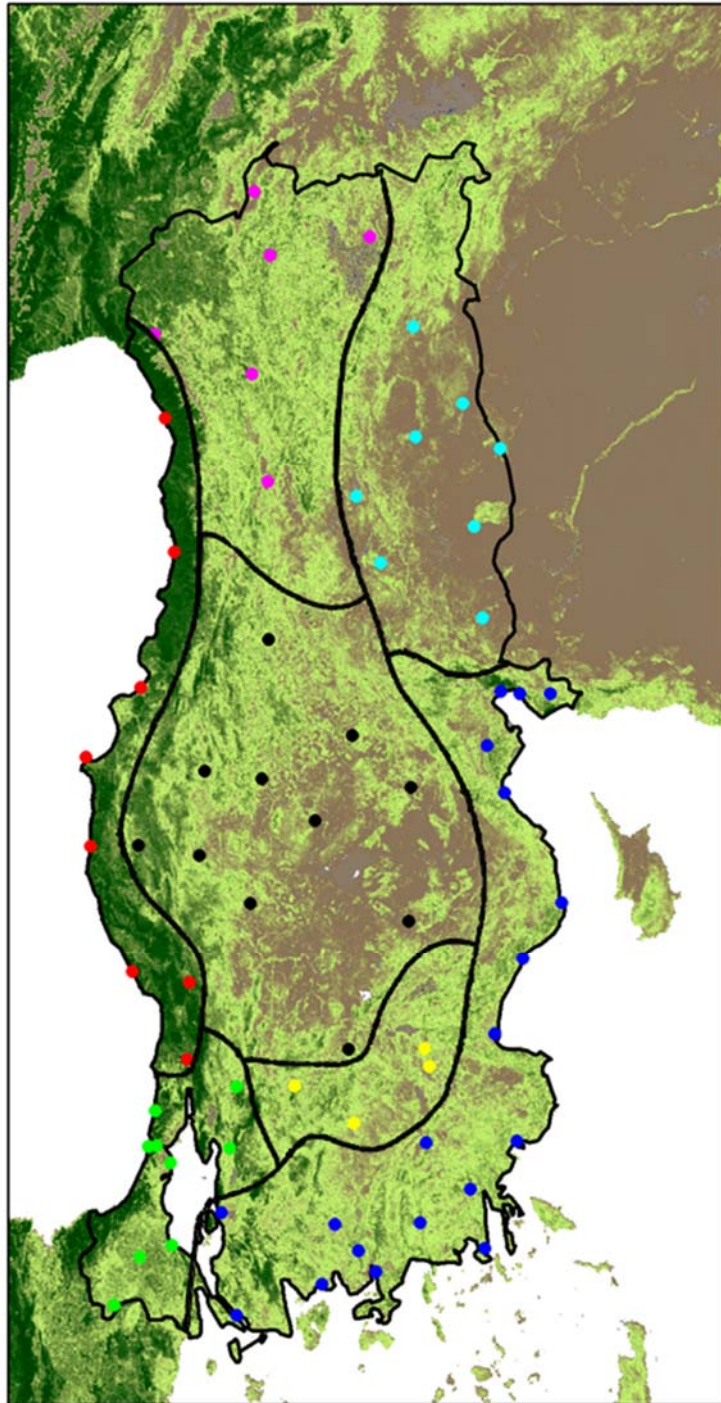


Figure 3.3 Locations of Selected Stations (Red Points= BLS, Black points= CCAN, Pink Points= CEAN, Light Blue Points= CMED, Blue points= MED, Yellow Points= MEDT, Green Points= MRT)

Daily data of AO, NAO, SOI and WeMO are also utilized in this study. Even though daily data of remaining three are easily accessible, it is not the case for WeMO. Therefore, daily WeMO indices are manually calculated by taking the daily SLP difference between Cadiz-San Fernando and Padua. After obtaining daily datasets for all climate indices, the standardization process are done. Climate indices are standardized by dividing each data to the last 30-years mean. The purpose of the standardization is to handle the data in a single order when there is a lot of difference between the data. Yearly averages of standardized daily climate indices can be examined in Figure 3.4.

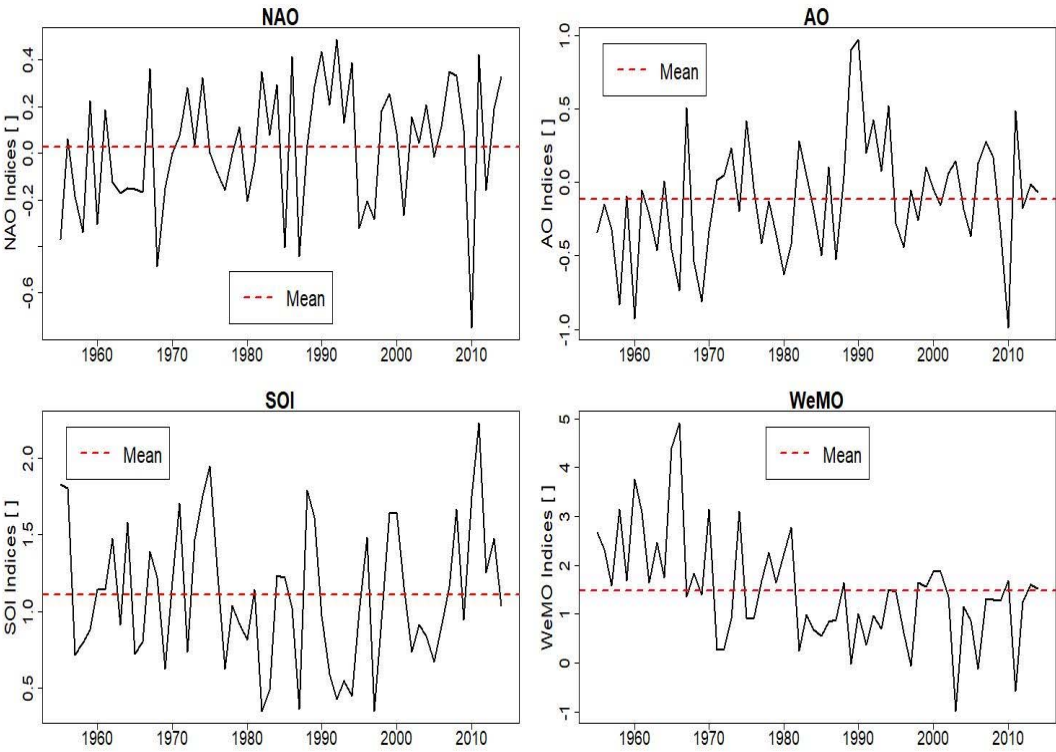


Figure 3.4 Time series of climate indices for the study period

CHAPTER 4

RESULTS AND DISCUSSION

4.1 Analyses of total precipitation

Before performing extreme precipitation variability analysis, total precipitation variability of Turkey is analyzed to have an idea on general precipitation behavior of Turkey. First of all, daily mean values are calculated for each region by taking the mean of the daily precipitation of the stations which are placed in these regions. Annual total precipitation over each of 7 different regions are calculated in two different ways: by summing the daily precipitation for each year separately and by summing the 10-year moving averaged daily precipitation. The main purpose of using the moving average method with 10-years block is to determine whether there are visible trends in the decadal period by smoothing the sharp changes that can occur from year to year. This is crucial since weather is the expression of current atmospheric conditions and it is chaotic. For example, very small effects on the atmosphere can create big storms. Likewise, a region that has been suffering from drought for a long time may face its highest precipitation due to a simple reason. In other words, when climate variability is examined, using short-term scales may be misleading since climate is the long-term average of the atmospheric conditions. Thus, in this study the decadal effects of the precipitation data are observed for this reason.

Moving average method is applied to daily precipitation data, where the block containing 10-years daily data is shifted with a moving step of 1 day. For instance, the arithmetic average of daily precipitation data between 1 January 1955 and 31 December 1964 are used to predict the daily precipitation value of 1 January 1960.

Similarly, in the next step, the daily precipitation value corresponding to 2 January 1960 is obtained from the average of daily data between 2 January 1955 and 1 January 1965. Then, daily data is converted into annual total by summing the moving averaged daily precipitation values in each year. The change of the total precipitation values obtained by using the moving average method can be seen in Figure 4.1. Besides, this figure shows the variation of annual total precipitation according to the years at different regions.

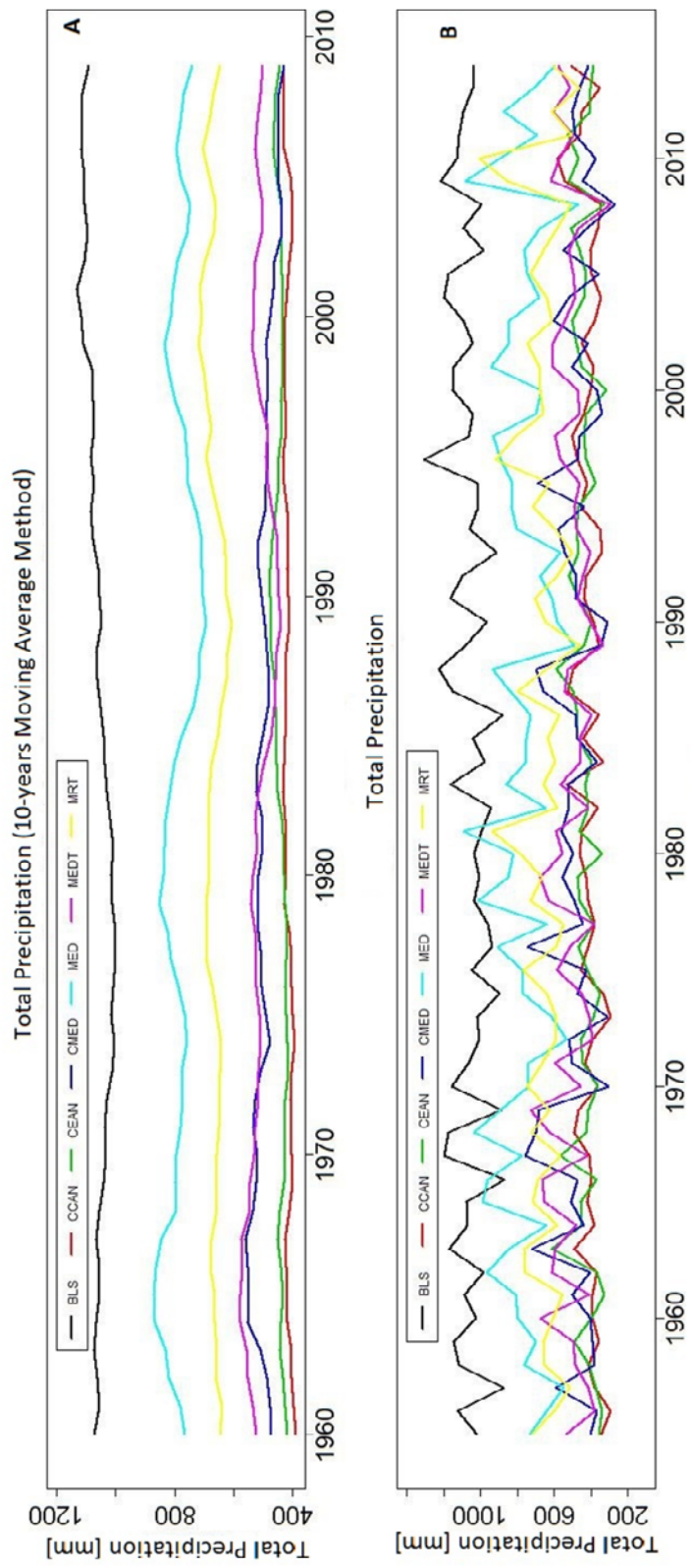


Figure 4.1 Total precipitation variation of Turkey

Describing precipitation variation of regions with reference to their long-term mean values are also important to more clearly see the anomalies from the mean. In parallel, Figure 4.2 represents the fluctuations of standardized total precipitation values over the years. Both natural and moving averaged total rainfall data are standardized based on the formula below:

$$TR'_k = (TR_k - \mu_i) / \sigma_i \quad (8)$$

where;

TR'_{ik} = Standardized annual total precipitation of i^{th} region at k^{th} year

TR_{ik} = Annual total precipitation of i^{th} region at k^{th} year

μ_i = Mean of annual total precipitation in the time-series of i^{th} region

σ_i = Standard deviation of annual total precipitation in the time-series of i^{th} region

Figure 4.1 indicates the distribution of average precipitation over Turkey; in particular BLS region has the highest and CCAN & CEAN regions have the lowest precipitation. Moreover, this figure shows the precipitation variability in Turkey over different regions. While the average precipitation in CCAN is around 380-400 mm in certain years, only the average precipitation difference between consecutive years in BLS is equal to this amount. Furthermore, in MED, the region with highest precipitation amount after BLS, noticeable fluctuations exist over the last 60 years. The early 1990s, especially in decadal scale, seem quite dry for MED region. Although the extent of decrease in the amount of precipitation at the early 1970s and 2000s for MED region rises, they do not reach the amount of early 1990s.

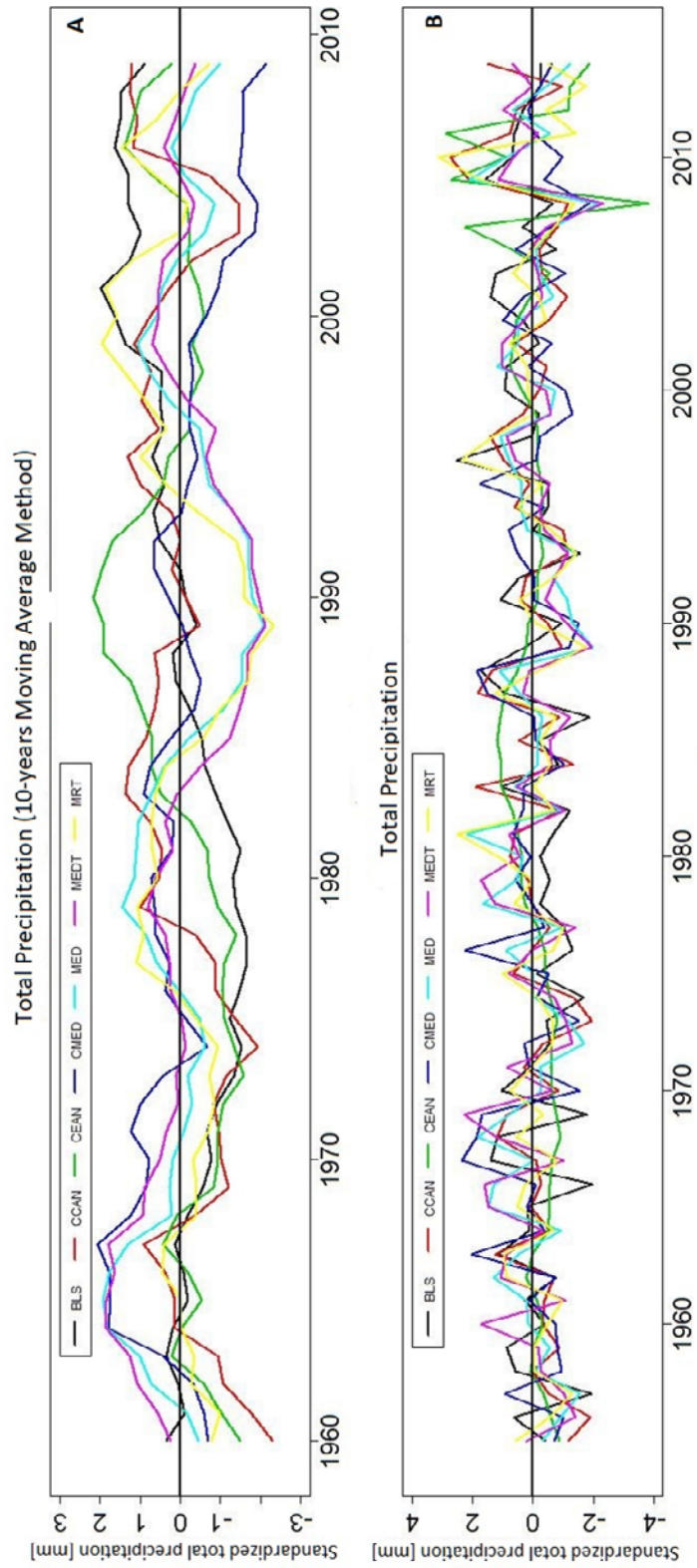


Figure 4.2 Standardized total precipitation variation of Turkey

Additionally, Figure 4.1 (B) displays a remarkable water shortage throughout all regions in Turkey during 2008. Figure 4.2 (B) shows the extent of the water shortage in 2008 with respect to the regions. During this year, it can be observed that the precipitation amounts in all regions drop below their long-term averages and notably the drop in the CEAN region is quite high. In addition, Figure 4.2 (A) demonstrates considerable drop in precipitation amount in the early 1990s for many of regions. While the precipitation amounts in the MEDT, MED and MRT regions are remarkably low, only the CEAN region appears to be above its long-term rainfall average.

4.2 Analyses of decadal precipitation anomaly in the high extremes

In the following parts of this section, decadal high extreme precipitation oscillation outcomes obtained by QPM are analyzed. The outcomes are reported separately for each rainfall region with respect to seasons as well as the individual responses of the stations over decades. Primarily, it is precious to state that Turkey receives most of its precipitation in winter. Therefore, it is crucial to thoroughly discuss winter extremes in order to have a complete understanding on extreme precipitation behavior of the country. During the Monte Carlo Confidence Interval Analyses, the significance of the anomalies is tested at 5% significance level.

4.2.1 The summary of all regions

The succeeding interpretations for the autumn, winter, spring and summer parts are grounded on the results shown in . The area between the maximum and the minimum region anomaly values are represented in Figure 4.4. The region anomaly values are obtained by taking median of the stations in the region in question.

4.2.1.1 Autumn

First of all, the fluctuations in the region anomaly of autumn are more than the fluctuations of winter and spring region anomaly. Turkey's rainfall regions contain lower quantile perturbations in the 1960s since Turkey receives less precipitation in autumn when compared to spring and winter. Different from this, higher quantile perturbations are explored in CEAN, CMED and BLS towards the end of the 60's. After the higher quantile perturbations in the 1960s, CMED shows lower quantile perturbations at 20% in the 1970s. In contrast, the higher quantile perturbations are noticed in the MEDT and MED regions. A common trend in the movement for the regions along the 1980s and 1990s can not be distinguished. However, the contrast movements of the region anomalies of MEDT and CMED should be taken into consideration. The increase in the anomaly of CMED that begin in the early 1980s, results in high perturbations up to 20% in the mid-1990s. On the other hand, the decrease in the anomaly of MEDT starting in the early 1980s ends up with low perturbations up to 10% in the mid- 1990s. Lastly, the regions mostly have high oscillations of anomalies in the 2000s except for CEAN, which has low oscillation of anomalies.

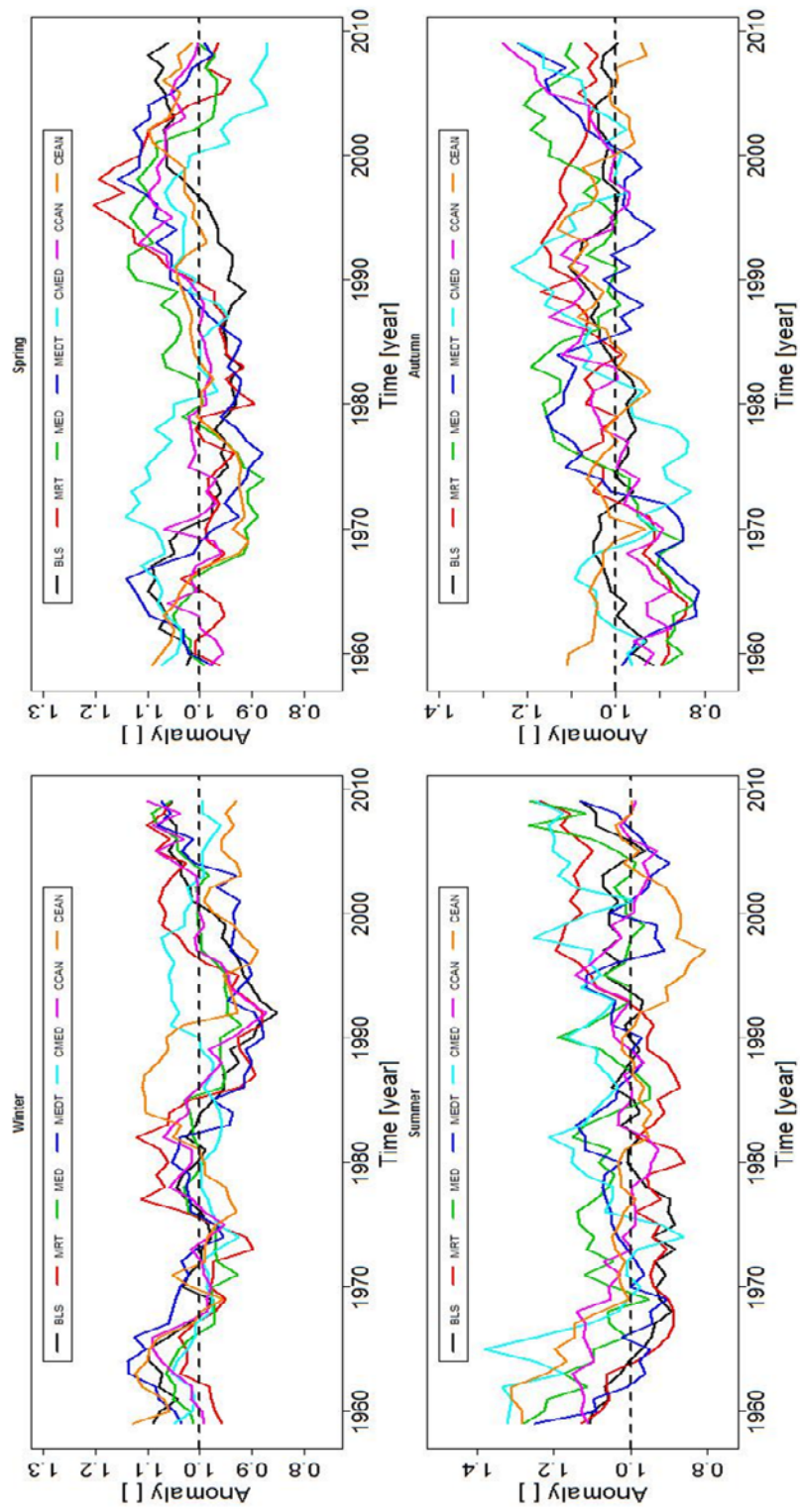


Figure 4.3 Comparison of the region anomalies with respect to sesason

4.2.1.2 Winter

In the first part of data obtained for the 1960s, an increase in the anomaly values is detected. All regions have positive anomalies in the mid-1960s, even the anomalies at the stations of MRT and CMED regions are slightly higher than the baseline. The peak anomalies are identified in the MEDT and CEAN for the same time slot. As a result of the tendency in the anomalies to decrease, the negative anomalies are almost encountered at all regions in the 1970s. Different from the others, the positive anomalies occur in the MRT for the 1970s. The extreme precipitation of Turkey's rainfall regions, excluding CMED and CEAN, show declining tendency after the first part of the 1980s. Especially, in the early 1990s, there are very low negative perturbations at the remaining 5 regions. Besides, it can be claimed that the 1990s pass with negative anomalies except for CMED. After this dry period in terms of extreme precipitation, the anomaly amount starts to rise along the 2000s and turn into positive anomalies in the early 2010s. Nevertheless, there are anomalies approximately identical to baseline in CMED and negative perturbations in CEAN. Also, Figure 4.4 indicates that the median of the region anomalies is commonly under the baseline average between the early 1970s and 2000s. This tendency signifies the decline in the amount of precipitation extremes for the given period. Both and Figure 4.4 prove that the decreases in extreme precipitation amounts are very high at the beginning of the 1990s. In this period, the median of region anomalies is pretty close to the minimum region anomaly value. There is a substantial decrease in the anomaly values at most of the regions. If two graphs are compared, it can be deduced that the maximum values in both region anomalies for this period originate from the anomalies in CMED region. Besides, it can be claimed that the 1960s and 2000s frequently compose of positive anomalies by checking the median of the region anomalies. In other words, an increase in the amount of extreme precipitation during the winter months is observed after the early 2000s.

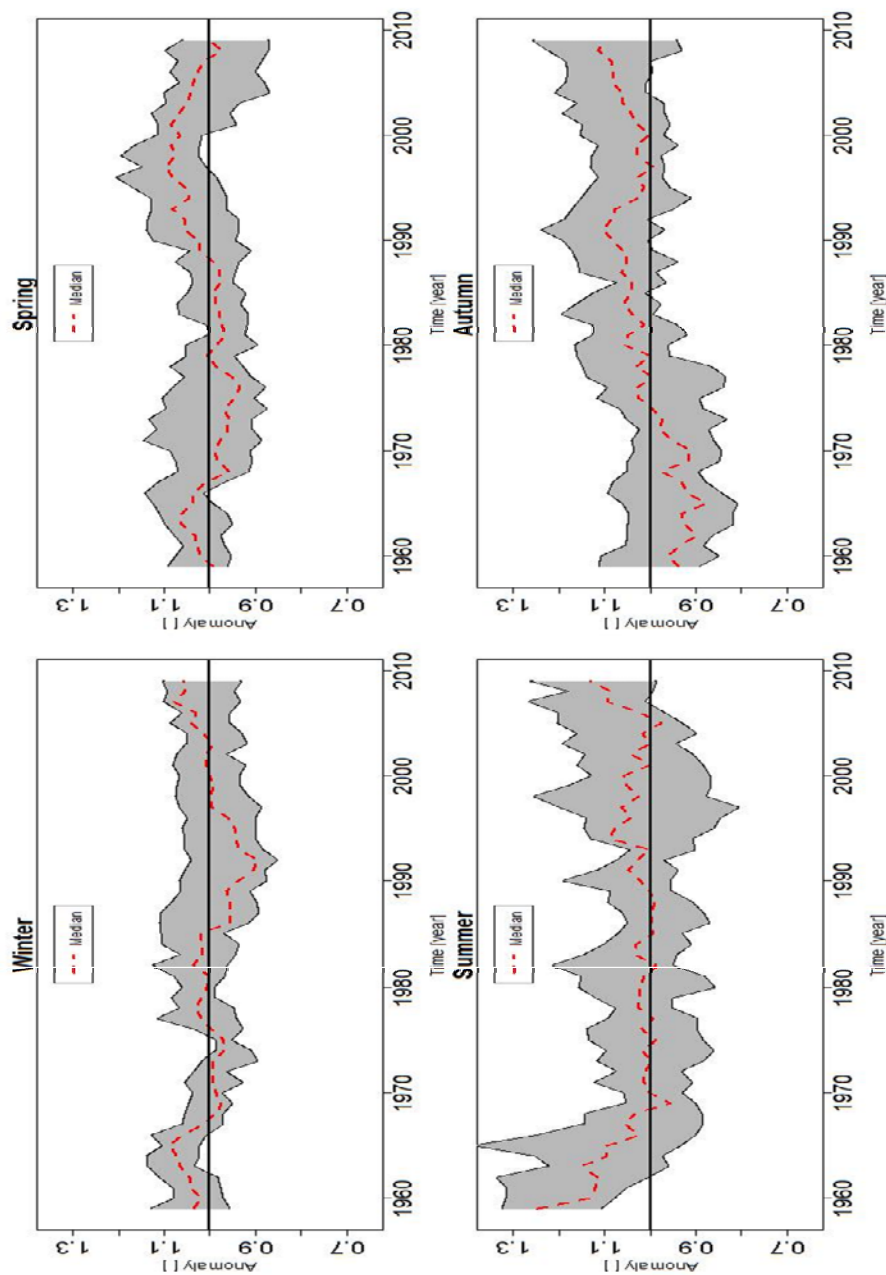


Figure 4.4 The Areas of the anomaly variability in the region anomalies with respect to all seasons

4.2.1.3 Spring

In the first part of the 1960s records, the positive anomalies are commonly observed in the region anomalies except for MRT and CCAN. Nevertheless, the decrease in

the anomalies starting from the second part of the 1960s continues until the 1980s as negative anomalies in all regions. Yet, the situation is different for the CMED region. The region has positive anomalies for the 1970s and also lower perturbation anomalies for the 1980s. However, this time the exception is the MED region which shows positive anomalies for the 1980s. Although the BLS keeps its lower perturbation attitude in the 1990s, the other regions mainly display higher perturbations. There are very high perturbations especially in the MRT region. Both the positive and the negative anomalies are monitored for the 2000s. Nonetheless, negative anomalies are encountered more rather than the positive anomalies. In CMED region, the median anomalies decrease almost to 13% less than the baseline.

4.2.1.4 Summer

The extreme precipitation behavior of the each individual station is examined and anomaly results obtained via QPM are reported with respect to different seasons along forthcoming sections of 4.2. However, summer part is omitted from this section since Turkey receives low precipitation during summer months. In the periods of low rainfall, small changes in precipitation amounts of quantiles point higher fluctuations. This is due to the fact that QPM investigates change of quantiles in reference to long-term baseline (Tabari and Willems, 2016). The high level of these fluctuations also makes it difficult to find decadal trends at the stations for the summer period. Thus, it seems more reasonable to interpret the decadal oscillations of summer anomalies based on region anomalies rather than individual stations. Afterwards it is possible to obtain general idea about extreme precipitation behavior of regions. It is also helpful to recall that the region anomalies are collected by taking the median of the stations in those regions. Namely, even if individual stations are not examined, it is expected that region anomalies give an idea of the general decadal behavior in the regions.

In the first half of the 1960s, the positive anomalies attract the attention. There are pretty high positive anomalies in MED, CEAN and CMED. The positive anomalies

rising up to 40% higher than the baseline are encountered in CMED during this period. Moreover, in the CMED region, the region anomalies are always positive except for the first half of the 1970s. Similarly, MED faces with higher quantile perturbations much more than lower quantile perturbations in summer months. Especially at the early 1960s, early 1990s and the end of the 2000s, an increase of about 20% is observed in the region anomalies of MED. For the time slot of this study, region anomalies of the MED are observed to be below the baseline for only a few times. This condition indicates that at least some of the 19 stations in the MED meet the positive anomalies almost every year. In the light of this information, it can be concluded that the MED region may be prone to flooding in the summer months. Unlike the MED, MRT has negative anomalies beginning from the second half of the 1960s to the mid-1990s. Yet, the region anomalies of MRT are positive after the mid-1990s until the present time-slot. Besides, higher quantile perturbations are noticed in all of the remaining regions except for the region anomalies of CCAN and CEAN which are around the baseline. The lowest extreme rainfall during the summer months occurs in the second half of the 1990s. The rate of CEAN's region anomaly drops below 80% of the baseline level at this time period. If the median of the region anomalies is examined (Figure 4.4), it can be seen that higher quantile perturbations cover nearly fifty year time period. Especially in the early 1960s and in the end of the 2000s, the level of the higher quantile perturbations is very high. In parallel with the outcome of the MED region, it can be concluded that there may be a fragility against flood events in summer not only in MED but also throughout Turkey. Furthermore, the propagation area, which is the area between minimum and maximum region anomaly, reaches the largest value in summer.

Based on the results, in the 1960s, high-level of positive anomalies take place in winter, summer and spring all over Turkey. Especially in the first half of the 1960s, higher anomalies are observed compared to the second half. Likewise, in the second half of the 2000s, the high-level of positive anomalies are observed in winter, summer and autumn. According to QPM results, these two-time period are unique in covering three different seasons with such highly positive anomaly values. If the QPM results are compared with the number of flood events (Figure 4.5) that

occurred (MGM, 2010), it can be seen that an overlap between QPM results and the occurred flood number exists. In accordance with the records, approximately 140 flood events occurred throughout Turkey in 1963 and 2008. Additionally, in 2009, 160 flood events happened. These three years are detected by QPM to cover the largest flood numbers for the time period of this study. Again according to the QPM results, the extreme precipitation amounts, reach very high values during these years, which is accepted as one of the most important factors that causes flood. Besides, it is determined that the number of flood events per year all along 1960s and in the second part of the 2000s are generally above the long-term yearly flood number average, although they are not in considerable amounts. In addition, based on QPM the high-level of the negative anomalies is at the early 1990s in winter, which is the climatic season with highest rain in Turkey. Correspondingly, the MGM records show that flood number that occurred is below the long-term yearly value in the years between 1989 and 1998. Further, in 1970, which experienced least floods in the time period of this study, the median of the region anomalies are negative for all of the climatic seasons.

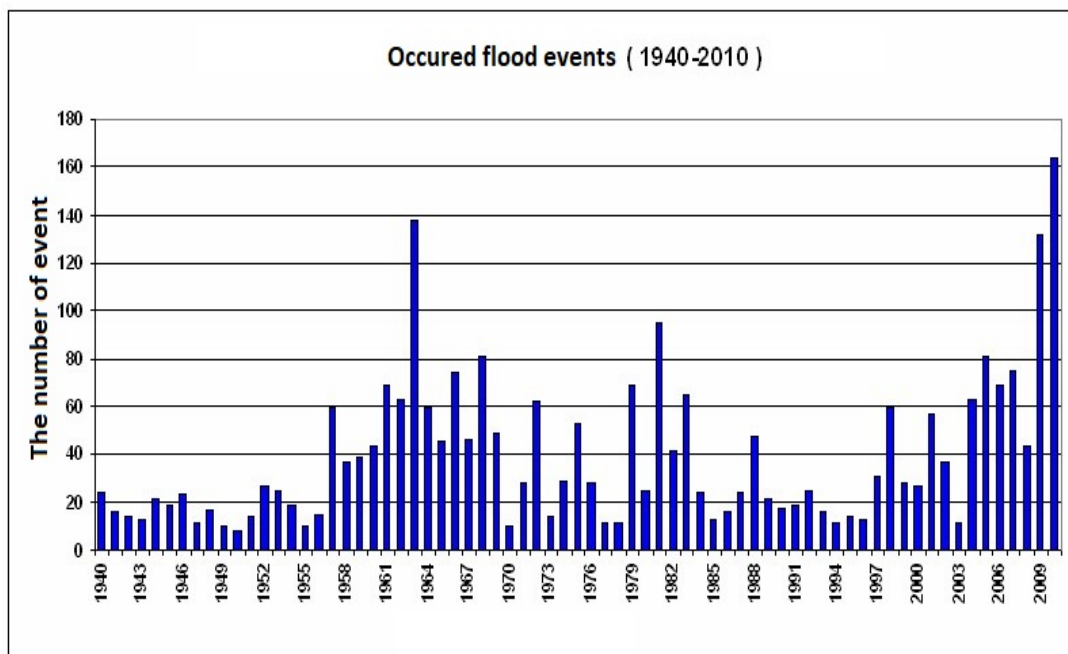


Figure 4.5 The number of floods occurred in Turkey between 1940 and 2010 (Retrieved from <https://www.mgm.gov.tr/arastirma/dogal-afetler.aspx?s=taskinlar>)

4.2.2 Black Sea Region (BLS)

4.2.2.1 Autumn

At the beginning of the 1960s, lower perturbation tendency is observed in daily precipitation extremes at 7 out of 8 stations. Significant negative anomalies are detected in Zonguldak, Sinop and Sakarya stations for this period. In general, slightly positive and negative deviations are observed in the late 1960s except for Samsun and Bolu. There are significant positive anomalies at Samsun station while the same period the city of Samsun faced damaging flood in 1967 (T.C. Orman ve Su İşleri Bakanligi, 2015). This flood may be a consequence of the significant positive anomalies. Even though they are not statistically significant, positive anomalies, which are very close to the upper limit of confidence interval, are specified at Bolu station. The 1970s were generally dry during autumn season. Significant lower quantile perturbations in precipitation extremes are found at İnebolu, Sinop, Rize and Giresun stations. Unlike 1970s, the 1980s can be regarded as a transitional period for the alteration from negative anomalies to positive anomalies. An example is the change of the precipitation extremes during 1980s and early 1990s from significant negative to positive anomalies in Zonguldak, İnebolu, Sinop and Rize (Figure 4.6). As for the 1990s, the negative and positive anomalies that are not significant with respect to Monte Carlo Confidence Interval, are both recognized. The direction of the anomalies for stations show differences from each other for this time slot. When arriving to the 2000s, it is seen that BLS region continues to show difference in terms of the direction of anomalies. While Sinop, Giresun and Rize stations were wet with significant positive anomalies, Samsun, Sakarya and Bolu were dry with negative anomalies in respect to precipitation extremes.

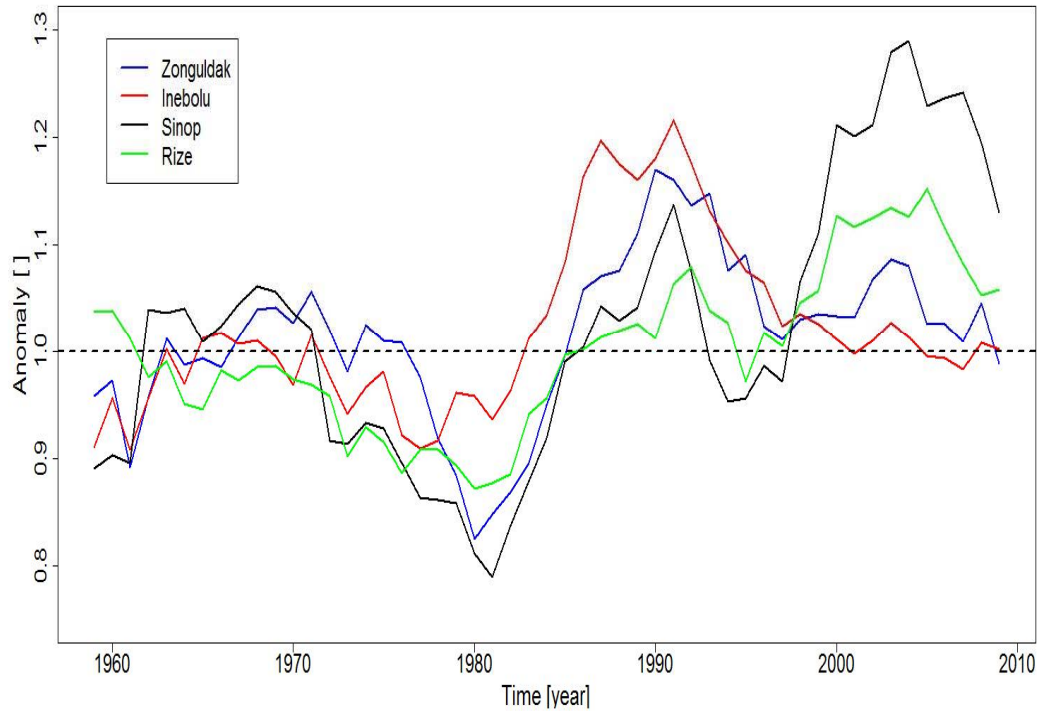


Figure 4.6 Decadal precipitation variation of the declared stations for the autumn season

4.2.2.2 Winter

The action of winter extreme precipitation can be regarded as generally similar for the decadal periods since the BLS is the region that receives the highest winter rainfall in Turkey. However, Sakarya and Bolu are excluded from this generalization. Decadal winter extreme precipitation behaviors of these stations are in agreement with MRT further than BLS at some decadal time periods. Accordingly, the drivers that control the extreme precipitation in MRT most probably have a higher impact on anomaly movement of Sakarya and Bolu. The comparative graphs of these cities with the Kireçburnu and İnebolu stations are shown in Figure 4.7. These stations are examples of general anomaly behavior of MRT and BLS, respectively. In addition, the least variability among all stations is observed at Rize station. Based on our data, Rize is the wettest precipitation area in Turkey. This can be related to the lower variability of precipitation in humid areas (

Tabari and Willems, 2016). In the 1960s, all stations except Bolu and Sakarya were wet in terms of extreme precipitation. Statistically significant high perturbations are detected especially in Sinop, Samsun and Giresun stations. These results also intersect with the flood event in Samsun reported by the OSIB in the winter of 1966. (T.C. Orman ve Su İşleri Bakanligi, 2015). Contrary to 1960s, lower quantile perturbations are seen over 6 of 8 stations in the 1970s. There are significant negative anomalies at Sinop and Rize stations. Apart from these 6 stations, significant positive anomalies are determined in Sakarya and Bolu for the 1970s. The most variable behavior of the extreme precipitations for stations are seen for the 1980s. However, most of the stations indicate higher quantile perturbations for the data provided from the beginning of 1980s and all stations demonstrate lower quantile perturbations towards the end of the 1980s. Similarly, all stations except Rize show significant low anomalies for the 1990s. Moreover, decreases of up to 25% are explored at Samsun and Giresun. Finally, although they are not statistically significant, the leaning of positive perturbation in extreme precipitation for the 2000s are examined at all stations.

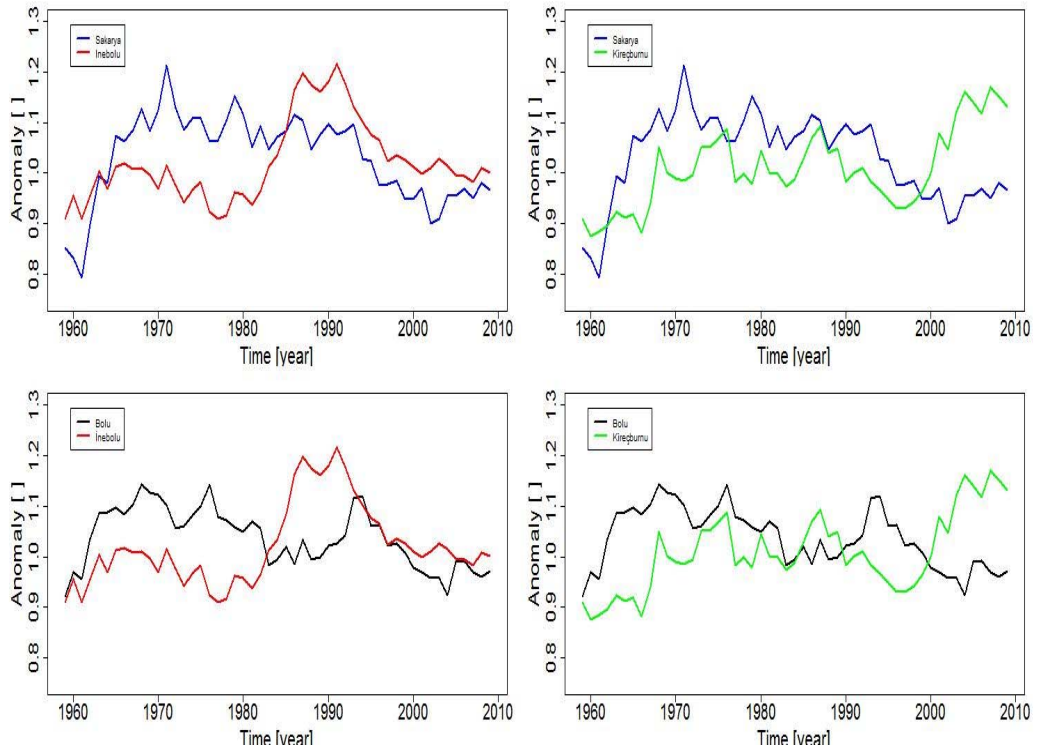


Figure 4.7 The comparison of the winter anomalies of Sakarya and Bolu with İnebolu and Kireçburnu

4.2.2.3 Spring

The spring season has more deviations from baseline than autumn and winter season in BLS since this season takes relatively less precipitation than others. In the 1960s, significant higher quantile perturbations occur in BLS with six stations. Particularly, the deviations up to 25% take place in Rize. The decline in the amount of anomalies starting from the beginning of 1970s result in the change of anomalies to negative perturbations for the 1980s. However, the significant positive anomalies at Samsun station in the early 1970s is in accordance with the flood event that lead to 831.025\$ financial damage in Samsun in spring, 1971 (T.C. Orman ve Su İşleri Bakanlığı, 2015). The lower tendency in 1980s continues until the mid-1990s. Zonguldak, İnebolu, Samsun and Bolu stations show approximately the same extreme precipitation behavior with negative anomalies during this period. After mid-1990s,

there are rising positive tendencies in the spring anomalies and significant higher perturbations are observed at Sinop and İnebolu stations in the end of the 2000s. Besides, the anomalies that are very close to the upper limit of confidence interval are caught in Samsun. In parallel with this situation, two big flood events appeared in Samsun on 27.05.2005 according to OSIB reports and the total cost of these flood events were approximately 2.127.008 \$ (T.C. Orman ve Su İşleri Bakanligi, 2015).

4.2.3 Continental Central Anatolia (CCAN)

4.2.3.1 Autumn

The variations for autumn extreme anomalies are quite high, especially in Kayseri, for CCAN region. The 1960s are wet with 8 stations having significant positive anomalies. Although most of the stations demonstrate very similar movement to the baseline, it is encountered with significant negative anomalies in Çorum, Kayseri, Niğde and Sivas during 1970s. Analogous with 1960s, the 1980s are also wet with 6 stations showing higher quantile perturbations. There are differences in the anomalies of the stations of CCAN in the 1990s. While Kayseri and Çankırı have significant positive anomalies, Kırşehir, Afyon and Konya have statistically significant negative anomalies with respect to the Monte Carlo Confidence Interval results. The significant higher quantile perturbations are dominant in the 2000s. The anomalies are significantly positive at 8 stations during that decadal period.

4.2.3.2 Winter

Analysis of winter anomalies of CCAN show that, negative anomalies are mostly observed at the stations Çorum, Sivas and Kayseri for the 1960s. In Kayseri, the negative anomalies exceed the lower limit of confidence interval down to 30%. In fact, Kayseri is one of the stations with highest negative/positive perturbations from the baseline for decades (Figure 4.8). The positive anomalies are prevalent for the

remaining seven stations during the same time interval. Moreover, it is probable that the flood event occurred on 03.12.1968 in Ankara and caused the death of seven people (SU PEK Proje ve Müşavirlik A.Ş., 2016) is originated by the given positive anomalies. Similarly, another flood event is noted in Yozgat, where the significant positive anomalies are identified by QPM for this station, in 1966 (T.C. Orman ve Su İşleri Bakanlığı, 2015). The anomalies of six of the eleven stations are below the baseline in the early 1970s, notably Kayseri and Niğde. If Sivas and Kayseri are excluded, the region draws a declining figure along 1980s. It is dry with nine stations that have negative anomalies, most of which are significant, in the early 1990s. In addition, the region has maintained its tendency to decrease in extreme precipitation during the 1990s. In this decadal period, significant lower quantile perturbations are seen in eight of the eleven stations. However, movement of Kayseri station is different from the general behavior. It has significant higher quantile perturbations along 1990s as well as along 2000s. Yet, not only Kayseri but also all stations show increasing inclination in the anomalies in the 2000s. Besides, there are significant positive anomalies at four stations for the following time period.

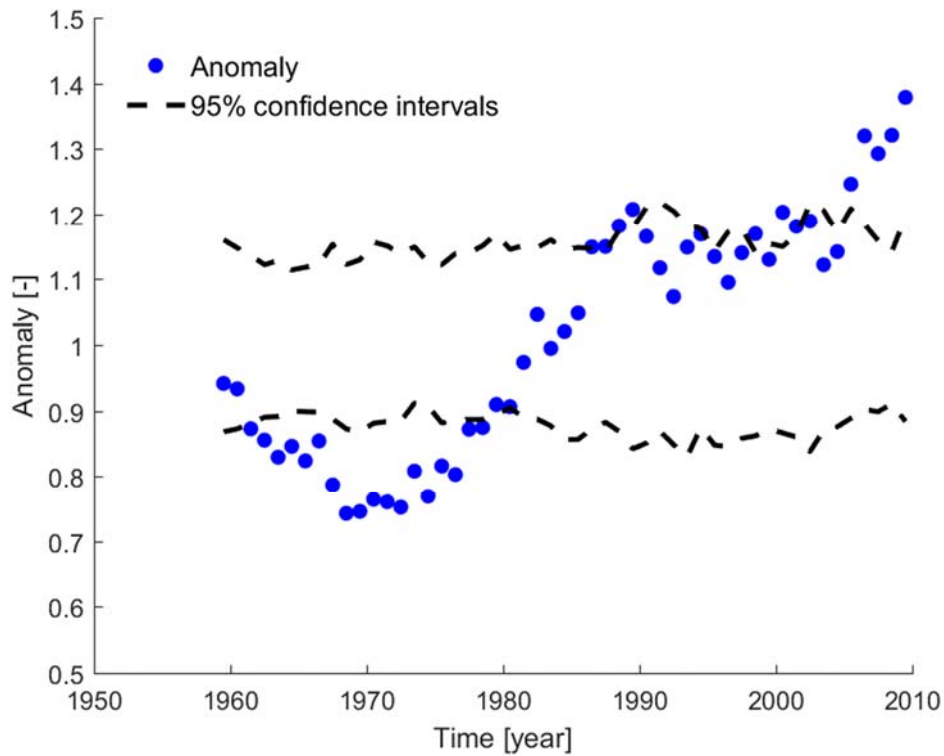


Figure 4.8 Decadal extreme precipitation fluctuation of Kayseri

4.2.3.3 Spring

A common movement is not observed for all stations in the spring extremes for 1960s. Çorum, Sivas, Yozgat and Kayseri show significant negative anomalies. Despite that, significant positive anomalies are revealed in Afyon, Niğde and Kırşehir. Similar to 1960s, differences are studied in the anomaly values for different stations in the 1970s. However, the anomalies aren't generally significant according to Monte Carlo Confidence Intervals. There are significant negative and positive anomalies only in Çankırı and Konya respectively. The prevailing behavior has lower tendency in the 1980s. Furthermore, the negative anomaly that is 25% lower than baseline is discovered for Afyon station. In general, most of the stations have positive anomalies in the 1990s and 2000s. In 1990s, 9 of the 12 stations show

positive anomalies and 6 of these 9 stations show significant positive anomalies. In the 2000s, higher quantile perturbations persist. Like the 1990s, 9 of the 12 stations exhibit positive anomalies. Nonetheless, there are distinctly significant negative anomalies at Kırşehir and Konya stations. Also, it is important to mention that in Sivas, one of the stations, which has the positive anomalies in the early 2000s, the harmful flood event is recorded by OISB in 2001 (T.C. Orman ve Su İşleri Bakanlığı, 2015).

4.2.4 Continental Eastern Anatolia (CEAN)

4.2.4.1 Autumn

The CEAN region is one of the most mountainous areas in Turkey. It is worthwhile to note that this mountainous terrain prevents the damp wind coming from the Black Sea to reach the region. Consequently, it receives very little rainfall compared to BLS. According to our data, while the annual average precipitation of Rize is 2250 mm, the areas such as Erzurum or Erzincan, which are not very far from Rize, receive rainfall between 380mm and 400mm on average per year. When focused on 1960s, higher quantile perturbations are specified for all stations. Specially, significant higher quantile perturbations are found in the early 1960s for Ağrı and Iğdır. Though the 1970s differ from station to station in terms of showing slightly high or low tendency from the baseline for autumn extreme anomalies, Erzurum displays positive anomalies at the end of the 1970s and including the early 1980s. The rest of the 1980s were generally dry at three stations that are Artvin, Ağrı and Van. In contrast to 1980s, five stations demonstrate higher quantile perturbations, 3 of which are statistically significant in the 1990s. Yet only Erzurum is dry with very low extreme anomalies from the baseline along that period. Lastly, all the stations, except for Artvin, indicate lower perturbations in the 2000s.

4.2.4.2 Winter

In winter, the higher perturbations are noticed for 4 of 6 stations in the 1960s. There are very high and significant perturbations at Iğdir station in the early 1960s. During the same period, significant negative anomalies are observed in Artvin. The 1970s are commonly dry. Opposite to 1960s, four of the six stations display lower quantile perturbations. All of the stations include positive anomalies in the 1980s. Moreover, Artvin, Ağrı and Erzurum outpace the upper limit of the confidence interval. When the anomalies of 1990s are analyzed, it is understood that all of the stations exhibit lower fluctuations from baseline except Artvin. Almost all of the negative anomaly values are significant for Erzurum during this decade. Similar to the 1990s, the downward movement remains in the winter anomalies of the 2000s. Exclusively, Erzurum, Ağrı, Iğdir and Artvin have a visible decrease in their winter anomalies. Only in Van, the positive anomalies arise towards the 2010s. Herein, it is essential to state that when examining the anomalies of the CEAN region, it may be necessary to evaluate Artvin separately from the others. In general, the winter extremes of Artvin show different fluctuations from the rest of the CEAN region. This can be related to the fact that Artvin is much closer to the seaside than the other stations. Consequently, the amount of total rainfall of Artvin is almost equal to a few stations in the BLS area. To further explain this, the mean and the median of average annual precipitation of the stations in BLS and CEAN (excluding Artvin) are compared with each other and average annual precipitation of Artvin (Figure 4.9). It is seen that Artvin shows up as a transition area between these two rainfall regions in terms of rainfall amount. The median of the stations is also compared since the annual rainfall amount at Rize station is even higher than other stations in the BLS, where the average annual rainfall is very high. If Figure 4.9 is carefully examined, the CEAN's mean and median values are almost identical, whereas the mean value in BLS is distinguishably higher than the median value.

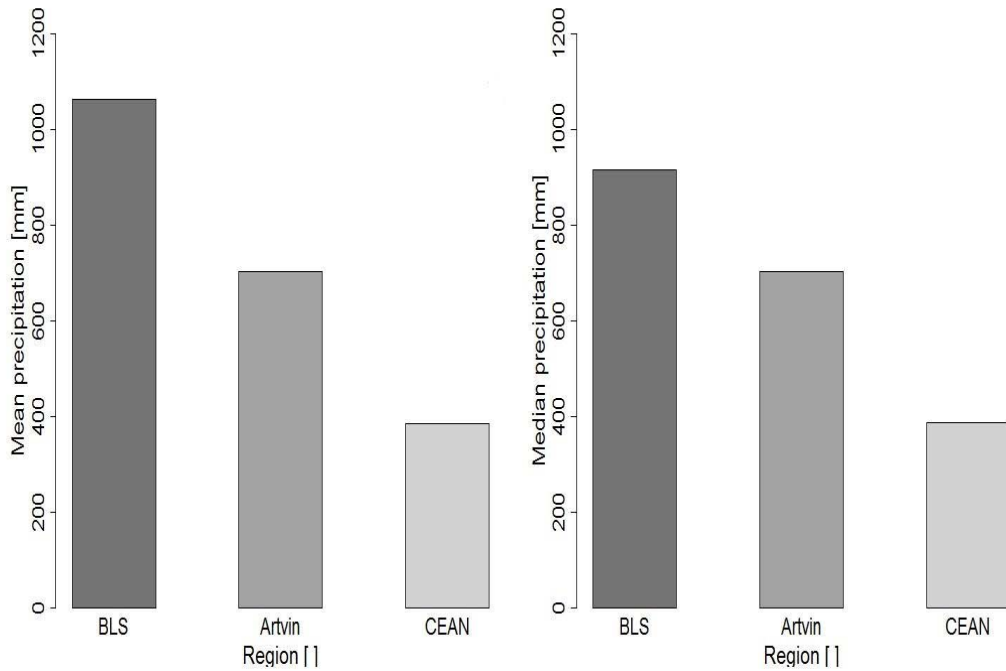


Figure 4.9 Comparison of the mean and the median of long-term average annual precipitation of the stations in BLS and CEAN with Artvin

4.2.4.3 Spring

All the six stations exhibit positive anomalies at the early 1960s for the spring season, whereas negative anomalies towards the late 1960s. Anomaly values are mostly negative during 1970s. Furthermore, there are significant negative anomalies at Erzurum, Erzincan and Ağrı. Apart from other stations, significant higher quantile perturbations are caught at Artvin in the 1980s. The remaining stations also have higher perturbation leaning but none of them represent statistically significant perturbations. In the 1990s, whereas most of the stations move identical to the baseline, the significant positive perturbations in Erzincan and the significant negative perturbations in Erzurum are identified. The significant negative anomalies at 1990s in Erzurum change place with the significant positive anomalies in the 2000s. Likewise, Ağrı station has the significant positive anomalies for the same time span.

4.2.5 Continental Mediterranean (CMED)

4.2.5.1 Autumn

The majority of stations in CMED region illustrate analogous extreme precipitation variability over decadal periods. Overall, the positive anomalies are observed over CMED region for 1960s considering autumn season and significant positive anomalies at Malatya and Elazığ stations are observed as well. Unlike the 1960s, all of the stations were dry with lower quantile perturbations all along 1970s. Also, the significant lower perturbations take place in the stations: Ceylanpınar, Mardin, Şanlıurfa, Gaziantep and Malatya. The 1980s exhibit high oscillation positive anomalies for all stations. Further, it is encountered with the positive significant anomalies at 4 stations. It can be claimed that 1990-2000 is a conversion period for anomalies altering from the positive perturbations to negative perturbations. In conjunction with the former statement, the negative anomalies are broadly seen at the beginning of the 2000s apart from Ceylanpınar and Gaziantep. Lastly, the positive anomalies are examined at the early 2010s.

4.2.5.2 Winter

In the 1960s, high fluctuations in anomalies are determined. The significant fluctuations are found to be leading at Şanlıurfa and Ceylanpınar stations. When arriving to 1970s, it is understood that the situation is conflicting with the 1960s. The 1970s are usually dry with four stations facing significant lower quantile perturbations. As reported with QPM, the 1980s is a changeover period for anomalies transferring from the negative phase to the positive phase. After the changeover period, the 1990s indicate widely the positive anomalies. Furthermore, there are significant positive anomalies in Gaziantep. Even though the station movements alter from station to station in terms of anomaly in the 2000s, low oscillations are detected in 4 stations. Again for this time slot, the significant positive

anomalies appear at Gaziantep station while the significant negative anomalies appear at Şanlıurfa, Mardin, and Ceylanpınar stations.

4.2.5.3 Spring

The 1960s were wet in terms of extreme precipitation in CMED for spring season like autumn and winter seasons. Six stations showed positive anomalies. The oscillation anomalies keep getting higher for the region over the 1970s. 5 stations possess the significant positive anomalies. Still, there are significant negative anomalies in Siirt. Higher oscillations of the anomalies decrease all along the 1980s and when coming to the early 1990s, the lower quantile perturbations take place. After a decade, the lower quantile perturbations turn into higher quantile perturbations. However, quite significant decrease of the anomaly amounts is determined at late 2000s. CMED has the greatest decrease by percentage on the subject of spring anomaly values at the end of the 2000s.

In Figure 4.10, the area between the maximum and the minimum anomaly values for each year at the stations of CMED region can be examined. As noted before, in summer when the rainfall amount is minimum in CMED, the stations exhibit more variable anomaly values with respect to each other. Concordantly, the least variability shows up in winter. Moreover, Ceylanpınar station, which has very low average annual precipitation rate (282mm), constitutes a large part of the maximum and / or minimum anomaly boundaries.

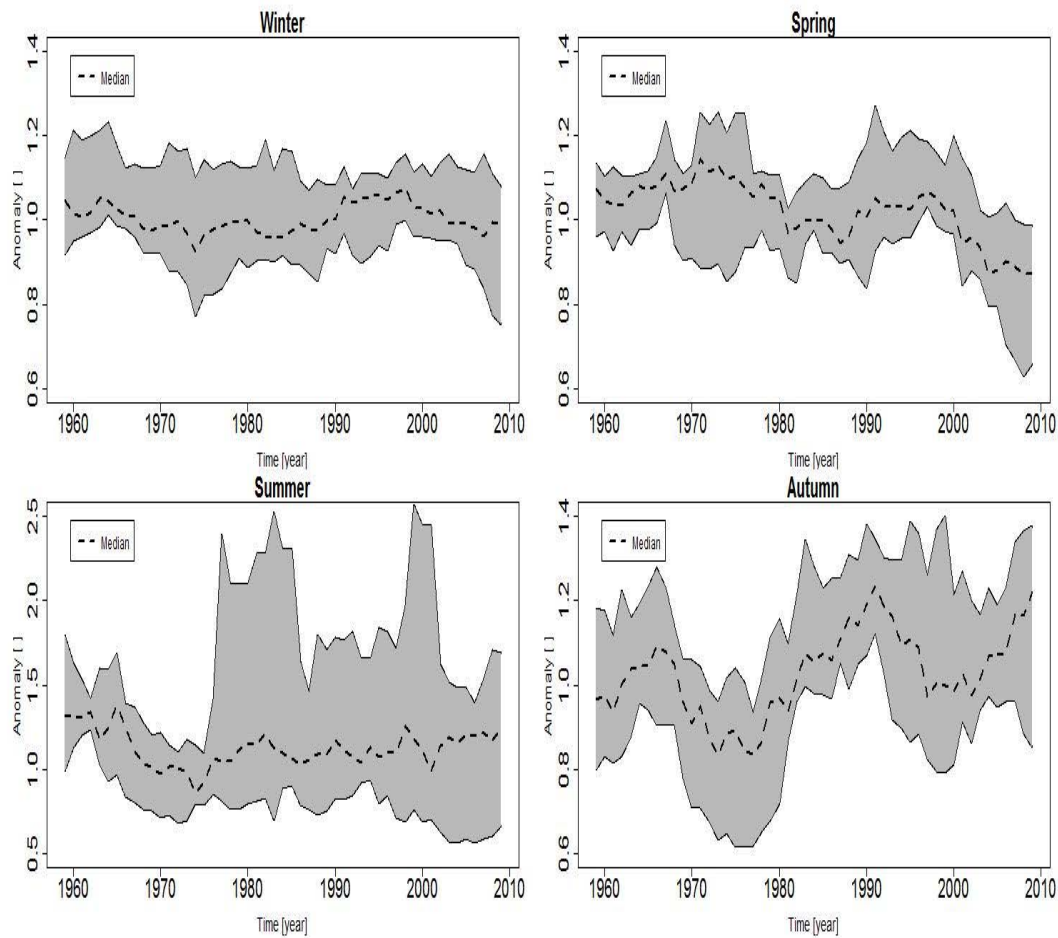


Figure 4.10 The Areas of the anomaly variability in the CMED stations with respect to all seasons

4.2.6 Mediterranean (MED)

4.2.6.1 Autumn

To begin with, the fluctuations of extreme precipitation anomalies in the fall season for the MED region, which receives a lot of precipitation in winter, is very high. For the 1960s, taking 19 stations into account, the lower quantile perturbations are confirmed to be similar. There are 12 stations with significant negative anomalies in the MED zone at the 1960s. In contrary with 1960s, the positive anomalies are

disclosed in the 1970s. Principally, statistically significant high perturbations are observed in geographically close and comparable regions such as İzmir, Denizli, Muğla and Fethiye. During 1980s and in the 1990s, anomaly attitudes vary from station to station. For instance, Aydın and Bodrum have negative anomalies whereas Adana, İskenderun, Dörtyol have positive anomalies for 1980s. Besides, even if the significant positive anomalies are detected at Dikili, Akhisar, Antalya and Adana, there are the significant lower oscillations in Denizli in the 1990s. In the 2000s, the significant positive anomalies are studied for 11 stations. Exclusively, the significant positive anomalies in Antalya may cause the flood occurred on 23.03.2002 (T.C. Orman ve Su İşleri Bakanlığı, 2016). In contrast with this, the significant negative anomalies show up in Mersin, Adana, İskenderun and Antakya.

4.2.6.2 Winter

The Monte Carlo Confidence interval affirms that the significant high oscillations locate in 6 of all stations in the 1960s. These significant high oscillations largely arise in the 1960s. Differently, the negative anomalies occupy 1970s with 11 stations. For example, 15% deterioration from the baseline is uncovered at Çanakkale station. In accordance with QPM results, it is not possible to allege that an associative movement exists for stations during the 1980s. The anomaly values ordinarily accumulate around the baseline. However, quantile perturbations are lower in the 1990s. 11 stations have significant negative anomaly during the decade. The larger part of those significant negative anomalies come to light in the early 1990s. Bandırma, Denizli, Bodrum and Anamur stations are among the 11 stations mentioned before. In the 2000s, the most notable positive anomalies are observed in Antalya. In addition, Antalya was exposed to two distinct floods during 2003 winter and five people died in one of these floods (T.C. Orman ve Su İşleri Bakanlığı, 2016).

4.2.6.3 Spring

Similar to the autumn anomalies, spring anomalies are also highly variable for the same reasons. Accordingly, negative anomalies are obtained for 1960s and 1970s and the reverse for 1980s and 1990s. The latter decades are generally wet with higher quantile perturbations. The anomalies of 2000s typically assemble around the baseline. At this point, there are also two stations which should be highlighted. The anomaly behaviors of Adana and Iskenderun are rather comparable with each other and compared with other stations, different trends are observed in their graphs. According to the QPM results, the 1960s contain significant higher perturbations for these two stations, but the stations have significant lower perturbations in the 1970s. Thus, their anomaly values remain around the baseline with a slight downward inclination.

As mentioned before, summers are hot and arid and winters are warm and rainy in the Mediterranean region. Consequently, comparing the variations of the median anomalies of all seasons, it can be understood that the highest variability in the median of anomalies with respect to years is found in summer and the lowest in winter. In addition, the variability of the median of autumn and spring anomaly stay at a value between summer and winter months (Figure 4.11).

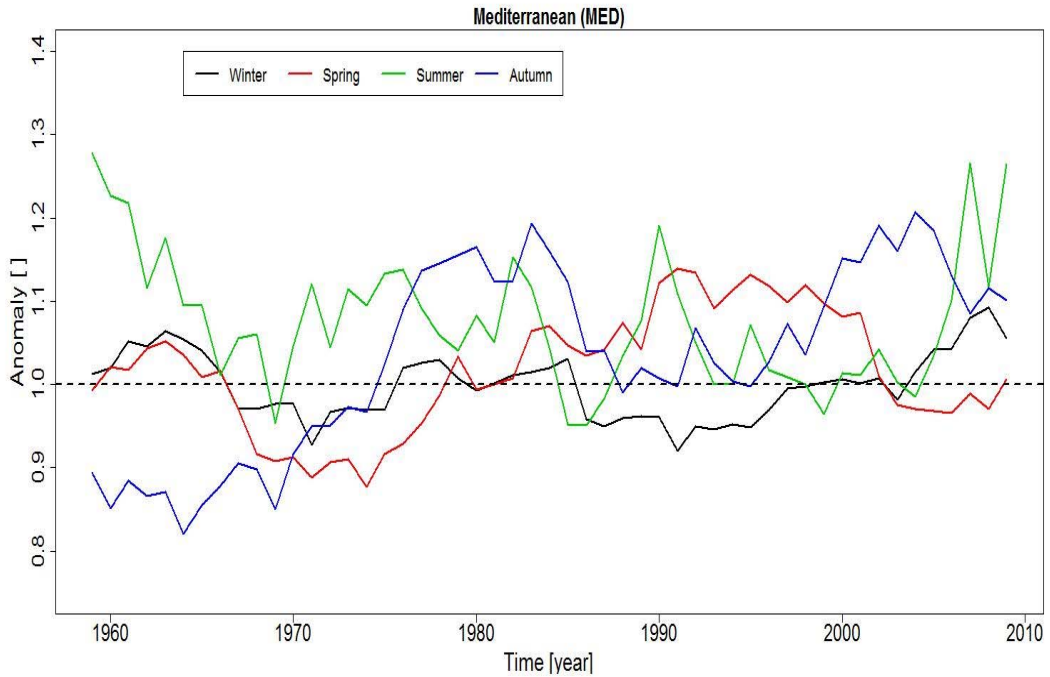


Figure 4.11 Comparison of the median anomalies in the Mediterranean with respect to seasons

4.2.7 Mediterranean Transition (MEDT)

4.2.7.1 Autumn

The low oscillation anomaly is recognized in the 1960s at 4 of the 4 stations. Moreover, the significant low oscillation anomalies are caught at Uşak, Burdur and Kütahya. When considering the 1970s, there are statistically significant positive anomalies at Uşak and Kütahya. The other two stations: Isparta and Burdur are different than the other two. Their anomaly values are below the baseline still not below the lower limit of the confidence interval. The low oscillation anomaly attracts the attention in the 1980s at all stations except for Burdur. In the 1990s, Kütahya remains at its lower tendency but the others are identical to the baseline. The upward tendency, which begins at the end of the 1990s, causes high oscillation anomalies to appear in the 2000s. At the end of the 2000s, it is encountered with the significant

high oscillation anomalies. Specifically, very high positive perturbations are discovered in Isparta.

4.2.7.2 Winter

The positive anomalies exist in the 1960s at all stations and these positive anomalies are significant for the Kütahya and Isparta stations. Uşak resumes its high oscillation behavior along 1970s. Yet, the other stations demonstrate low oscillation anomalies. In the early 1980s, Kütahya and Usak show positive anomalies, while negative anomalies are observed in Burdur and Isparta. There are negative anomalies at all stations in the early 1990s. Also, the significant negative anomalies up to 30% are seen in Kütahya. The 1990s as well as the early 2000s are commonly dry except Burdur. Thereafter, anomalies increase in the positive direction towards the late 2000s. Moreover, there are anomaly values which are very close to upper limit of confidence interval in Uşak for this time interval. The decadal winter anomaly behavior of all stations in the MEDT region are shown in the Figure 4.12.

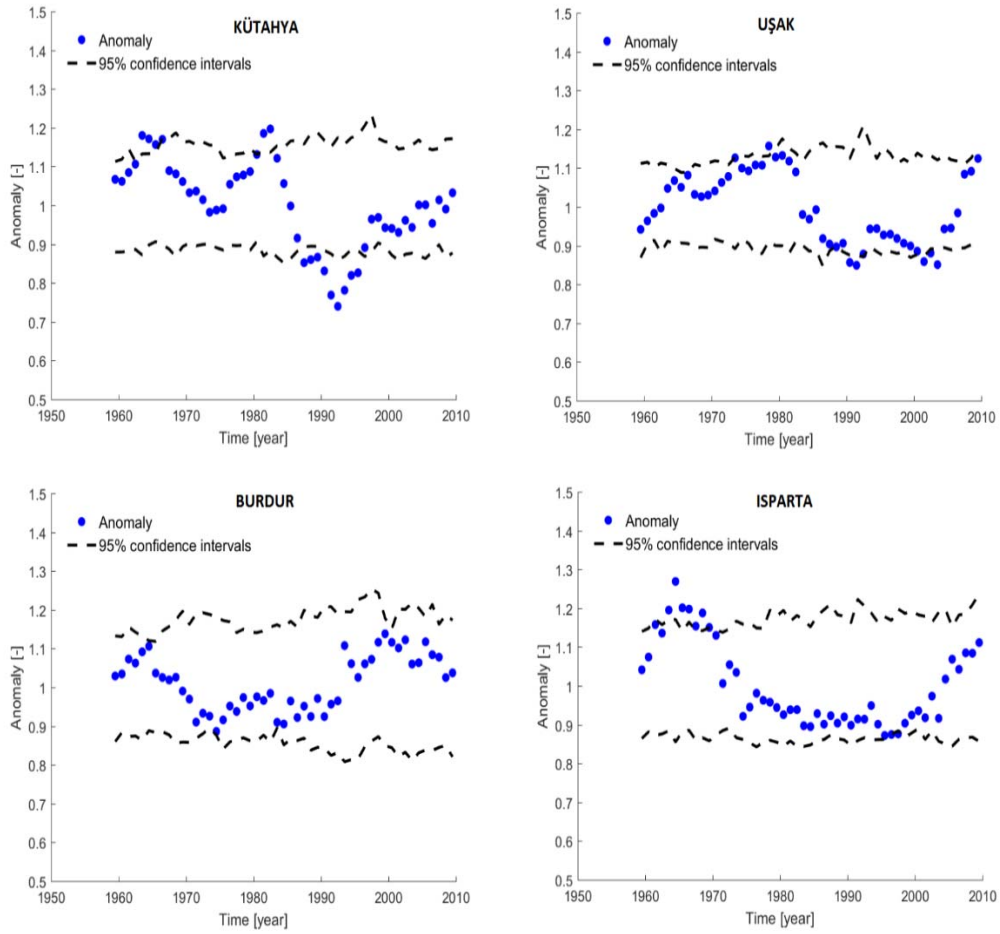


Figure 4.12 Decadal anomaly fluctuations of the stations in the MEDT region

4.2.7.3 Spring

The low oscillation of the anomalies is noticed only at Burdur station in the 1960s. Apart from this, other stations have high oscillation anomalies. Besides, there are statistically significant perturbations at Kütahya. The negative perturbations are defined at four of the four stations in the 1970s and 1980s. The 1990s are widely wet in terms of anomaly for three stations except Kütahya. Opposite to each other, the significant high perturbations take place in Uşak and the significant low perturbation are detected in Kütahya in early 1990s. Finally, the positive anomalies are disclosed in Uşak in the early 2000s. Nevertheless, the reduction is also discovered in the

amount of anomaly values towards the 2010s for this station. Lastly, Burdur has high and significant positive anomalies all along 2000s.

4.2.8 Marmara Transition (MRT)

4.2.8.1 Autumn

The 1960s are wet considering the anomalies for MRT. The negative anomalies are obtained at all 9 stations. Five station that are Bursa, Bilecik, Edirne, Tekirdağ, Florya have the significant negative anomalies. However, it is hard to comment on the anomaly action of the 1970s for the autumn season. Both the negative and the positive anomaly variations are analyzed. Great extend of the MRT region present high oscillation of anomalies in the 1980s. Furthermore, Bursa and Florya present high oscillation of anomalies. As the 1970s, stations don't have a common movement in the 1990s. The negative anomalies are discovered in Kumköy while the significant positive anomalies are observed in Edirne, Bursa, Bilecik and Florya. The negative anomalies take place at Kumköy and Kireçburnu stations in the 1990s but they have the positive anomalies in the 2000s along with Tekirdağ and Bursa. Also, negative anomalies are detected in Edirne and Florya in contrast with 1990s. The negative anomaly values are not significant at these stations but still they are very close to the lower limit of the confidence interval.

4.2.8.2 Winter

In the 1960s, 5 of 9 stations show positive anomalies while the remaining shows negative anomalies. Nevertheless, a common movement of the anomalies in the 1970s is observed. The lower quantile perturbations cover the 7 stations. In addition to that, there are approximately 20% lower perturbations in Edirne. However, the higher perturbations that begin in the second half of the 1970s cause significant positive anomalies to exist until the end of the first half of the 1980s. This is

principally valid for the Kireçburnu and Kumköy stations. In the late 1980s and early 1990s, the negative anomalies are discovered in 8 of the 9 stations. The significant negative anomaly is found at least once at 7 of these 8 stations. There is an increasing motion in the anomalies at stations towards the end of the 90's after this era of lower perturbations. distinct from the other stations, the significant negative anomalies occupy almost whole decade for Bursa. In the 2000s, all of the stations have either positive anomalies or the anomalies slightly above and/or below the baseline. The significant positive anomalies take part in the stations: Edirne, Tekirdağ, Kireçburnu and Bursa.

4.2.8.3 Spring

The lower quantile perturbations are seen in 8 out of the 9 stations in the 1960s. Only in Bilecik, even though it is not significant, higher quantile perturbations are detected. Low perturbation anomalies are spotted in the 1970s, unless Edirne is considered. The low trend does not seem significant, but it is very close to the lower limit of the confidence interval. In contrast, Edirne shows significant high perturbation for this period. Moreover, negative anomalies are still detected in the 1980s. For this region, unlike all other regions, we can refer to a period of the lower perturbation of 30 years, covering between the years 1960 and 1990 in the spring anomaly precipitation. Nevertheless, when it comes to the 1990s, the positive anomalies take place. Especially for the early 2000s, very high positive anomalies occur. After that period, recurrence of the negative anomaly domination is noted.

4.3 Analyses of decadal precipitation anomaly in the low extremes

In this part of the study, decadal low anomaly oscillations of the regions is are recorded. Similar to the region anomalies of high extremes, the region anomalies of low extremes are also calculated by taking the median of the anomalies at the stations that are in those regions. It is crucial to emphasize that low extreme

anomalies with respect to seasons are obtained by using QPM data based on annual dry day number of these seasons. During the decision of the amount of dry days in a climatic season, the days which receive precipitation less than 0.3 mm, are accepted as dry day. In addition, interpretations of low extreme results for different seasons are performed on the grounds of Figure 4.13.

4.3.1.1 Autumn

In the years between 1960 and 1980 positive anomalies in dry days are dominant in every region. The relatively higher positive anomalies are perceived in BLS through 1960s as well as in BLS and MRT through 1970s. The decreasing trend in dry day number is common for all rainfall regions in the 1980s. The negative anomalies are determined in CMED, CCAN, CEAN during this period. In the 20-year period among 1990s and 2010, the rainfall regions usually have a dry day number around baseline. The dry day number is slightly higher than the baseline in the mid-1990s whereas it is slightly lower than the baseline in the mid-2000s. On the contrary, CMED region has the positive anomalies during this 20-year era.

4.3.1.2 Winter

Along the 1960s a decline in regard to baseline is found in the amount of dry days. There is an increase between 5%-10% in wet day number especially in CCAN, MED, MEDT and MRT during this period. Also, in the former chapters, the tendency to increase is generally detected in the high extreme precipitation anomalies throughout Turkey. In parallel with this situation, the wet day number seems to rise during this same period. Nevertheless, the 1970s are drier than 1960s according to QPM results. The highest decrease in wet day number is determined in MRT. Similarly, in the 1970s, the negative high extreme anomalies are reached in the MRT. A different behavior can be mentioned in CMED. In the second half

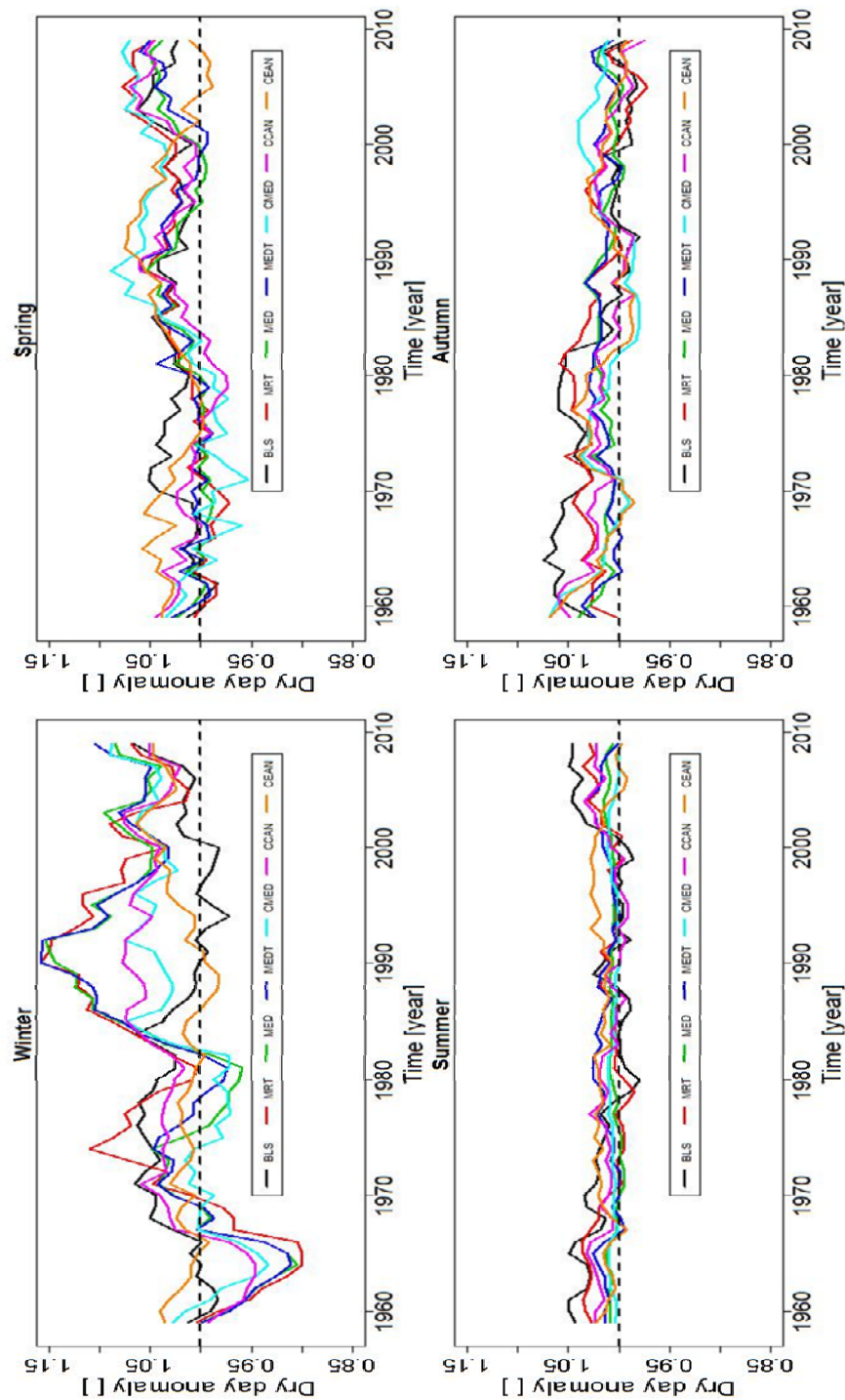


Figure 4.13 Decadal low extreme oscillations of the regions with respect to seasons

of 1970s, there is a decrease in high extreme precipitation amount despite the increase in the number of rainy days in this region. However, both of these situations do not appear to be significant because they are only 2-3% different from the baseline. The uprising in the dry day number starting from early 1980s reaches to

very high levels in the early 1990s in all regions excluding BLS and CEAN. Dry day numbers that are 15% higher than the baseline are encountered in MED, MEDT and MRT. This situation also coincides with decreasing high extreme precipitation anomaly behavior in most of the regions. Yet, after this time-slot, a very critical circumstance comes into light. The high extreme precipitation amounts, which increase after the early 1990s, turn into the positive anomalies in the second half of the 2000s. Although the high extreme precipitation amount increases in the 5 of 7 regions, the number of dry days also increase for all regions in the second half of 2000s. To investigate this situation, the correlation between high extreme precipitation and dry day numbers of different regions are shown in Table 4.1 with respect to different time intervals. In the regions except CMED, the extent of positive correlation based on the data between the periods of 1992-2009 increases compared to the correlation in the period of 1959-1992. The most remarkable increment is seen in the MEDT region. The correlation between high extreme precipitation and dry day number in MEDT is -0.948 between the years 1959 and 1992. However, it becomes 0.235 in the period of 1992-2009. In other words, while the inverse correlation is almost perfect for these two variables between 1959 and 1992, the high extreme precipitation amount increases as the number of dry day increases after 1992. Another significant change in correlation coefficient is observed in CEAN. The correlation coefficient, which is -0.251 at the first period, alters to 0.266 at the second period. Another region that encounters a high change in correlation is MED. The correlation evolves into -0.811 from -0.284. Remarkably, even if the correlation in the second period is negative, there is obviously tendency towards positive relation. Albeit the data length of the second half of 2000s is not enough to define a reasonable correlation, by analyzing the winter parts of and Figure 4.13 the positive relationship between the number of dry day and the high extreme precipitation amount can be understood. In addition to this, Figure 4.2 (A) indicates that the total precipitation of the rainfall regions do not have a meaningful decrease except for CMED. The total precipitation of other regions are about their long-term mean level. So, assuming that there is no meaningful change in the total precipitation amount of these six regions, proves that approximately same amount of precipitation starts to

fall into ground in less days than before as both the high extreme precipitation amount and dry day number rise. In other words, the number of the showers, which may cause floods, raise. The climb of occurred flood events towards the end of the 2000s (Figure 4.5) accompanies the possible consequence. Moreover, the overlap of relationship between high extreme precipitation and the dry day number carries on growing in an unprecedented manner in the recent period. In fact, the increase in the percentages of the extreme precipitation against total precipitation has been noted previously (Yucel and Onen, 2013). Unless realistic solutions to reduce anthropogenic sources that impair the balance of precipitation behavior are found, it is inevitable that amount of flood events increase.

Table 4.1 Correlation between decadal high extreme precipitation anomalies and decadal dry day number anomalies

Region	Spearman's Rank Order Correlation		
	1959-1992	1992-2009	1959-2009
BLS	0.127	0.705	0.197
CCAN	-0.639	-0.525	-0.530
CEAN	-0.251	0.266	-0.493
CMED	0.128	-0.226	0.153
MED	-0.811	-0.284	-0.547
MEDT	-0.948	0.235	-0.784
MRT	-0.562	-0.314	-0.378

4.3.1.3 Spring

The higher perturbation anomalies in the dry day number at the early 1960s decrease towards the 1970s at the 6 of the 7 rainfall regions excluding CEAN. At CEAN, the dry day number is higher than the baseline in the early 1970s. Actually, it can be said that the dry day number of CEAN in spring is frequently higher than the baseline all through the study period. Particularly, the increase of the dry day number reaches to roughly 6-7% higher than baseline condition in the early 1990s for this region. In

fact, it is common for all rainfall regions in the early 1990s. This condition is quite analogous to the dry day number behavior of the early 1990s in winter. It can be understood that the early 1990s is quite dry in Turkey considering the decrease in the extreme rainfall amount of the winter, the increase in spring and winter dry day numbers and the decrease in total rainfall amount. Specifically in the MED, MEDT and MRT regions which include 32 stations, the drought reaches very high levels. Meanwhile, for low extremes of spring, it is noticed that CMED and CCAN exhibit parallel dry day anomaly behavior during this season. In these two regions, negative anomalies are detected in the dry day number from the second half of the 1960s to the end of the first half of the 1980s. After that point, positive anomalies prevail these regions until 2010s. It can be stated that the dry day anomaly behaviors in the second half of the 2000s are similar to winter dry day anomaly behavior. Like winter, a rise in the dry day numbers is discovered in the regions excluding CEAN. On the other hand, unlike winter, there is no extraordinary rise in the high extreme precipitation amount of spring.

4.3.1.4 Summer

The number of rainy days varies from season to season in Turkey. This variation can be understood by examining Table 4.2, which shows the average number of dry days and the average standard deviation of the dry day numbers based on 65 stations for a 60-year period. This table displays that the climatic season with the uppermost average number of rainy days in Turkey is obviously winter. Thus, the excessive perturbations in winter dry day number may give rise to drought events. In addition to this, the season with the uppermost average standard deviation is also winter. In parallel, Figure 4.13 indicates that the higher oscillations in dry day number occurs in winter season. Beside, Table 4.2 demonstrates that the season with highest average dry day number belongs to summer. The average dry day number is 82.06 in this season. In other words, an average of 10 days are wet during summer period in Turkey. Moreover, the lowest standard deviation 3.94, is detected for summer. Therefore, it is expected to have lower decadal oscillations of summer dry day

number. The QPM results showed in Figure 4.13 verifies this statement. For most of the regions, the decadal oscillations of dry day number in summer are small enough to be neglected. Analogous to other QPM analyses, the dry day number behaviors in the early 1960s and the second half of 2000s are similar to each other. The highest positive anomalies are found in these two periods. The positive anomalies reach up to 5% higher than the baseline in BLS and 3% higher than the baseline in MRT. The rainiest region of Turkey, BLS, does not receive precipitation for an average of 70.35 days in summer. 5% increase of dry day number in BLS corresponds to 3.5 days. Accordingly, there is an increase of 3.5 days in the average dry day number of BLS when the most extreme conditions of the 60-year working period arise. This proves that the change of the dry number in summer months are not so effective on generating water scarcity. As shown in section 4.2.1.4, it is more reasonable to focus on the decadal high extreme precipitation oscillations in order to take precautions for potential floods in summer rather than to focus on the decadal dry day number oscillations that may cause drought. Lastly, it can be noted that in general, the higher quantile perturbations are identified in summer months for all regions. Exceptionally, the lower quantile perturbations are defined in the early 1980s at BLS and MRT and in the early 2000s at BLS.

Table 4.2 Average dry day numbers and average standard deviations of the stations according to seasons

	Average dry day number	Average standard deviation
Autumn	71.93	5.31
Spring	63.73	6.60
Summer	82.06	3.94
Winter	57.70	8.09

4.4 Relationship between the teleconnection patterns and the decadal high extreme precipitation variability

The relationship between extreme precipitation anomalies and climate indices anomalies are tested to find out possible causes in extreme precipitation variability. The NAO, AO, SOI and WeMO are selected as climate indices to investigate whether they have a significant effect on the extreme precipitation variability of Turkey.

When analyzing the relationship, both linear and non-linear methods are used. The significance of the correlation and the relation coefficients obtained from different methods are measured with respect to t-test. During the determination of threshold correlation value for significance levels, the effective sample size is taken into consideration as well the actual sample size. The threshold value obtained with the effective sample size is used to minimize errors that may occur while interpreting the results. QPM includes a filtering process during defining anomalies which leads to an autocorrelation. Since all precipitation data and climate indices are subjected to the same process and autocorrelation, correlation between compared data becomes higher than expected. At this point effective sample size is used to eliminate the effect of autocorrelation. It is calculated by dividing the sample size to the selected block length. In our case, 5-years and 10-years block length are picked. Thus, the effective sample sizes are found as 12 and 6 for selected block lengths respectively. Besides, the significance of the results is checked with the 5% significance level. The threshold values with respect to actual and effective sample size can be seen in Table 4.3 separately. It should be noted that in the following parts, the significance of the correlations are interpreted on the basis of effective sample size unless otherwise is stated. In addition, the correlations designated as significant considering the actual sample size are represented in the relation result tables.

Table 4.3 Threshold values with respect to actual and effective sample size

	Actual sample size	Effective sample size
Threshold	0.215	0.730

4.4.1 The single relationship analysis

Initially, the relationships are studied with single inputs in order to see one-to-one relations between extreme precipitation and each climate index. By doing so, the individual effects of NAO, AO, SOI and WeMO on Turkey's extreme precipitation are tested. Furthermore, a linear and a non-linear relation method is used for analyses with the single inputs. Through this the linearity of the relationship by comparing outputs of linear and non-linear methods are inspected. The results are shown in detail in the following sections.

4.4.1.1 NAO responses

i) Spearman's rank-order correlation (SROC)

According to the Spearman correlation analysis, the negative correlation coefficients are usually effective on the relationship in winter. Five stations show statistically significant correlation at 5% significance level in winter and all of them have negative correlation with NAO. These stations are Samsun and Giresun from BLS, Konya from CEAN, Kütahya and Isparta from MEDT. Nonetheless, the station numbers having significant correlation with NAO decrease in other seasons. There is only one station for which the relation is significant with NAO in spring and three stations in summer. Moreover, it is not encountered with the significant correlations in autumn.

As stated before, the precipitation data of this study consist of point measurements, which are taken from 65 different stations throughout Turkey. Likewise, the relationship analyses demonstrate the relation between climate indices and the extreme precipitation data at these 65 points. Exhibiting the continuous distribution

of the correlation coefficients across Turkey is also quite essential for this kind of study. In line with this purpose, the correlation coefficients obtained from 65 stations are propagated over Turkish map by the help of inverse-distance weighting (IDW) method. IDW method is applied to obtain the correlation coefficient of unsampled regions. The basic idea of this is taking the weighted average of correlations at the neighboring points that are sampled, with respect to their weights. The weights should be taken into consideration as inversely proportional to the distance between the prediction point and each sampled neighboring point (Gotway et al, 1996). Figure 4.14 shows the continuous map of spearman correlation coefficients between NAO and extreme precipitation of each season. By analyzing the figure, it can be observed that NAO is not a significant driver of extreme precipitation in Turkey except winter months. It has been stated that, NAO was found very effective on Turkey's precipitation variability in winter (e.g. Türkeş, 2003; Cullen et al, 2000). However, it is not possible to see the same effect of NAO on decadal extreme precipitation variability of Turkey according to our results. Still, in parallel with the cited studies above, decadal behavior of the number of dry days in winter months is assessed as crucially related to NAO in section 4.5.1.1. On the basis of all these information, even though NAO is one of the basic drivers of extreme precipitation in winter for some regions of Turkey, it is not as a prevailing driver as it is for the total precipitation. Moreover, Figure 4.14, based on SROC method, indicates that the decadal extreme precipitation data are markedly connected to NAO at a notable part of CCAN and central BLS along with a small part of eastern BLS during winter. Additionally, NAO is an important driver for decadal extreme precipitation in the western part, which includes some big cities such as İzmir, Manisa and Balıkesir.

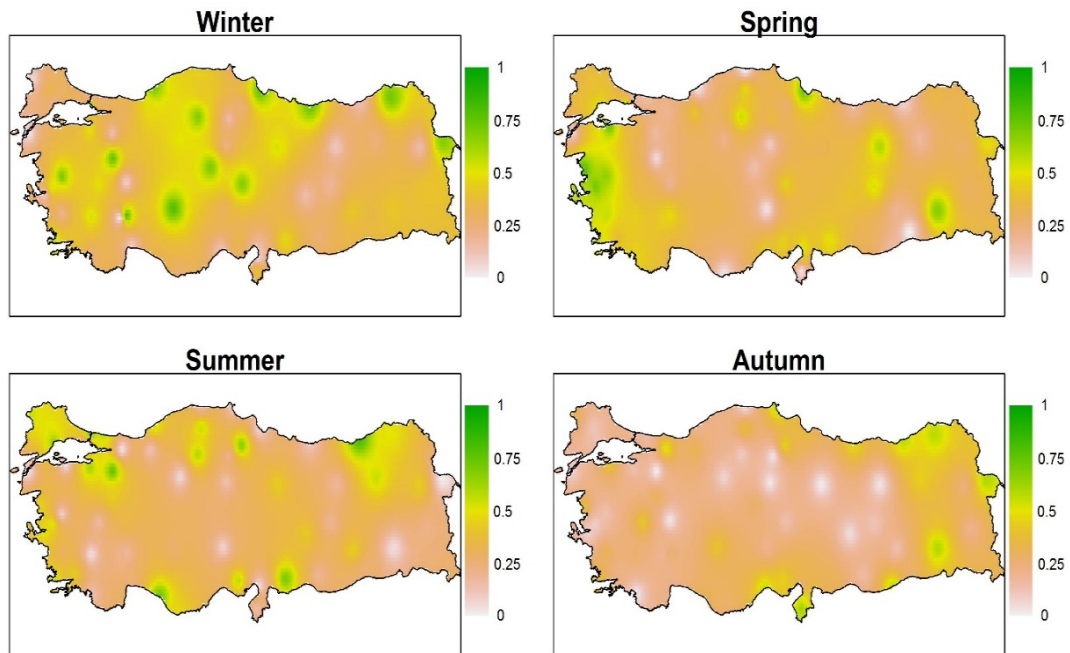


Figure 4.14 The continuous map of spearman's rank order correlation coefficient between NAO and extreme precipitation with respect to seasons

In addition to these, if the significance of the correlations at the stations are checked referring to threshold obtained with the actual sample size, the number of stations having the significant correlation shows a great increase. In this case, the extreme precipitation of 45 stations is found significantly related to NAO in winter. Table 4.4 shows the distribution of these 45 stations by region. The region with the highest number of stations in which extreme precipitation behavior is significantly correlated to NAO is MED with 12 stations. Further, the rate of presenting a significant relationship according to total station numbers is the highest in the BLS and CCAN. 7 of the 8 stations in BLS and 9 of the 11 stations in CCAN indicates significant correlations with NAO.

Table 4.4 The number of station having significant correlation with NAO in winter with regard to actual sample size threshold

Rainfall Region	Total number of the station	Number of station having significant correlation
BLS	8	7
CCAN	11	9
CEAN	6	4
CMED	8	6
MED	19	12
MEDT	4	3
MRT	9	4

ii) Power Law Regression (PLR)

In winter, six stations display significant relation with NAO. Samsun, Konya, Kayseri, Iğdır, Akhisar and Isparta have significant relation with NAO. However, the number of stations having the significant relationship decreases in other seasons identical with Spearman’s rank-order correlation method. The extreme precipitation amount of two MED stations, Bandırma and Dikili, are significantly related to NAO in spring season. Also, the significant relations are detected at Rize, Alanya and Bilecik stations in summer. Finally, the autumn extreme precipitation is not significantly connected to NAO based on the power law regression results.

The continuous distribution of PLR coefficient over Turkey are displayed in Figure 4.15. If it is compared with Figure 4.14, it is obvious that the relationship results of PLR are quite similar to SROC results except for the minor discrepancies. In general, SROC defines slightly higher relationship in winter and spring whereas PRL finds marginally higher relationship in summer and autumn. Apart from these, the regions where the relationship is high or low are detected to be the same in both figures. Further, the relationship coefficients obtained by the two methods at different stations can be seen in the Table 4.5. These coefficients, give an insight on the

similarity or dissimilarity between the relationship results of two methods at each station.

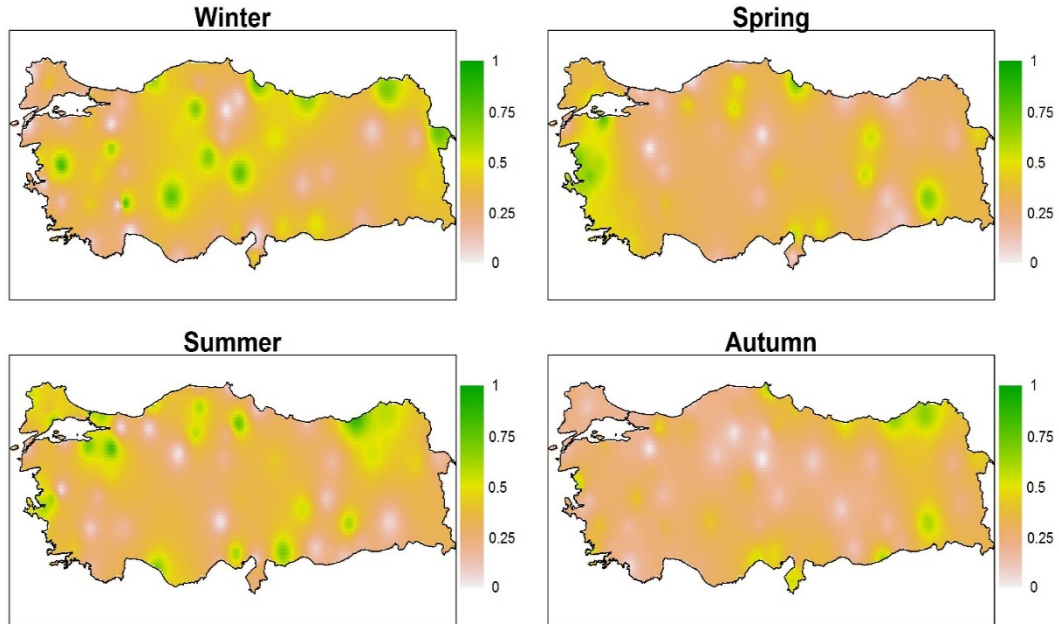


Figure 4.15 The continuous map of non-linear power law regression coefficient (R) between NAO and extreme precipitation with respect to seasons

When the significance of PLR results are analyzed in regard to the actual sample size threshold, it can be seen that in winter, the significant relationship is identified at 40 stations. If the relation coefficients obtained by PLR is compared with the correlation coefficients obtained by SROC, it is observed that PLR gives higher relation coefficients at 28 stations while SROC gives higher coefficients at 37 stations. Herein, it is worthy to declare that when comparing the results, absolute values of SROC coefficients are used since PLR does not represent the negative relationship. Although PLR determine higher relationship at lower number of stations in comparison to SROC in total, the number of stations with the significant relationship coefficient based on the effective sample size threshold is higher than SROC results. However, it is not reasonable to claim that there is a substantially difference between the results of these two methods. In order to see the similarity or dissimilarity of the results of these methods, the correlation coefficient between the 65 correlation coefficients gained by SROC and the 65 relationship coefficient gained by PLR are

calculated by the help of Pearson correlation coefficient method. The values are found to be 0.94, 0.95, 0.93 and 0.90 for spring, summer, autumn and winter respectively. Namely, it can be inferred that the results of PLR and SROC are parallel to each other. The executed linear and non-linear methods characterize quite similar relationship of the extreme precipitation over Turkey with NAO.

Table 4.5 The relationship between anomaly of extreme precipitation and NAO anomaly (*Bold black numbers= The significant relationship for the effective sample size and the actual sample size, Red Numbers: The significant relationship for the actual sample size, Black Numbers= The insignificant relationship*)

Station	Region	Spearman's rank order correlation				Non-linear power law regression (R value)			
		Spring	Summer	Autumn	Winter	Spring	Summer	Autumn	Winter
Adana	MED	0.451	-0.564	0.447	0.343	0.321	0.629	0.479	0.429
Afyon	CCAN	0.193	-0.358	-0.030	0.095	0.129	0.371	0.148	0.212
Ağrı	CEAN	0.282	-0.438	-0.252	-0.161	0.173	0.454	0.222	0.179
Akhisar	MED	0.655	0.090	-0.135	-0.696	0.595	0.042	0.265	0.829
Alanya	MED	0.263	0.727	-0.324	0.330	0.299	0.682	0.240	0.364
Anamur	MED	0.017	0.468	-0.271	-0.259	0.161	0.445	0.285	0.120
Ankara	CCAN	0.218	-0.064	0.076	-0.505	0.218	0.026	0.097	0.476
Antakya	MED	-0.032	-0.164	0.625	-0.403	0.074	0.242	0.553	0.455
Antalya	MED	0.348	-0.251	-0.224	-0.096	0.346	0.332	0.231	0.002
Artvin	BLS	0.353	-0.507	-0.577	0.712	0.303	0.580	0.670	0.703
Aydın	MED	0.552	-0.309	-0.316	-0.209	0.460	0.329	0.396	0.142
Bandırma	MED	0.708	-0.043	-0.417	-0.364	0.771	0.147	0.358	0.132
Bilecik	MRT	-0.159	-0.747	-0.011	-0.142	0.266	0.826	0.005	0.026
Bodrum	MED	0.552	0.549	-0.443	-0.580	0.528	0.377	0.524	0.396
Bolu	BLS	-0.409	-0.137	0.325	-0.475	0.460	0.051	0.348	0.424
Burdur	MEDT	0.446	0.215	-0.188	0.002	0.260	0.194	0.221	0.016
Bursa	MRT	0.355	-0.615	-0.141	-0.488	0.302	0.708	0.213	0.418
Çanakkale	MED	-0.089	0.041	-0.083	0.035	0.168	0.152	0.160	0.041
Çankırı	CCAN	0.553	-0.592	-0.105	-0.678	0.541	0.584	0.026	0.693
Ceylanpınar	CMED	-0.159	-0.260	-0.558	-0.340	0.102	0.107	0.601	0.390
Çorum	CCAN	-0.368	0.220	-0.036	-0.159	0.230	0.229	0.077	0.005
Denizli	MED	0.444	0.048	0.263	-0.528	0.411	0.084	0.168	0.439
Dikili	MED	0.787	-0.462	-0.396	-0.300	0.729	0.481	0.594	0.514
Diyarbakır	CMED	-0.195	-0.444	0.142	0.423	0.097	0.622	0.167	0.341
Dörtöyol	MED	0.545	-0.013	0.236	-0.148	0.627	0.067	0.225	0.019
Edirne	MRT	-0.347	-0.548	0.320	-0.061	0.334	0.539	0.247	0.049
Elazığ	CMED	-0.523	0.203	0.123	-0.184	0.557	0.106	0.211	0.191
Erzincan	CEAN	0.594	0.180	0.032	-0.116	0.554	0.166	0.169	0.360
Erzurum	CEAN	0.174	0.549	0.450	-0.247	0.225	0.537	0.410	0.087
Fethiye	MED	0.463	0.144	-0.024	-0.260	0.481	0.189	0.053	0.127
Florya	MRT	0.640	0.213	0.220	-0.227	0.596	0.127	0.171	0.079
Gaziantep	CMED	-0.496	-0.694	-0.313	0.469	0.490	0.705	0.369	0.482
Giresun	BLS	-0.179	-0.122	-0.473	-0.731	0.099	0.165	0.512	0.667
İğdır	CEAN	0.485	0.011	0.598	-0.675	0.464	0.160	0.444	0.745

Table 4.5 Continued

Inebolu	BLS	-0.005	-0.177	-0.069	-0.449	0.122	0.234	0.172	0.402
İskenderun	MED	0.398	0.337	0.543	-0.051	0.331	0.396	0.539	0.071
Isparta	MEDT	0.487	-0.177	-0.263	-0.780	0.429	0.190	0.344	0.800
İzmir	MED	0.569	-0.504	-0.068	0.099	0.627	0.631	0.130	0.028
Kastamonu	CCAN	-0.475	-0.549	-0.382	-0.422	0.534	0.606	0.281	0.232
Kayseri	CCAN	0.444	0.299	0.145	0.679	0.411	0.367	0.124	0.770
Kireçburnu	MRT	-0.104	-0.672	-0.069	-0.136	0.075	0.697	0.139	0.069
Kırşehir	CCAN	0.141	-0.259	0.284	-0.694	0.175	0.268	0.392	0.692
Konya	CCAN	-0.340	0.271	0.410	-0.775	0.285	0.360	0.414	0.760
Kumköy	MRT	0.112	-0.713	0.208	0.133	0.218	0.674	0.190	0.226
Kütahya	MEDT	-0.052	0.440	0.303	-0.738	0.007	0.489	0.307	0.650
Lüleburgaz	MRT	0.393	-0.513	-0.118	0.340	0.344	0.394	0.105	0.434
Malatya	CMED	-0.407	0.427	0.052	0.152	0.257	0.553	0.088	0.137
Manisa	MED	0.709	-0.501	-0.086	-0.528	0.705	0.634	0.144	0.481
Mardin	CMED	-0.007	-0.252	0.271	-0.361	0.090	0.189	0.204	0.170
Mersin	MED	-0.433	-0.287	0.548	-0.127	0.345	0.213	0.554	0.209
Muğla	MED	0.394	0.434	0.224	-0.402	0.467	0.421	0.217	0.348
Niğde	CCAN	-0.038	0.084	-0.205	0.307	0.164	0.026	0.216	0.350
Rize	BLS	-0.078	-0.800	-0.573	-0.140	0.038	0.864	0.652	0.356
Sakarya	BLS	0.192	-0.037	0.502	-0.296	0.124	0.053	0.477	0.140
Samsun	BLS	-0.709	-0.078	0.373	-0.741	0.693	0.106	0.422	0.750
Şanlıurfa	CMED	-0.315	-0.197	-0.162	-0.259	0.296	0.094	0.135	0.516
Siirt	CMED	0.671	-0.050	0.587	0.420	0.689	0.069	0.610	0.349
Şile	MRT	0.141	-0.552	0.144	0.251	0.070	0.659	0.159	0.344
Sinop	BLS	0.340	-0.093	-0.624	-0.272	0.323	0.083	0.668	0.348
Sivas	CCAN	0.335	0.439	0.019	0.525	0.279	0.423	0.093	0.516
Tekirdağ	MRT	0.488	-0.641	-0.119	0.208	0.552	0.630	0.200	0.206
Uşak	MEDT	0.342	-0.169	0.430	-0.493	0.306	0.190	0.417	0.450
Van	CEAN	0.303	-0.225	0.214	-0.410	0.356	0.341	0.238	0.448
Yozgat	CCAN	-0.101	0.140	0.027	-0.230	0.025	0.201	0.000	0.149
Zonguldak	BLS	0.039	-0.533	-0.203	-0.695	0.033	0.562	0.146	0.636

4.4.1.2 AO responses

i) Spearman's rank-order correlation

Based on the Spearman correlation analysis it can be claimed that, results that AO provides have less effect on extreme precipitation variability in Turkey in comparison to NAO results. There are only two stations for which the correlation coefficient is significant at 5% significance level in winter. These stations are Ankara and Kayseri. While the negative correlation coefficient exists between Ankara and AO, the positive correlation coefficient exists between Kayseri and AO. As stated before, the high fluctuations take place in winter extreme precipitation of Kayseri. AO may be regarded as one of the possible drivers for high fluctuations with respect to that result. Like NAO, AO is generally not a significant driver for extreme precipitation in other seasons. When the other seasons are controlled, it is understood that the only significant correlation appears at Uşak station in autumn.

The influence of AO on extreme precipitation in Turkey is mapped in Figure 4.16. When the results are checked against Figure 4.14, it can be noticed that the regions having the advanced correlation with NAO and AO in winter and spring are fairly identical. In order to verify this observation, the correlation coefficient between NAO and AO anomalies are calculated. These coefficients are 0.90 and 0.92 for winter and spring. Namely, the decadal anomalies of NAO and AO indices are significantly connected in winter and spring months. In addition to these, even if their domains are similar, NAO broadly shows a higher correlation with extreme precipitation in Turkey than AO. Besides, the impact of AO drops in summer and autumn just like NAO. The only remarkable effect in these seasons is determined in autumn. In this season, the relatively high correlation between AO and extreme precipitation anomalies is detected along the region extending from southwest coast to CMED.

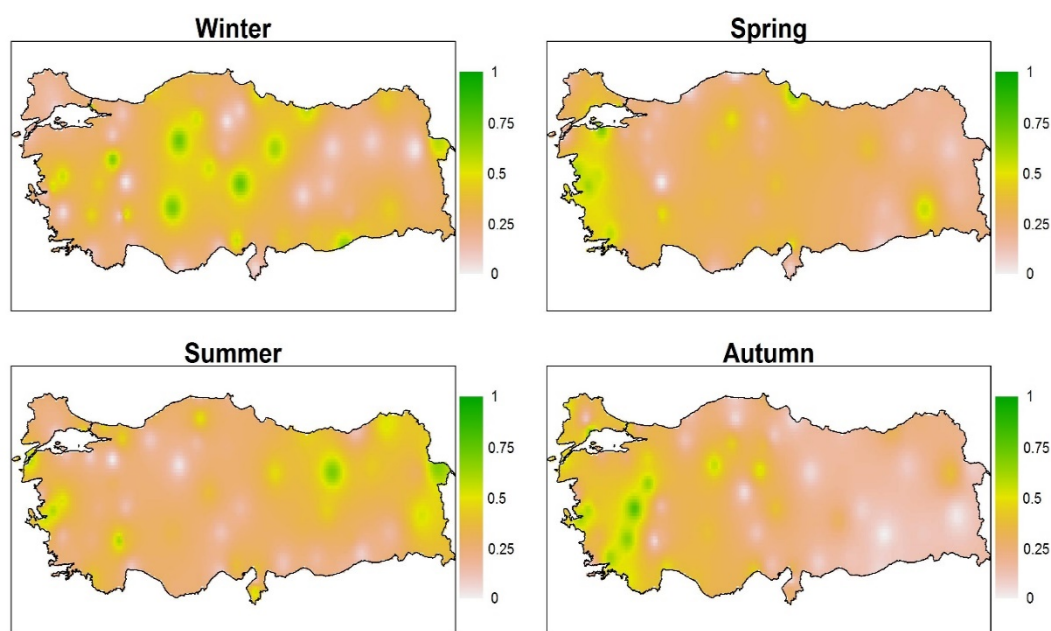


Figure 4.16 The continuous map of spearman rank order correlation coefficient between AO and extreme precipitation with respect to seasons

The significance of the relation between AO indices and extreme precipitation anomalies is also evaluated based on the threshold acquired by the actual sample size. In consequence of this supervision, the significant relation is disclosed at 38 stations. At this juncture, it is valuable to remind that the relationship with NAO has been identified as significant at 45 stations. Likewise, the number of station having significant relationship with AO and NAO are pretty close in regard to regions (Table 4.6). This situation may suggest that AO and NAO have similar effects on extreme precipitation behavior of Turkey, but NAO is the more effective driver.

Table 4.6 The comparison of the number of station having significant correlation with AO and NAO in winter with regard to actual sample size threshold

Rainfall Region	Number of station having significant correlation with AO	Number of station having significant correlation with NAO
BLS	7	7
CCAN	8	9
CEAN	3	4
CMED	6	6
MED	9	12
MEDT	3	3
MRT	2	4

ii) Power Law Regression

When the AO teleconnection pattern is examined, the significant relationship is detected only at Kayseri station during the winter months. Still, even though they are not significant, the relation coefficients that are very close to the threshold value are evaluated at Ankara and Konya stations. The Bandirma station has a significant relation with the AO as well as with the NAO in spring. No significant relation is observed between AO and any another station in spring. Significant relations are seen in autumn at two MEDT stations; Kütahya and Uşak. There is no significant relationship with AO at the 5% significance level in any station for the summer season.

The distribution of PLR coefficient (R) is drawn in Figure 4.17. In order to interpret PLR and SROC results together, the Figure 4.16 and Figure 4.17 are comparatively examined. These figures express that the regions where the extreme precipitation relationship is relatively high with AO are parallel for PLR and SROC results. Nevertheless, it can be said that the relationships defined by the PLR are commonly higher. Differently from SROC, the PLR defines AO as a more effective variable on the extreme precipitation of northeastern Turkey in summer and western Turkey in spring.

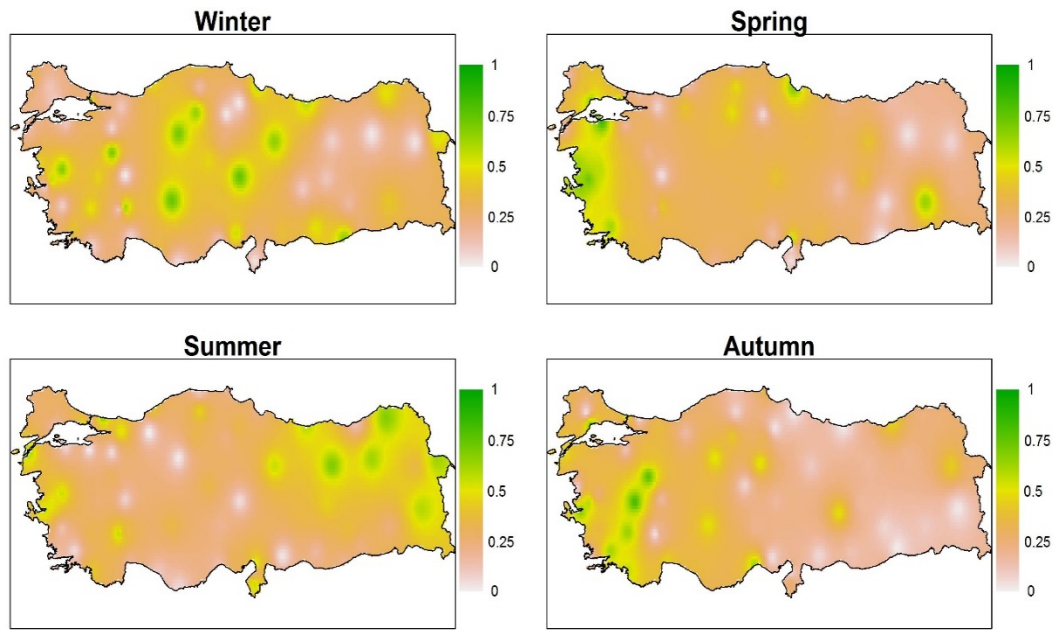


Figure 4.17 The continuous map of non-linear power law regression coefficient (R) between AO and extreme precipitation with respect to seasons

According to PLR, the R coefficients between the winter extremes and AO is higher than actual sample size threshold at 39 stations. This number is 38 for the SROC coefficients. Consequently, the count of the significant relationships defined by SROC and PLR is approximately the same for the actual sample size threshold. However, when the SROC and PLR coefficients are measured station by station, it can be understood that PLR method detects a higher relationship than SROC at more of stations. The coefficient values of PLR are higher than SROC coefficients at 37, 40, 34 and 40 stations for spring, summer, autumn and winter seasons respectively. All the coefficient values are remarked in Table 4.7.

Table 4.7 The relationship between anomaly of extreme precipitation and AO anomaly (Bold black numbers= The significant relationship for the effective sample size and the actual sample size, Red Numbers: The significant relationship for the actual sample size, Black Numbers= The insignificant relationship)

Station	Region	Spearman's rank order correlation				Non-linear power law regression (R value)			
		Spring	Summer	Autumn	Winter	Spring	Summer	Autumn	Winter
Adana	MED	0.378	-0.380	0.132	0.555	0.164	0.314	0.047	0.550
Afyon	CCAN	0.001	0.142	0.158	-0.012	0.041	0.081	0.178	0.015
Ağrı	CEAN	0.095	-0.304	-0.384	-0.024	0.075	0.361	0.438	0.037
Akhisar	MED	0.551	-0.529	0.398	-0.563	0.580	0.547	0.257	0.678
Alanya	MED	0.323	0.271	-0.395	0.322	0.315	0.104	0.374	0.361
Anamur	MED	0.127	0.232	0.333	-0.040	0.215	0.047	0.325	0.038
Ankara	CCAN	0.412	0.026	0.566	-0.734	0.363	0.017	0.509	0.708
Antakya	MED	0.074	-0.534	0.285	0.053	0.045	0.545	0.284	0.030
Antalya	MED	0.361	-0.102	0.481	-0.140	0.337	0.201	0.455	0.078
Artvin	BLS	0.172	0.522	-0.236	0.424	0.193	0.674	0.237	0.502
Aydın	MED	0.490	0.161	0.330	-0.044	0.486	0.138	0.361	0.089
Bandırma	MED	0.712	0.127	0.222	-0.203	0.821	0.062	0.303	0.104
Bilecik	MRT	-0.138	0.004	0.479	-0.091	0.299	0.047	0.377	0.072
Bodrum	MED	0.447	-0.190	0.062	-0.309	0.510	0.074	0.084	0.230
Bolu	BLS	-0.269	-0.100	0.131	-0.335	0.409	0.000	0.165	0.340
Burdur	MEDT	0.327	0.625	0.049	-0.080	0.212	0.567	0.035	0.110
Bursa	MRT	0.191	0.082	0.261	-0.255	0.182	0.016	0.131	0.294
Çanakkale	MED	-0.140	-0.599	0.496	-0.142	0.190	0.596	0.472	0.159
Çankırı	CCAN	0.504	0.163	0.446	-0.542	0.493	0.338	0.414	0.640
Ceylanpınar	CMED	-0.065	0.182	-0.064	-0.667	0.006	0.208	0.187	0.650
Çorum	CCAN	-0.166	-0.237	0.365	0.024	0.063	0.230	0.324	0.025
Denizli	MED	0.361	0.237	0.673	-0.471	0.342	0.333	0.636	0.501
Dikili	MED	0.627	0.159	0.192	-0.395	0.643	0.347	0.068	0.453
Diyarbakır	CMED	-0.138	-0.304	0.004	0.218	0.052	0.378	0.071	0.168
Dörtöyol	MED	0.537	0.428	0.364	0.284	0.607	0.537	0.229	0.308
Edirne	MRT	-0.168	0.232	0.491	-0.186	0.175	0.254	0.334	0.313
Elazığ	CMED	-0.240	-0.450	-0.083	0.114	0.386	0.452	0.167	0.118
Erzincan	CEAN	0.399	-0.702	-0.177	0.073	0.401	0.686	0.175	0.085
Erzurum	CEAN	-0.155	-0.431	0.100	-0.083	0.037	0.623	0.204	0.023
Fethiye	MED	0.253	-0.422	0.520	-0.112	0.358	0.434	0.553	0.080
Florya	MRT	0.610	0.533	0.294	-0.186	0.650	0.541	0.260	0.134
Gaziantep	CMED	-0.289	-0.120	0.084	0.417	0.360	0.029	0.062	0.386
Giresun	BLS	-0.282	-0.450	-0.142	-0.570	0.229	0.568	0.025	0.571
İğdır	CEAN	0.182	-0.681	-0.087	-0.588	0.255	0.620	0.261	0.530

Table 4.7 Continued

Inebolu	BLS	-0.014	-0.205	-0.090	-0.356	0.186	0.105	0.131	0.405
İskenderun	MED	0.159	-0.096	0.025	0.145	0.026	0.225	0.054	0.118
Isparta	MEDT	0.521	-0.367	0.225	-0.549	0.439	0.353	0.229	0.633
İzmir	MED	0.508	-0.564	0.616	-0.093	0.663	0.544	0.665	0.096
Kastamonu	CCAN	-0.333	-0.500	-0.055	-0.255	0.476	0.454	0.066	0.157
Kayseri	CCAN	0.397	0.163	0.394	0.754	0.399	0.047	0.173	0.746
Kireçburnu	MRT	0.008	0.304	0.401	-0.191	0.017	0.419	0.386	0.317
Kırşehir	CCAN	0.353	-0.381	0.044	-0.545	0.334	0.347	0.075	0.466
Konya	CCAN	-0.355	-0.336	0.388	-0.710	0.299	0.350	0.492	0.733
Kumköy	MRT	0.281	0.210	0.578	-0.003	0.358	0.299	0.689	0.016
Kütahya	MEDT	-0.184	-0.295	0.645	-0.695	0.208	0.304	0.763	0.702
Lüleburgaz	MRT	0.334	0.211	0.100	0.145	0.396	0.290	0.038	0.118
Malatya	CMED	-0.277	-0.342	-0.297	0.063	0.152	0.360	0.491	0.106
Manisa	MED	0.629	-0.601	0.598	-0.540	0.716	0.520	0.582	0.559
Mardin	CMED	0.154	0.088	0.105	-0.411	0.221	0.238	0.017	0.251
Mersin	MED	-0.384	0.114	0.446	-0.110	0.323	0.143	0.619	0.126
Muğla	MED	0.577	0.243	0.623	-0.329	0.613	0.057	0.613	0.401
Niğde	CCAN	-0.249	-0.122	-0.120	0.384	0.343	0.195	0.197	0.385
Rize	BLS	-0.221	-0.113	-0.320	-0.218	0.148	0.127	0.456	0.264
Sakarya	BLS	0.150	0.457	0.331	-0.116	0.079	0.520	0.373	0.112
Samsun	BLS	-0.649	-0.266	0.051	-0.513	0.675	0.244	0.019	0.554
Şanlıurfa	CMED	-0.263	0.173	-0.120	-0.405	0.281	0.176	0.134	0.497
Siirt	CMED	0.566	0.172	-0.114	0.434	0.633	0.247	0.104	0.418
Şile	MRT	0.241	0.473	0.176	0.236	0.163	0.651	0.048	0.178
Sinop	BLS	0.364	0.205	-0.308	-0.259	0.302	0.212	0.353	0.314
Sivas	CCAN	0.355	-0.481	-0.057	0.626	0.343	0.552	0.103	0.649
Tekirdağ	MRT	0.473	0.095	0.655	-0.058	0.619	0.166	0.660	0.089
Uşak	MEDT	0.363	-0.229	0.789	-0.446	0.360	0.254	0.806	0.448
Van	CEAN	0.158	-0.527	0.025	-0.241	0.218	0.584	0.030	0.297
Yozgat	CCAN	0.225	0.260	0.525	-0.170	0.305	0.283	0.519	0.252
Zonguldak	BLS	-0.059	0.305	-0.148	-0.456	0.162	0.401	0.277	0.452

4.4.1.3 SOI responses

i) Spearman's rank-order correlation

SOI relationships are found significant at Ağrı and Antalya stations with 5% significance level in winter. Unlike former two indices NAO and AO, the number of the stations with significant correlation is the highest in summer. While there is the positive significant correlation between Erzurum station and SOI in summer, there is the negative significant correlation at the stations Zonguldak and Çankırı. In addition, Bolu shows a significant correlation with SOI in spring. The significant correlation is not detected for autumn season.

In parallel with the statement above, the season, in which the influence of SOI on high extremes is the most, is summer according to Figure 4.18. Regionally, the highest correlations in summer is specified at the northeast of Turkey. In addition, the impact area of SOI is smaller in winter. The SOI is may be thought as a driver of the extreme precipitation in the area which covers Kars, Ağrı and Iğdır. Lastly, SOI has a very small power on spring extremes while it is almost no power on autumn extremes.

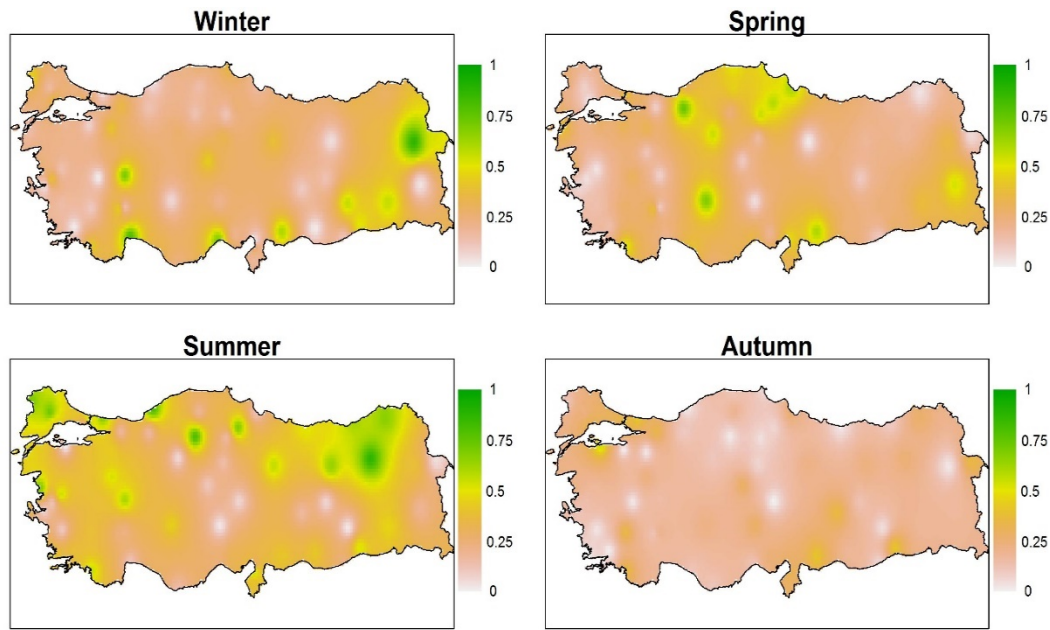


Figure 4.18 The continuous map of spearman rank order correlation coefficient between SOI and extreme precipitation with respect to seasons

When the significance of the correlations are measured with reference to the actual sample size threshold, there are 45 stations which are significantly correlated to SOI in summer. Also, 36 of the stations express the significant correlation with SOI in winter. However, if these results are studied by data provided by Figure 4.18, it can be understood that the correlations usually does not reach the 0.60 level. In other words green areas are rarely encountered. This implies that the number of stations that are significantly related to SOI is about the same with NAO and AO, but the value of these correlations is lower than the other two indices. Simply, SROC results notify that SOI is the weaker driver of extreme precipitation in Turkey than both NAO and AO excluding summer.

ii) Power Law Regression

After testing the relation between SOI indices and extreme anomalies, it is seen that there is no significant relation at stations during spring and autumn. However, significant relation at two stations in winter and at three stations in summer period

are present. While Ağrı and Antalya exhibit significant relations with SOI for the winter season; Zonguldak, Çankırı and Erzurum exhibit significant relations in the summer months.

The spread of R coefficient between extreme precipitation and SOI is portrayed in Figure 4.19. The output is pretty analogous to spread of SROC coefficient. The relationship coefficient are generally not significant in spring and autumn as such in SROC map. Still, it can be mentioned about the small differences in winter and summer. In winter, PLR shows more relationship than SROC, this is especially valid for the inner parts of the country. In summer, the opposite is the case. The partially high correlation defined by SROC at the northwestern of Turkey is overlooked by PLR.

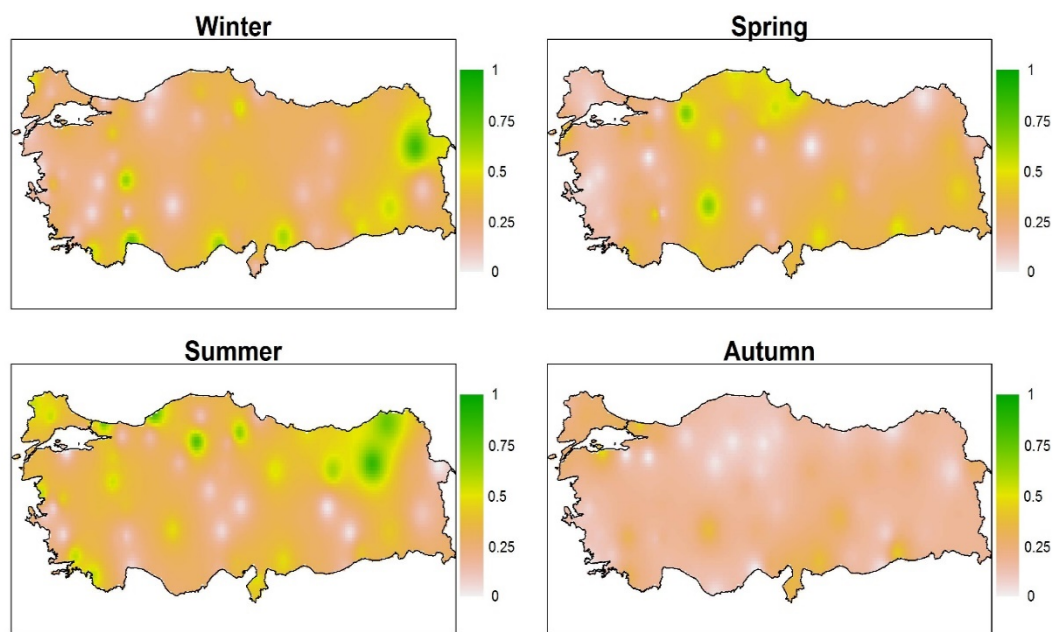


Figure 4.19 The continuous map of non-linear power law regression coefficient (R) between SOI and extreme precipitation with respect to seasons

PLR assigns the 43 stations as significant with respect to the actual sample size threshold in summer and winter. These numbers are 45 and 36 according to SROC method. As it can be realized, there is a noteworthy increase in the number of stations that have significant relationship with SOI for winter whereas the number of

stations is approximately the same for summer. As supported by Figure 4.19, it can be deduced that the PLR better describes the relationship in winter and the SROC better explains the relationship in the summer. In order to further consolidate this finding, PLR and SROC coefficients are compared station by station. It is detected that PLR finds higher correlation at 40 stations in winter while SROC finds higher correlation at 41 stations in summer (Table 4.8).

Table 4.8 The relationship between anomaly of extreme precipitation and SOI anomaly (Bold black numbers= The significant relationship for the effective sample size and the actual sample size, Red Numbers: The significant relationship for the actual sample size, Black Numbers= The insignificant relationship)

Station	Region	Spearman's rank order correlation				Non-linear power law regression (R value)			
		Spring	Summer	Autumn	Winter	Spring	Summer	Autumn	Winter
Adana	MED	-0.192	-0.326	-0.249	0.206	0.142	0.378	0.274	0.265
Afyon	CCAN	0.079	-0.604	0.155	0.696	0.157	0.397	0.204	0.656
Ağrı	CEAN	0.354	-0.388	-0.029	-0.864	0.377	0.270	0.054	0.831
Akhisar	MED	0.030	0.544	-0.170	-0.131	0.038	0.458	0.167	0.152
Alanya	MED	-0.401	0.281	0.116	-0.339	0.439	0.252	0.136	0.245
Anamur	MED	-0.261	0.151	0.111	0.234	0.391	0.258	0.041	0.383
Ankara	CCAN	0.554	0.060	0.114	0.273	0.515	0.154	0.030	0.225
Antakya	MED	-0.322	0.395	-0.284	-0.176	0.365	0.436	0.347	0.138
Antalya	MED	-0.211	-0.125	-0.171	0.800	0.199	0.070	0.149	0.748
Artvin	BLS	-0.036	-0.667	-0.275	-0.294	0.027	0.729	0.197	0.305
Aydın	MED	-0.134	-0.103	0.029	0.155	0.097	0.055	0.111	0.307
Bandırma	MED	-0.285	0.005	0.545	0.181	0.188	0.001	0.495	0.373
Bilecik	MRT	0.328	-0.434	0.022	0.412	0.339	0.454	0.006	0.452
Bodrum	MED	-0.131	0.452	0.007	0.190	0.134	0.226	0.017	0.378
Bolu	BLS	0.739	-0.168	0.104	-0.131	0.701	0.148	0.059	0.069
Burdur	MEDT	0.395	-0.237	-0.128	0.442	0.493	0.202	0.136	0.391
Bursa	MRT	0.318	-0.384	0.015	0.078	0.335	0.298	0.006	0.250
Çanakkale	MED	0.396	0.469	-0.222	0.148	0.409	0.336	0.276	0.087
Çankırı	CCAN	0.246	-0.799	-0.024	0.128	0.276	0.787	0.021	0.142
Ceylanpınar	CMED	-0.096	-0.232	-0.070	0.113	0.316	0.151	0.035	0.129
Çorum	CCAN	0.552	0.168	0.042	0.122	0.479	0.198	0.023	0.229
Denizli	MED	0.281	-0.389	0.360	-0.103	0.303	0.343	0.323	0.046
Dikili	MED	-0.280	-0.703	-0.216	0.248	0.232	0.595	0.176	0.032
Diyarbakır	CMED	-0.245	0.022	0.046	0.564	0.275	0.034	0.080	0.430
Dörtöyol	MED	-0.486	-0.278	-0.270	0.029	0.369	0.268	0.309	0.406
Edirne	MRT	0.259	-0.689	-0.130	0.444	0.116	0.558	0.189	0.501
Elazığ	CMED	-0.101	0.069	-0.131	0.131	0.193	0.025	0.163	0.180
Erzincan	CEAN	-0.184	0.641	-0.237	-0.046	0.157	0.619	0.237	0.147
Erzurum	CEAN	-0.179	0.868	0.256	-0.348	0.181	0.859	0.242	0.340
Fethiye	MED	-0.502	0.545	0.364	0.423	0.433	0.579	0.317	0.555
Florya	MRT	0.114	-0.190	-0.304	-0.306	0.084	0.137	0.311	0.333
Gaziantep	CMED	0.599	-0.416	-0.411	0.605	0.502	0.476	0.385	0.620
Giresun	BLS	-0.273	0.517	0.029	0.266	0.262	0.475	0.090	0.293
İğdir	CEAN	0.059	0.042	-0.358	-0.521	0.135	0.008	0.283	0.524

Table 4.8 Continued

Inebolu	BLS	0.518	-0.280	-0.117	-0.256	0.542	0.343	0.117	0.331
İskenderun	MED	-0.409	0.571	-0.341	0.298	0.356	0.584	0.383	0.401
Isparta	MEDT	0.102	-0.224	0.206	0.143	0.077	0.093	0.207	0.093
İzmir	MED	0.062	-0.076	0.114	-0.041	0.060	0.096	0.097	0.095
Kastamonu	CCAN	0.455	-0.190	-0.199	0.146	0.474	0.121	0.146	0.408
Kayseri	CCAN	0.263	0.067	-0.007	0.279	0.248	0.053	0.123	0.402
Kireçburnu	MRT	0.652	-0.529	0.404	0.275	0.472	0.585	0.335	0.342
Kırşehir	CCAN	-0.101	-0.116	0.290	-0.441	0.262	0.088	0.206	0.374
Konya	CCAN	-0.682	0.447	-0.229	0.063	0.682	0.482	0.377	0.045
Kumköy	MRT	0.163	-0.480	0.296	0.079	0.113	0.417	0.260	0.134
Kütahya	MEDT	0.119	0.529	0.240	-0.275	0.005	0.548	0.175	0.158
Lüleburgaz	MRT	0.083	-0.717	-0.235	0.169	0.092	0.563	0.292	0.144
Malatya	CMED	-0.248	0.170	-0.365	-0.100	0.438	0.287	0.342	0.129
Manisa	MED	-0.039	0.117	0.146	0.393	0.022	0.068	0.081	0.396
Mardin	CMED	-0.273	-0.513	-0.413	-0.509	0.522	0.402	0.428	0.512
Mersin	MED	-0.359	-0.243	0.119	-0.700	0.335	0.199	0.005	0.672
Muğla	MED	-0.144	0.387	-0.016	0.020	0.118	0.573	0.094	0.107
Niğde	CCAN	0.045	0.025	-0.291	0.199	0.081	0.059	0.236	0.350
Rize	BLS	-0.158	-0.612	-0.098	-0.335	0.227	0.502	0.028	0.407
Sakarya	BLS	0.090	-0.178	0.343	0.358	0.087	0.125	0.282	0.378
Samsun	BLS	0.609	-0.125	0.265	0.175	0.611	0.146	0.187	0.140
Şanlıurfa	CMED	-0.249	-0.418	-0.182	0.018	0.321	0.288	0.147	0.163
Siirt	CMED	-0.378	-0.461	-0.181	-0.559	0.307	0.419	0.156	0.552
Şile	MRT	0.276	-0.684	-0.436	0.043	0.242	0.743	0.474	0.037
Sinop	BLS	0.505	-0.308	0.060	0.385	0.564	0.338	0.115	0.353
Sivas	CCAN	-0.019	0.561	-0.223	-0.385	0.006	0.521	0.249	0.290
Tekirdağ	MRT	0.032	-0.460	0.333	0.366	0.016	0.349	0.246	0.310
Uşak	MEDT	0.303	0.386	0.024	-0.010	0.271	0.365	0.201	0.054
Van	CEAN	-0.528	0.192	0.176	0.034	0.451	0.121	0.191	0.114
Yozgat	CCAN	0.160	-0.148	0.070	-0.335	0.098	0.213	0.071	0.348
Zonguldak	BLS	0.313	-0.799	0.031	-0.059	0.379	0.810	0.171	0.012

4.4.1.4 WeMO responses

i) Spearman's rank-order correlation

Among the four climatic indices included in this study, WeMO has the least impact on precipitation extremes in Turkey. There is no station that is significantly correlated to WeMO in winter. In parallel, only 1 station has significant relationship in autumn. This station is Van from CEAN rainfall region. Also, the correlation of 3 stations are defined as significant in spring and summer. In summer, Zonguldak and İnebolu from BLS and Kütahya from MEDT are the stations having the correlations higher than the effective sample size threshold. Finally, Ankara, Alanya and Anamur stations show significant correlation with WeMO in summer.

The small impact of WeMO on winter extremes can also be perceived from Figure 4.20. As noted before, winter is the rainiest season of Turkey. Therefore, while evaluating the impact of a climate index, the responses of winter have great importance. Nevertheless, WeMO seems to be the most appropriate climate index in summer. In previous sections, it has been stated that summer extremes may create flooding risks since their anomalies are usually positives and variations are great. Herein, identifying an efficient driver such as WeMO can be an important part of taking precautions against possible hazards originated by extreme precipitation during the summer. Besides, the regions where the summer extremes are governed by SOI or WeMO appear to be complementary for each other. It may be beneficial to take advantage of these two indices while evaluating summer extremes.

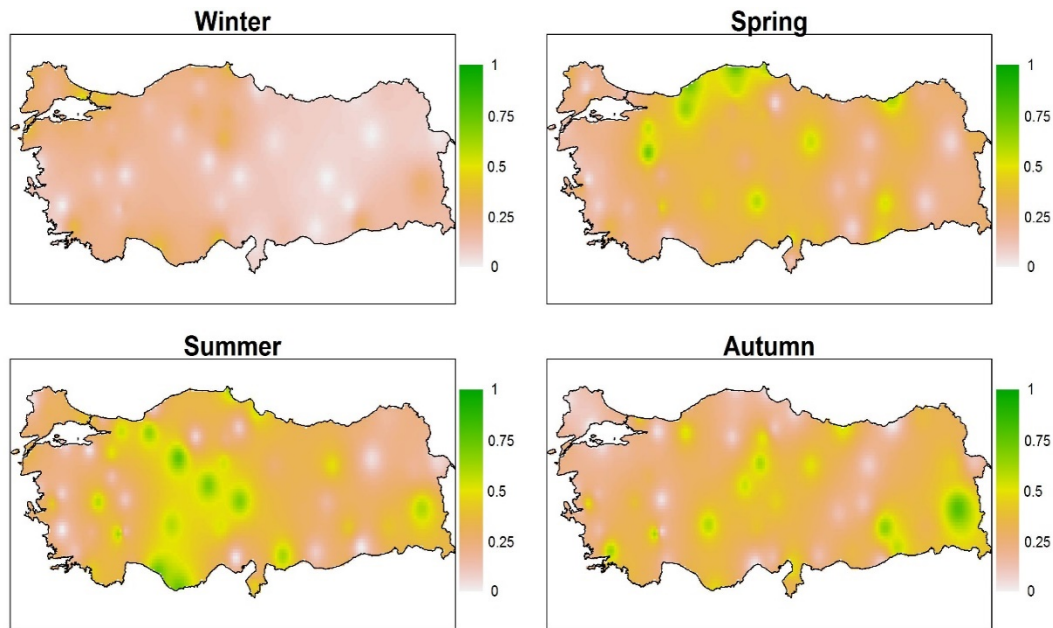


Figure 4.20 The continuous map of spearman rank order correlation coefficient between SOI and extreme precipitation with respect to seasons

The number of stations having significant relationship with WeMO are checked, more particularly for summer, considering the actual sample size threshold. The correlation coefficients that are higher than the actual sample size, 0.215, designated at 44 stations in summer. Moreover, the 13 of the 19 stations in MED have significant correlation with WeMO. Lastly, the correlations values with WeMO are higher than the actual sample size at 40, 36 and 23 stations in spring, autumn and winter respectively.

ii) Power Law Regression

According to PLR results, there is no significant relation between precipitation extremes at stations and WeMO in winter. Still, the significant relations are caught at two stations in spring and at one station in autumn. In spring, Zonguldak and İnebolu stations which are located in BLS shows significant relation with WeMO whereas Van station, from CEAN, shows significant relation with WeMO in autumn. Similar to SROC results, PLR results also prove that WeMO is a more effective climate

index on Turkey's high extreme precipitation in summer rather than the other seasons. In CCAN, two stations are significantly related to WeMO during summer. These are Ankara and Kırşehir. In addition to these two stations, R coefficient of the relationship between Kayseri station and WeMO is very close the effective sample size threshold even if it does not exceed this threshold. Also, Alanya is the another station which's R coefficient is significantly high for summer extremes.

The distribution of the R coefficients between extreme precipitation and WeMO is represented on Turkey's map in Figure 4.21. The outcome is approximating to SROC results. Like Figure 4.20, the existence of quite low relationship coefficients in winter extremes can also be seen in this figure. Besides, the spring and autumn relationships defined by PLR are parallel to the spring and autumn relationships defined by SROC. When the relationships in summer are examined, it can be distinguished that even if there is no very high differences between PLR and SROC results, PLR identifies the higher relationships in general between precipitation extremes and WeMO than SROC.

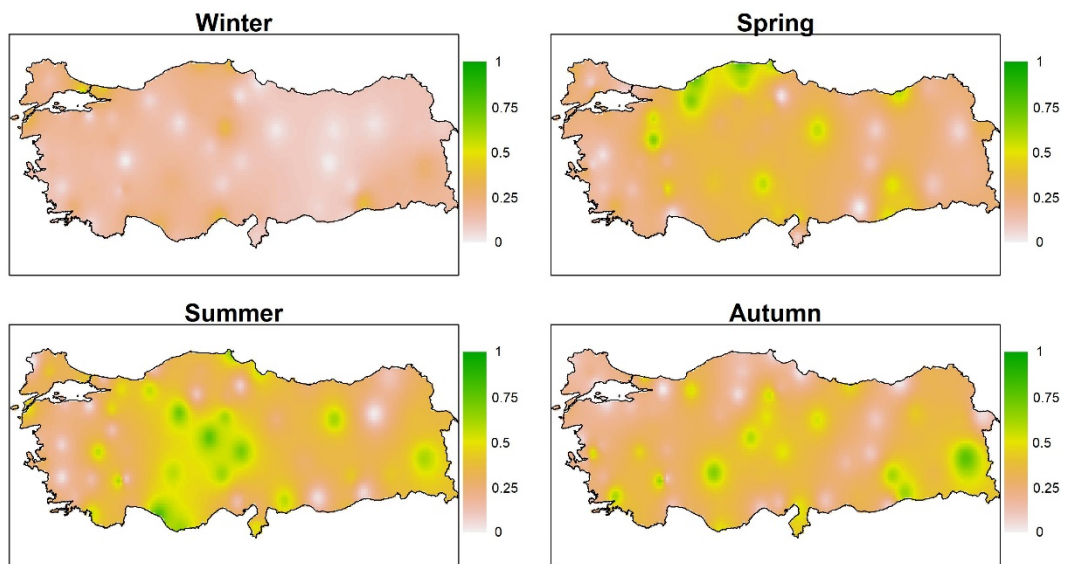


Figure 4.21 The continuous map of non-linear power law regression coefficient (R) between WeMO and extreme precipitation with respect to seasons

The PLR finds the 46 stations as significant with respect to the actual sample size threshold in summer. This number is 44 for SROC method. In fact, it can be said that the PLR and SROC results are very close to each other only by looking at these numbers. However, when comparing Figure 4.20 and Figure 4.21, it can be noticed that the PLR map contains more dark parts in summer season. The reason for this darkness is that the PLR explores higher associations between the summer extremes and WeMO than SROC at 37 stations. Thus, these results claim that the PLR explains higher relationship in summer. In addition, 42, 34 and 21 stations exceed the actual sample size threshold in spring, autumn and winter. To give more detailed representation, coefficient values of the PLR and SROC methods are denoted in Table 4.9 for each station.

Table 4.9 The relationship between anomaly of extreme precipitation and WeMO anomaly
(Bold black numbers= The significant relationship for the effective sample size and the actual
sample size, Red Numbers: The significant relationship for the actual sample size, Black Numbers=
The insignificant relationship)

Station	Region	Spearman's rank order correlation				Non-linear power law regression (R value)			
		Spring	Summer	Autumn	Winter	Spring	Summer	Autumn	Winter
Adana	MED	0.384	0.016	-0.145	0.112	0.447	0.142	0.143	0.176
Afyon	CCAN	0.211	0.106	-0.035	0.032	0.208	0.276	0.207	0.002
Ağrı	CEAN	0.065	0.191	0.439	0.087	0.067	0.377	0.374	0.116
Akhisar	MED	0.150	0.074	0.152	-0.184	0.030	0.066	0.181	0.147
Alanya	MED	-0.193	-0.746	-0.341	0.393	0.277	0.802	0.285	0.316
Anamur	MED	-0.347	-0.738	-0.474	0.250	0.347	0.645	0.501	0.144
Ankara	CCAN	0.321	0.760	0.263	0.084	0.287	0.731	0.201	0.038
Antakya	MED	0.113	0.454	-0.315	0.069	0.076	0.513	0.451	0.081
Antalya	MED	-0.052	-0.290	-0.138	-0.291	0.006	0.267	0.134	0.259
Artvin	BLS	0.223	0.170	0.363	0.115	0.175	0.119	0.327	0.121
Aydın	MED	-0.081	0.002	-0.151	0.003	0.108	0.035	0.188	0.060
Bandırma	MED	-0.186	-0.078	0.047	0.275	0.293	0.111	0.024	0.133
Bilecik	MRT	0.573	0.511	0.224	0.175	0.553	0.488	0.203	0.127
Bodrum	MED	-0.117	-0.320	-0.189	-0.014	0.134	0.279	0.180	0.093
Bolu	BLS	0.656	0.659	0.524	0.135	0.685	0.572	0.525	0.069
Burdur	MEDT	0.243	-0.635	-0.634	0.094	0.262	0.622	0.674	0.092
Bursa	MRT	0.264	-0.014	0.175	0.175	0.247	0.034	0.120	0.040
Çanakkale	MED	0.120	0.345	-0.236	0.380	0.242	0.494	0.251	0.356
Çankırı	CCAN	0.305	0.068	0.079	0.272	0.303	0.113	0.045	0.221
Ceylanpınar	CMED	-0.517	-0.290	0.086	-0.091	0.521	0.357	0.092	0.068
Çorum	CCAN	-0.387	0.225	-0.523	0.288	0.391	0.270	0.555	0.232
Denizli	MED	0.161	-0.222	-0.326	0.233	0.135	0.150	0.345	0.182
Dikili	MED	-0.093	0.130	-0.130	-0.035	0.161	0.184	0.056	0.098
Diyarbakır	CMED	-0.529	0.421	-0.666	-0.009	0.519	0.424	0.623	0.056
Dört Eylül	MED	-0.517	0.270	-0.472	0.058	0.496	0.252	0.521	0.211
Edirne	MRT	-0.332	-0.039	0.042	0.323	0.323	0.004	0.093	0.241
Elazığ	CMED	0.139	0.179	-0.121	-0.001	0.117	0.359	0.107	0.011
Erzincan	CEAN	0.123	0.489	0.089	-0.077	0.088	0.617	0.108	0.031
Erzurum	CEAN	0.372	-0.044	-0.304	0.007	0.287	0.014	0.429	0.032
Fethiye	MED	-0.193	0.451	-0.363	0.204	0.195	0.548	0.380	0.070
Florya	MRT	0.174	-0.426	-0.135	0.608	0.022	0.430	0.196	0.623
Gaziantep	CMED	0.399	0.615	-0.144	-0.146	0.295	0.580	0.116	0.114
Giresun	BLS	0.207	0.311	-0.534	-0.086	0.190	0.269	0.473	0.104
İğdır	CEAN	0.334	-0.053	-0.114	-0.021	0.338	0.359	0.044	0.091

Table 4.9 Continued

Inebolu	BLS	0.774	-0.351	-0.086	0.318	0.808	0.373	0.133	0.353
İskenderun	MED	0.250	0.235	-0.511	-0.031	0.236	0.320	0.520	0.088
Isparta	MEDT	0.479	-0.142	0.052	-0.207	0.511	0.087	0.094	0.220
İzmir	MED	-0.328	0.303	-0.147	-0.109	0.306	0.309	0.157	0.121
Kastamonu	CCAN	0.581	0.344	0.163	-0.120	0.600	0.280	0.106	0.225
Kayseri	CCAN	-0.313	-0.691	-0.449	-0.020	0.333	0.705	0.514	0.071
Kireçburnu	MRT	0.120	0.334	-0.252	0.329	0.099	0.322	0.306	0.253
Kırşehir	CCAN	-0.242	0.703	-0.553	-0.035	0.298	0.769	0.597	0.095
Konya	CCAN	-0.413	0.585	-0.593	-0.182	0.412	0.578	0.685	0.240
Kumköy	MRT	-0.067	0.531	-0.289	0.346	0.116	0.609	0.288	0.464
Kütahya	MEDT	0.731	-0.134	-0.309	0.256	0.684	0.132	0.303	0.209
Lüleburgaz	MRT	-0.053	0.305	0.109	0.177	0.084	0.415	0.209	0.138
Malatya	CMED	-0.144	-0.292	-0.142	0.076	0.287	0.279	0.163	0.100
Manisa	MED	-0.018	0.444	-0.505	-0.151	0.066	0.208	0.540	0.180
Mardin	CMED	-0.361	0.009	-0.576	0.279	0.436	0.053	0.640	0.384
Mersin	MED	-0.296	0.315	-0.010	0.424	0.351	0.352	0.093	0.391
Muğla	MED	-0.348	0.123	-0.631	0.363	0.335	0.166	0.613	0.257
Niğde	CCAN	0.591	0.526	-0.405	-0.075	0.578	0.631	0.373	0.070
Rize	BLS	0.619	0.251	-0.004	0.042	0.585	0.282	0.012	0.112
Sakarya	BLS	0.356	0.562	0.036	0.232	0.315	0.492	0.009	0.229
Samsun	BLS	0.269	-0.537	-0.069	-0.025	0.254	0.544	0.021	0.016
Şanlıurfa	CMED	0.067	-0.093	-0.349	0.015	0.005	0.040	0.342	0.073
Siirt	CMED	-0.077	-0.407	-0.331	0.155	0.114	0.416	0.357	0.206
Şile	MRT	0.244	0.147	-0.459	0.452	0.177	0.104	0.490	0.445
Sinop	BLS	0.643	-0.621	0.035	-0.417	0.643	0.685	0.013	0.409
Sivas	CCAN	-0.558	0.263	-0.498	0.042	0.573	0.252	0.534	0.024
Tekirdağ	MRT	-0.314	0.298	0.006	0.182	0.335	0.291	0.049	0.192
Uşak	MEDT	0.278	0.592	-0.393	-0.090	0.230	0.580	0.469	0.147
Van	CEAN	-0.212	0.599	0.782	-0.269	0.196	0.609	0.766	0.265
Yozgat	CCAN	-0.365	-0.536	-0.614	0.343	0.277	0.622	0.510	0.364
Zonguldak	BLS	0.731	-0.104	0.254	0.226	0.737	0.140	0.311	0.178

4.4.2 The multiple relationship analysis

In the previous section, the single relation analyses are interpreted to see the individual effect of the climate indices on high precipitation extremes. Nevertheless, in this section, the collective effect of two climate indices are investigated. However, the pair of AO and NAO are omitted from the multiple relationship analyses since they are highly correlated to each other. Furthermore, the pair of SOI and WeMO is used as input variable only for summer season. The reason for this, the SOI and WeMO are generally influential on summer extremes as stated in section 4.4.1.3 and 4.4.1.4. Apart from these, all other climate indices pairs are tested as input variables and their multiple effects on precipitation extremes are inspected.

The multiple linear regression (MLR) is chosen as the linear method while the multivariate adaptive regression splines (MARS) is chosen to explain non-linear relationship between input and output variables.

All analyses results are clarified for the 10-years block anomalies as in the previous sections.

4.4.2.1 NAO and SOI responses

i) Multiple Linear Regression (MLR)

MLR defines the significant relationships at 9 stations in winter. If the locations of these stations are checked, there are 2 stations from BLS and CCAN, 3 stations from CEAN and 1 station from MED and MEDT rainfall regions. Moreover, the summer extremes of 6 stations include the significant relationship with NAO and SOI pair. These 6 stations disperse over 4 rainfall regions; BLS, CCAN, CEAN and MRT. While two of the stations are located in BLS and MRT, one of the stations is located in CCAN and CEAN. When the results of spring anomalies are examined, it can be

seen that the extreme precipitation variation of 5 stations are significantly related to NAO and SOI at 5% significance level. BLS contains two of these stations as while CCAN, CEAN, MRT contain one of these stations. Finally, each CCAN and MRT have 1 station which have correlation coefficient higher than the effective sample size threshold.

The domain of the SOI and NAO pair on extreme precipitation of Turkey are figured on Figure 4.22. The effect of this climate indices couple on winter extreme precipitation seems greater than in other seasons. In particular, the winter extreme oscillations in the northeastern part of the BLS and CEAN are determined to depend on the NAO and SOI extremes. In addition, it can be mentioned about the similar effect for CCAN region. This climate indices pair is also an important driver for the northeastern side of the BLS in summer. Apart from this region, the effectiveness of NAO and SOI pair are detected in some small regions for this region. Finally, the relationships defined by MLR are weaker in spring and autumn.

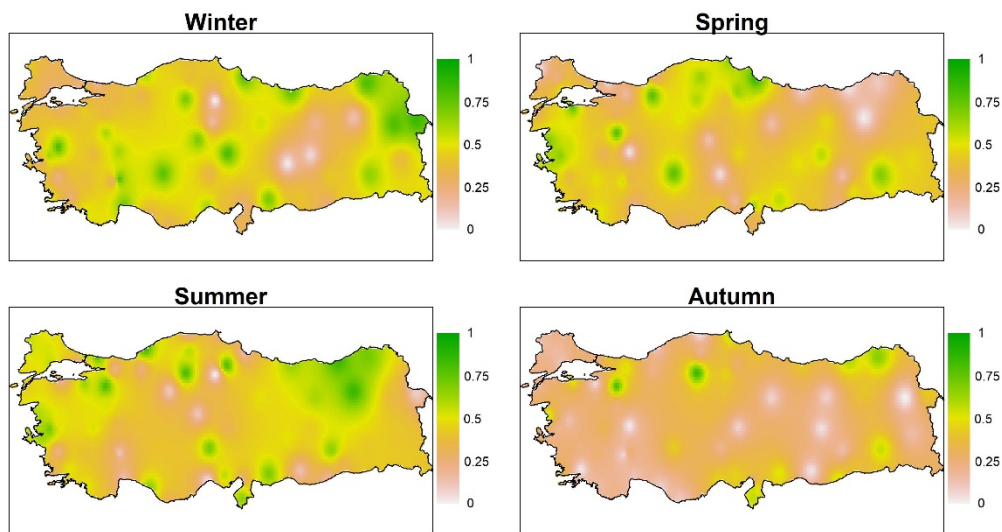


Figure 4.22 The continuous map of multiple linear regression coefficient between NAO and SOI pair and extreme precipitation with respect to seasons

When the actual sample size threshold, 0.215, tests the significance of the multiple correlation coefficients, the results show that 56 stations have the higher coefficient

than 0.215 in winter. There are the significant correlation at all of 19 stations in MED and all of 4 stations in MEDT. Further, 6 of the 8 stations in CMED marks the significant correlation. In other words, the SOI and NAO pair seems to be an important driver for the extreme precipitation of the regions having Mediterranean climate. Also, a very similar situation comes out for the spring and summer seasons. In spring, 28 of 31 stations that are located in Mediterranean climate (i.e. CMED, MED, MEDT) possess the significant correlation with the NAO and SOI pair. This number is 25 for summer season. Thus, it can be made a deduction that the NAO and SOI pair is one of the vital driver on the extreme precipitation of the areas affected by the Mediterranean climate in winter, spring and summer. Finally, the correlation values of the 38 stations are higher than the actual sample size threshold in autumn.

ii) Multivariate Adaptive Regression Splines (MARS)

In this and next MARS sections, the MARS results are evaluated comparatively with MLR results. MARS finds the significant relationship between NAO and SOI pair and the winter extremes at 26 stations. It has been 9 stations in respect to MLR results. In addition, the relationship of the 19 stations are assigned as significant in spring and 10 stations are assigned as significant in summer. MLR has found the significant relationships at 5 and 6 stations for spring and summer seasons. The significantly related station number is 2 for both MARS and MLR result in autumn. Considering these conditions, it can be claimed that MARS defines much stronger relationships between extreme precipitation and the pair of NAO and SOI except for autumn. The number of stations with significant relationship in rainfall regions are represented in Table 4.10.

Table 4.10 The number of the station having the significant relationship with NAO and SOI pair based on the effective sample size threshold with respect to the rainfall regions and seasons

Rainfall Region	Total Station Number	Number of the station having the significant relationship			
		Spring	Summer	Autumn	Winter
BLS	8	4	2	0	2
CCAN	11	3	1	0	8
CEAN	6	1	2	0	3
CMED	8	5	1	1	4
MED	19	4	1	1	6
MEDT	4	0	0	0	2
MRT	9	2	3	0	1
Total	65	19	10	2	26

Dispersion of the mars coefficient between decadal extreme precipitation of Turkey and the couple of NAO and SOI are shown in Figure 4.23. By analyzing this figure, it can be understood that the relationship coefficients are quite high in winter and spring. Especially in winter, the coefficients are greater than 0.6 in almost every side of Turkey. In summer, there are some regions in where emphasized climate indices have impact on their decadal extreme precipitation oscillation, especially in the north east of Turkey. However, these areas are not as large as in spring and winter. In autumn, the influence areas of NAO and SOI climate indices are lower than in the other seasons.

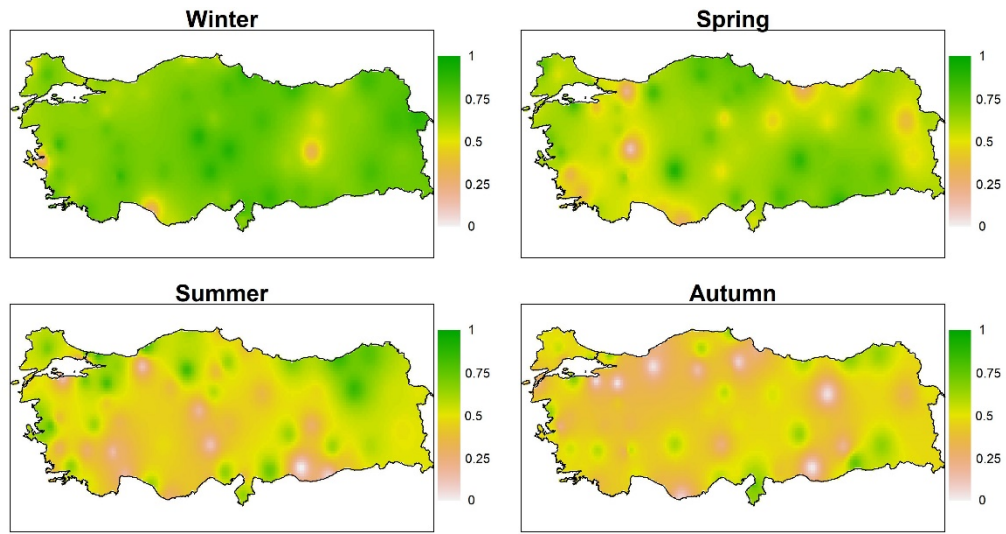


Figure 4.23 The continuous map of multivariate adaptive regression splines coefficient between NAO and SOI pair and extreme precipitation with respect to seasons

Finally, stations of which's relationship coefficients are higher than the actual sample size threshold are investigated. MARS results are almost higher than this threshold all in Turkey for winter and spring. In winter, the MARS coefficients of 64 stations are greater than the actual sample size limit of the significance measurement while in spring, the MARS coefficients of 63 stations are greater than the actual sample size limit of the significance measurement. Lastly, there are 56 and 57 stations having the significant relationship considering the actual sample size threshold in autumn and summer. In addition, to reveal the strength difference of the relationships defined by MARS and MLR, the relationship coefficients of MARS are checked against the relationship coefficients of MLR for all seasons. As a consequence, it is seen that the relationship coefficients of MARS are greater than the relationship coefficients of MLR at 63, 57, 52 and 45 stations for winter, spring, autumn and summer seasons respectively.

MLR and MARS result for all stations can be found in Table 4.11.

Table 4.11 The relationship between anomaly of extreme precipitation and the pair of NAO and SOI anomaly (Bold black numbers= The significant relationship for the effective sample size and the actual sample size, Red Numbers: The significant relationship for the a

		Multiple linear regression (MLR)				Multivariate adaptive regression splines (MARS)			
Station	Region	Spring	Summer	Autumn	Winter	Spring	Summer	Autumn	Winter
Adana	MED	0.176	0.572	0.452	0.379	0.745	0.658	0.498	0.667
Afyon	CCAN	-0.032	0.345	0.018	0.610	0.104	0.338	0.343	0.763
Ağrı	CEAN	0.368	0.366	0.000	0.790	0.374	0.540	-0.334	0.831
Akhisar	MED	0.554	0.492	0.136	0.789	0.597	0.385	0.351	0.830
Alanya	MED	0.375	0.661	0.084	0.346	0.433	0.635	0.347	0.265
Anamur	MED	0.281	0.328	0.093	0.314	0.279	0.273	0.058	0.560
Ankara	CCAN	0.517	-0.106	-0.355	0.482	0.617	0.380	0.370	0.712
Antakya	MED	0.294	0.676	0.579	0.324	0.525	0.650	0.668	0.664
Antalya	MED	0.248	0.148	0.123	0.706	0.485	0.179	0.517	0.725
Artvin	BLS	0.106	0.709	0.669	0.787	0.651	0.779	0.646	0.823
Aydın	MED	0.373	0.217	0.262	0.221	0.339	0.308	0.549	0.737
Bandırma	MED	0.746	-0.201	0.510	0.293	0.820	0.121	0.683	0.671
Bilecik	MRT	0.296	0.802	-0.798	0.356	0.597	0.808	0.024	0.582
Bodrum	MED	0.454	0.270	0.437	0.526	0.468	0.365	0.504	0.787
Bolu	BLS	0.763	-0.241	0.225	0.337	0.810	0.117	0.032	0.618
Burdur	MEDT	0.544	0.336	0.064	0.265	0.662	0.138	0.314	0.724
Bursa	MRT	0.403	0.637	-0.058	0.443	0.401	0.702	0.036	0.700
Ceylanpınar	CMED	0.221	-0.181	0.533	0.247	0.877	-0.055	0.509	0.765
Çanakkale	MED	0.327	0.441	0.209	-0.359	0.565	0.468	0.274	0.594
Çankırı	CCAN	0.597	0.798	-0.845	0.697	0.660	0.830	-0.153	0.764
Çorum	CCAN	0.379	0.003	-0.462	-0.004	0.736	0.378	0.402	0.736
Denizli	MED	0.493	0.393	0.261	0.378	0.499	0.277	0.585	0.657
Dikili	MED	0.705	0.614	0.548	0.391	0.734	0.674	0.667	0.647
Diyarbakır	CMED	0.152	0.663	-0.150	0.424	0.733	0.632	0.197	0.654
Dört Yol	MED	0.645	0.226	0.278	0.243	0.616	0.352	0.610	0.807
Edirne	MRT	0.073	0.549	0.151	0.436	0.767	0.558	0.508	0.496
Elazığ	CMED	0.583	-0.437	0.042	0.058	0.711	0.284	0.427	0.321
Erzincan	CEAN	0.476	0.611	0.088	0.199	0.506	0.469	0.034	0.539
Erzurum	CEAN	-0.012	0.843	0.407	0.137	0.746	0.844	0.462	0.663
Fethiye	MED	0.521	0.506	0.162	0.526	0.600	0.525	0.362	0.771
Florya	MRT	0.559	0.085	0.234	0.156	0.747	0.251	0.646	0.526
Gaziantep	CMED	0.574	0.686	0.514	0.700	0.798	0.731	0.408	0.847
Giresun	BLS	0.096	0.636	0.429	0.753	0.276	0.700	0.608	0.851
Iğdır	CEAN	0.418	-0.089	0.437	0.845	0.607	0.516	0.500	0.877

Table 4.11 Continued

Inebolu	BLS	0.483	0.232	-0.044	0.382	0.788	0.618	0.409	0.520
Isparta	MEDT	0.340	-0.115	0.269	0.785	0.477	0.288	0.568	0.855
İskenderun	MED	0.329	0.526	0.582	0.291	0.598	0.584	0.788	0.833
İzmir	MED	0.606	0.642	-0.223	-0.303	0.603	0.687	0.539	0.163
Kastamonu	CCAN	0.633	0.581	0.209	0.392	0.817	0.580	-0.607	0.697
Kayseri	CCAN	0.467	0.321	-0.078	0.802	0.574	0.369	0.493	0.894
Kırşehir	CCAN	0.136	0.117	0.368	0.694	0.727	0.182	0.476	0.898
Kireçburnu	MRT	0.376	0.700	0.217	0.237	0.531	0.855	0.448	0.631
Konya	CCAN	0.753	0.405	0.435	0.757	0.902	0.480	0.603	0.758
Kumköy	MRT	0.048	0.642	0.183	0.078	0.435	0.701	0.488	0.519
Kütahya	MEDT	-0.771	0.523	0.237	0.604	0.597	0.429	0.428	0.744
Lüleburgaz	MRT	0.230	0.533	0.163	0.315	0.520	0.708	0.564	0.772
Malatya	CMED	0.498	0.497	0.260	-0.019	0.864	0.636	0.648	0.628
Manisa	MED	0.668	0.712	-0.200	0.617	0.730	0.759	0.221	0.649
Mardin	CMED	0.486	0.330	0.400	0.438	0.719	0.410	0.746	0.688
Mersin	MED	0.449	0.032	0.466	0.613	0.588	0.358	0.585	0.679
Muğla	MED	0.389	0.506	0.029	0.262	0.347	0.651	0.482	0.598
Niğde	CCAN	-0.053	-0.699	0.209	0.350	0.494	0.125	0.242	0.882
Rize	BLS	0.040	0.845	0.597	0.420	0.456	0.853	0.669	0.560
Sakarya	BLS	-0.175	-0.217	0.526	0.343	0.202	0.648	0.336	0.591
Samsun	BLS	0.837	-0.161	0.402	0.754	0.808	0.416	0.213	0.864
Siirt	CMED	0.678	0.426	0.557	0.650	0.765	0.592	0.656	0.808
Sinop	BLS	0.660	0.243	0.610	0.447	0.832	0.407	0.691	0.548
Sivas	CCAN	0.152	0.489	0.079	0.536	0.450	0.364	0.530	0.812
Şanlıurfa	CMED	0.418	0.143	-0.037	0.405	0.664	0.001	0.021	0.766
Şile	MRT	0.073	0.759	0.431	0.187	0.513	0.858	0.683	0.681
Tekirdağ	MRT	0.500	0.574	0.108	0.223	0.586	0.568	0.362	0.701
Uşak	MEDT	0.321	0.526	0.331	0.374	0.597	0.635	0.357	0.675
Van	CEAN	0.470	0.411	0.160	0.380	0.484	0.490	0.470	0.697
Yozgat	CCAN	-0.362	0.343	-0.388	0.166	0.470	0.586	0.575	0.671
Zonguldak	BLS	0.260	0.805	-0.137	0.596	0.602	0.795	-0.230	0.637

4.4.2.2 AO and SOI responses

i) Multiple Linear Regression (MLR)

The significant relationship between precipitation extremes and the pair of AO and SOI is distinguished at three stations in winter season. Two of these three stations, Ankara and Kayseri, are located in CCAN while one of those stations, Ağrı, are located in CEAN region. In addition, the relationship coefficient is higher than the effective sample size threshold at four stations in spring. BLS includes two of these four stations. Samsun and Bolu are the stations, which belong to BLS region. Also, the extreme precipitation behavior of Konya, from CCAN, and Bandırma, from MED are significantly related to the pair of AO and SOI in spring according to the MLR results. Besides, in autumn, there are significant relationship at two stations that are Kütahya and Uşak stations from MEDT region. Finally, the higher relationships are specified at the stations in the northeastern part of Turkey for summer.

The distribution of the influence of AO and SOI pair on extreme precipitation fluctuation is demonstrated over Turkish map in Figure 4.24. This figure projects that the stated climate index pair is most effective on Turkey's extreme precipitation in winter even if the number of stations exceeding the effective sample size threshold is higher in spring. To support this projection, the relationship coefficients for spring and winter are compared. As a result of the comparison, it is seen that the relationship coefficients in winter are greater than the relationship coefficients in spring at 36 stations whereas the relationship coefficients in spring are greater than the relationship coefficients in winter at 29 stations. Furthermore, in the section 4.4.1.3, it has been stated that SOI is typically not a significant driver for autumn extremes. In parallel with this expression, the impact area of the AO and SOI pair is obtained in analogy to the impact area of AO for this season. In autumn, the relatively high correlation between the climate indices pair and the extreme

precipitation anomalies is detected along the region extending from southwest coast to CMED.

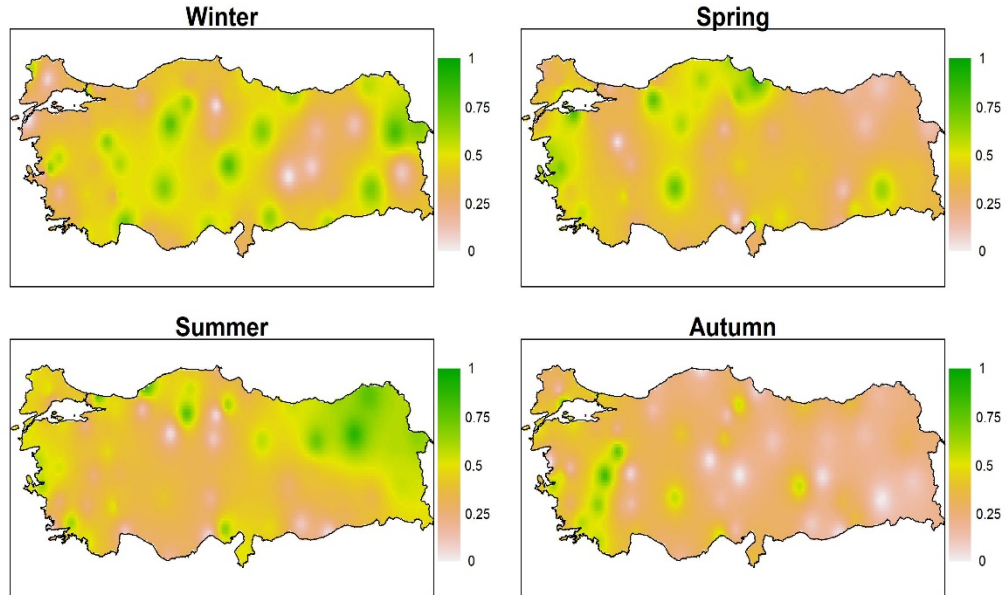


Figure 4.24 The continuous map of multiple linear regression coefficient between AO and SOI pair and extreme precipitation with respect to seasons

By taking the actual sample size threshold into consideration, 54 stations in spring and 53 stations in winter are significantly correlated to AO and SOI pair. Similar to NAO and SOI pair, 27, 25 and 26 of 31 stations that are under the effect of Mediterranean climate have significant relationship with AO and SOI pair. At this point, starting from this similarity, it is decided to compare MLR coefficients obtained by AO and SOI pair with MLR coefficients obtained by NAO and SOI pair for each station. The main purpose is to see which climate indices pair has the greater impression on the decadal extreme precipitation in Turkey. Therefore, it is realized that NAO and SOI pair is more effective in spring, summer and winter whereas AO and SOI pair is more effective in autumn.

ii) Multivariate Adaptive Regression Splines (MARS)

According to the MARS results, there are significant relationship between AO and SOI pair and winter extremes at 22 stations. According to MLR results it is only 3 stations. In addition, the relationship of the 9 stations are assigned as significant in spring and 8 stations are assigned as significant in autumn. MLR has found the significant relationships at 4 and 2 stations for spring and autumn season. There are also increase in the significantly related station number in summer from 5 to 7. Considering these conditions, it can be claimed that MARS defines much stronger relationships between extreme precipitation and the pair of AO and SOI than MLR. The number of stations with significant relationship in rainfall regions are represented in Table 4.12.

Table 4.12 The number of the stations with significant relationship for AO and SOI pair based on the effective sample size threshold with respect to the rainfall regions and seasons

Rainfall Region	Total Station Number	Number of the station having the significant relationship			
		Spring	Summer	Autumn	Winter
BLS	8	2	2	0	1
CCAN	11	2	1	1	7
CEAN	6	0	3	0	2
CMED	8	3	0	3	3
MED	19	2	0	2	6
MEDT	4	0	0	1	2
MRT	9	0	1	1	1
Total	65	9	7	8	22

The continuous map of the MARS relationship coefficient is also specified in Figure 4.25. In line with this figure, the pair of AO and SOI is one of the main drivers on winter extremes across Turkey with the exception of small areas. Besides, if the Figure 4.24 and Figure 4.25 are comparatively examined, it can be easily asserted that the MARS results give much higher relationship values than MLR. To reinforce this assertion, the relationship coefficients of MARS are checked against the

relationship coefficients of MLR for all seasons. In consequences of the check, it is seen that the relationship coefficients of MARS are greater than the relationship coefficients of MLR at 61, 50, 48 and 43 stations for winter, spring, autumn and summer seasons respectively. Besides, the power of the MLR coefficients obtained by AO and SOI pair are tested against MLR coefficients obtained by NAO and SOI pair for each station in previous section. The same test is also applied to MARS outcomes. Consequently, based on MARS outcomes, it is found out that the NAO and SOI pair is more decisive in spring, summer and winter. Yet, the AO and SOI pair is more active in autumn. It is worthwhile to remind that this condition is also the same for MLR outcomes.

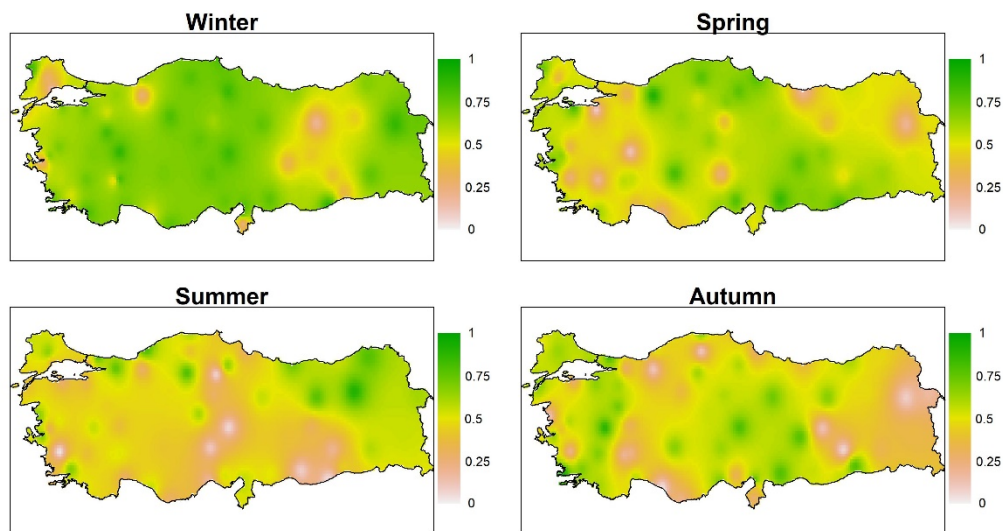


Figure 4.25 The continuous map of multivariate adaptive regression splines coefficient between AO and SOI pair and extreme precipitation with respect to seasons

Finally, the significance of the relationships are evaluated regarding actual sample size threshold. MARS results are almost higher than this threshold all in Turkey for winter and spring. In winter, the MARS coefficients of 63 stations are greater than the actual sample size limit of the significance measurement while in spring, the MARS coefficients of 60 stations are greater than the actual sample size limit of the

significance measurement. Lastly, there are 53 and 57 stations having the significant relationship considering the actual sample size threshold in autumn and summer.

Table 4.13 exhibits the MLR and MARS result of all stations included by this study.

Table 4.13 The relationship between anomaly of extreme precipitation and the pair of AO and SOI anomaly (Bold black numbers= The significant relationship for the effective sample size and the actual sample size, Red Numbers: The significant relationship for the actual sample size, Black Numbers= The insignificant relationship)

		Multiple linear regression (MLR)				Multivariate adaptive regression splines (MARS)			
Station	Region	Spring	Summer	Autumn	Winter	Spring	Summer	Autumn	Winter
Adana	MED	-0.048	0.654	0.156	0.522	0.779	0.530	0.324	0.741
Afyon	CCAN	-0.202	0.327	0.056	0.604	0.121	0.385	0.320	0.862
Ağrı	CEAN	0.320	0.593	0.313	0.802	0.194	0.571	0.091	0.850
Akhisar	MED	0.539	0.533	0.152	0.592	0.343	0.516	0.586	0.698
Alanya	MED	0.377	0.263	0.252	0.291	0.252	0.557	0.033	0.528
Anamur	MED	0.296	0.188	0.192	0.274	0.417	0.281	0.211	0.773
Ankara	CCAN	0.604	-0.041	0.424	0.776	0.648	0.479	0.370	0.794
Antakya	MED	0.272	0.512	0.393	-0.280	0.501	0.529	0.267	0.237
Antalya	MED	0.261	0.110	0.411	0.725	0.386	-0.301	0.571	0.724
Artvin	BLS	-0.114	0.770	0.173	0.577	0.497	0.779	0.467	0.680
Aydın	MED	0.419	-0.263	0.290	0.165	0.252	-0.025	0.212	0.579
Bandırma	MED	0.811	-0.493	0.493	0.273	0.802	-0.268	0.274	0.699
Bilecik	MRT	0.336	0.391	0.218	0.389	0.502	0.498	0.630	0.545
Bolu	BLS	0.755	-0.143	-0.151	0.232	0.905	0.291	0.114	0.259
Burdur	MEDT	0.508	0.520	-0.222	0.325	0.578	0.511	0.183	0.479
Bursa	MRT	0.289	0.228	-0.305	0.295	-0.085	-0.347	0.661	0.709
Ceylanpınar	CMED	0.192	-0.041	-0.036	0.607	0.823	0.040	0.561	0.868
Çanakkale	MED	0.341	0.526	0.496	-0.010	0.593	0.401	0.657	0.464
Çankırı	CCAN	0.527	0.776	0.281	0.660	0.533	0.785	0.619	0.706
Çorum	CCAN	0.360	0.050	0.138	-0.029	0.690	-0.075	0.520	0.679
Denizli	MED	0.420	0.258	0.663	0.464	0.185	0.393	0.678	0.724
Dikili	MED	0.623	0.600	-0.008	0.364	0.590	0.676	0.122	0.593
Diyarbakır	CMED	0.129	0.367	-0.349	0.311	0.487	0.196	-0.069	0.406
Dört Yol	MED	0.643	0.457	0.309	0.374	0.589	0.568	0.757	0.789
Edirne	MRT	-0.219	0.506	0.275	0.599	0.728	0.557	0.510	0.826
Elazığ	CMED	0.374	0.391	0.037	-0.078	0.676	0.319	0.128	0.427
Erzincan	CEAN	0.302	0.727	0.153	-0.171	0.379	0.763	0.670	0.189

Table 4.13 Continued

Erzurum	CEAN	-0.137	0.882	0.142	0.129	0.492	0.903	0.475	0.444
Fethiye	MED	0.430	0.523	0.576	0.512	0.614	0.498	0.613	0.787
Florya	MRT	0.623	0.490	0.326	0.183	0.631	0.424	0.631	0.513
Gaziantep	CMED	0.498	0.474	0.290	0.660	0.846	0.511	0.782	0.759
Giresun	BLS	0.235	0.547	-0.414	0.631	0.178	0.709	0.380	0.672
İğdir	CEAN	0.128	0.666	0.254	0.678	0.501	0.618	0.164	0.742
Inebolu	BLS	0.509	0.417	-0.041	0.413	0.692	0.594	0.655	0.720
Isparta	MEDT	0.344	0.373	0.138	0.546	0.566	0.515	0.214	0.805
İskenderun	MED	0.224	0.528	0.315	0.300	0.503	0.567	0.346	0.739
İzmir	MED	0.645	0.629	0.630	-0.169	0.720	0.681	0.640	0.236
Kastamonu	CCAN	0.608	0.553	-0.216	0.324	0.772	0.414	-0.111	0.778
Kayseri	CCAN	0.454	-0.377	0.008	0.793	0.592	-0.062	0.794	0.836
Kırşehir	CCAN	0.296	0.323	0.020	0.436	0.649	0.609	0.556	0.747
Kireçburnu	MRT	0.387	0.529	0.417	0.447	0.515	0.543	0.517	0.697
Konya	CCAN	0.746	0.413	0.568	0.690	0.800	0.408	0.665	0.709
Kumköy	MRT	0.263	0.323	0.691	-0.270	0.515	0.516	0.637	0.333
Kütahya	MEDT	0.034	0.473	0.743	0.677	0.503	0.442	0.705	0.808
Lüleburgaz	MRT	0.310	0.519	0.147	-0.060	0.366	0.656	0.643	0.276
Malatya	CMED	0.427	0.266	0.569	-0.013	0.766	0.392	0.774	0.340
Manisa	MED	0.687	0.497	0.529	0.676	0.666	0.330	0.410	0.684
Mardin	CMED	0.517	0.317	0.371	0.474	0.670	0.442	0.778	0.360
Mersin	MED	0.419	-0.047	0.541	0.605	0.644	0.175	0.678	0.682
Muğla	MED	0.570	0.623	0.588	0.333	0.519	0.679	0.682	0.532
Niğde	CCAN	0.242	-0.197	0.159	0.410	0.254	0.110	0.633	0.761
Rize	BLS	0.168	0.633	0.383	0.386	0.537	0.559	0.600	0.524
Sakarya	BLS	-0.291	0.479	0.337	0.332	0.326	0.746	0.301	0.648
Samsun	BLS	0.834	0.313	-0.068	0.513	0.766	0.321	-0.300	0.700
Siirt	CMED	0.640	0.356	0.014	0.705	0.630	0.586	0.339	0.745
Sinop	BLS	0.626	0.219	0.278	0.366	0.644	0.399	0.418	0.793
Sivas	CCAN	0.259	0.575	0.116	0.692	0.622	0.560	0.716	0.751
Şanlıurfa	CMED	0.392	0.109	-0.102	0.423	0.685	-0.089	0.554	0.600
Şile	MRT	0.147	0.763	0.420	-0.189	0.477	0.763	0.816	0.571
Tekirdağ	MRT	0.583	0.229	0.657	0.226	0.631	0.412	0.610	0.161
Uşak	MEDT	0.376	0.246	0.822	0.376	0.485	0.562	0.876	0.700
Van	CEAN	0.401	0.552	-0.105	0.105	0.538	0.554	0.354	0.662
Yozgat	CCAN	0.172	0.107	0.440	0.241	0.385	0.292	0.595	0.629
Zonguldak	BLS	0.300	0.799	0.174	0.388	0.628	0.802	0.493	0.633

4.4.2.3 NAO and WeMO responses

i) Multiple Linear Regression (MLR)

The main influence of the NAO and WeMO pair on decadal extreme precipitation of Turkey are determined in summer. In total, the MLR coefficients of 8 stations are higher than the effective sample size limit in summer. In detail, 2 stations belong to BLS, CCAN and MRT while each one of the remaining two stations belongs to CMED and MED rainfall regions. Furthermore, the decadal extreme precipitation of 5, 3, and 4 stations are significantly depended on NAO and WeMO couple in spring, autumn and winter.

Parallel to the above mentioned statement, Figure 4.26 displays that the impact of NAO and WeMO pair is highest for summer. In other seasons, relatively low relationships are defined by MLR. Previously, it has been stated that the winter receives the highest amount of rainfall in Turkey. In addition, it has been noted that NAO is the climate indices which shows the highest relationship with extreme precipitation of Turkey during winter according to the single relationship analyses. Further, the relationships calculated by the single fittings may be higher than the relationships calculated by the multiple fittings because cross-validation procedure is applied when forming multiple regression models to avoid overfitting. Herewith, the single analysis of NAO is compared with the multiple analysis of NAO and WeMO pair since the winter relationships seem to be low in Figure 4.26. As a result, it is seen that the single effect of NAO is higher than the multiple effect of NAO and WeMO pair.

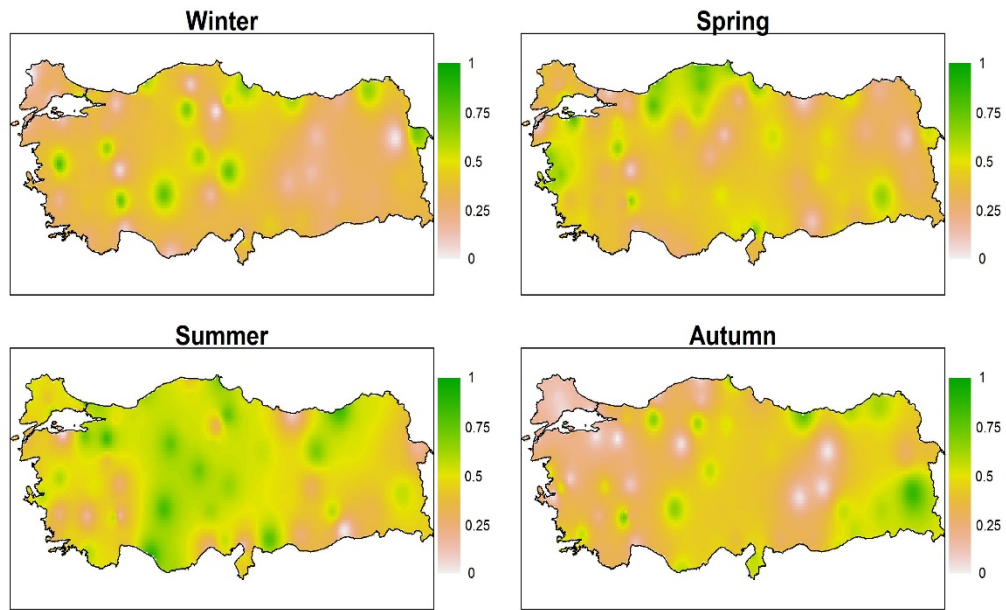


Figure 4.26 The continuous map of multiple linear regression coefficient between NAO and WeMO pair and extreme precipitation with respect to seasons

If the significance of the relationships are measured based on the actual sample size threshold, it is spotted that the summer anomalies of extreme precipitation are significantly connected to NAO and WeMO pair at 57 stations. Specifically in Mediterranean climate zones (CMED, MED, MEDT), the considerable amount of the stations indicates higher correlation values than 0.215. After summer, the utmost significant correlation is achieved in spring. 53 stations have the significant correlation with NAO and WeMO pair in this season. Finally, the significant relationships are caught at 46 stations for autumn and winter.

ii) Multivariate Adaptive Regression Splines (MARS)

Like in other climate indices pairs, MARS defines significant relationship at more stations than MLR. In summer, there is significant relationship between extreme precipitation anomalies and the couple of NAO and WeMO. It has been 8 stations in respect to MLR results. In addition, the relationship of the 8 stations are assigned as

significant in winter. MLR has found the significant relationships at 4 for winter. There are also increase in the significantly related station number in spring from 5 to 6 and in autumn from 3 to 6. The number of stations with significant relationship in rainfall regions are represented in Table 4.14.

Table 4.14 The number of the stations with significant relationship with NAO and WeMO pair based on the effective sample size threshold with respect to the rainfall regions and seasons

Rainfall Region	Total Station Number	Number of the station having the significant relationship			
		Spring	Summer	Autumn	Winter
BLS	8	2	3	2	1
CCAN	11	0	3	0	3
CEAN	6	0	3	1	1
CMED	8	0	3	0	0
MED	19	4	1	2	1
MEDT	4	0	1	1	1
MRT	9	0	5	0	1
Total	65	6	19	6	8

NAO and WeMO pair drives the summer extremes in the remarkable proportion of the Turkey (Figure 4.27). Exceptionally, it can be said that the values of the relationship drop in the western part of Turkey and in a part of CMED. Besides, It can be claimed that this climate indices couple is some more active over the western Turkey in winter and spring. Yet, in the autumn, the activity predominantly takes place in the southern part.

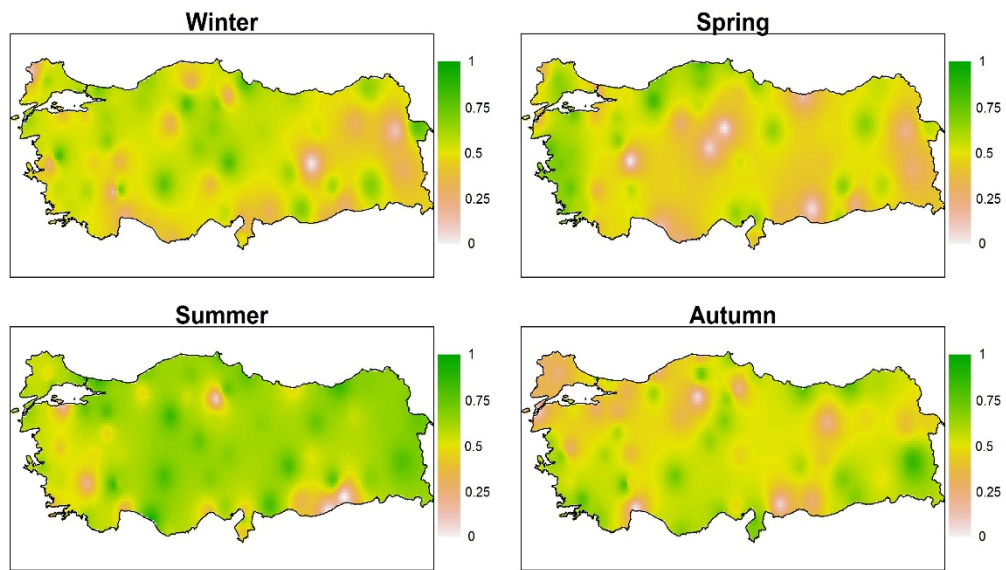


Figure 4.27 The continuous map of multivariate adaptive regression splines coefficient between NAO and WeMO pair and extreme precipitation with respect to seasons

As a final point, the significance of the relationships are tested based on the actual sample size threshold. MARS results are greater than this threshold at 60 stations for summer and autumn. In winter, the MARS coefficients of 61 stations are higher than the actual sample size limit of the significance measurement. Lastly, there are 58 stations having the significant relationship considering the actual sample size threshold in spring.

Table 4.15 exhibits the MLR and MARS result of all stations included by this study.

Table 4.15 The relationship between anomaly of extreme precipitation and the pair of NAO and WeMO anomaly (*Bold black numbers= The significant relationship for the effective sample size and the actual sample size, Red Numbers: The significant relationship for the actual sample size, Black Numbers= The insignificant relationship*)

		Multiple linear regression (MLR)				Multivariate adaptive regression splines (MARS)			
Station	Region	Spring	Summer	Autumn	Winter	Spring	Summer	Autumn	Winter
Adana	MED	0.513	0.564	0.379	0.346	0.652	0.643	0.463	0.574
Afyon	CCAN	0.086	0.257	0.105	-0.048	0.013	0.557	0.369	0.341
Ağrı	CEAN	-0.113	0.412	0.297	-0.020	0.209	0.660	0.388	0.128
Akhisar	MED	0.552	-0.601	0.074	0.792	0.666	-0.417	0.252	0.807
Alanya	MED	0.254	0.884	0.347	0.351	0.162	0.930	0.561	0.397
Anamur	MED	0.240	0.627	0.580	-0.081	0.237	0.569	0.684	0.347
Ankara	CCAN	0.277	0.748	0.036	0.395	0.259	0.849	-0.337	0.323
Antakya	MED	-0.344	0.432	0.570	0.340	-0.405	0.408	0.692	0.508
Antalya	MED	0.209	0.406	0.127	0.074	0.528	0.325	0.018	0.233
Artvin	BLS	0.208	0.531	0.622	0.645	0.564	0.677	0.597	0.657
Aydın	MED	0.377	0.229	0.365	-0.197	0.739	0.554	0.515	0.570
Bandırma	MED	0.768	-0.017	0.245	-0.134	0.744	0.125	0.525	0.380
Bilecik	MRT	0.540	0.830	-0.004	-0.255	0.599	0.782	-0.283	0.617
Bodrum	MED	0.453	0.301	0.541	0.280	0.730	0.354	0.649	0.467
Bolu	BLS	0.760	0.530	0.677	0.352	0.829	0.465	0.629	0.621
Burdur	MEDT	0.279	0.582	0.746	-0.432	0.498	0.840	0.794	0.154
Bursa	MRT	0.311	0.718	-0.022	0.283	0.403	0.740	0.260	0.436
Ceylanpınar	CMED	0.466	0.340	0.526	0.242	0.600	-0.014	0.557	0.328
Çanakkale	MED	0.073	0.363	0.177	0.192	0.367	0.655	0.118	0.637
Çankırı	CCAN	0.602	0.542	-0.632	0.702	0.562	0.546	-0.052	0.783
Çorum	CCAN	0.370	0.324	0.525	-0.016	0.413	0.076	0.649	0.675
Denizli	MED	0.356	-0.186	0.219	0.412	0.348	0.193	0.562	0.597
Dikili	MED	0.694	0.427	0.521	0.400	0.783	0.557	0.643	0.569
Diyarbakır	CMED	0.459	0.588	0.567	0.209	0.666	0.762	0.692	0.621
Dört Yol	MED	0.719	0.122	0.437	-0.251	0.682	0.382	0.600	-0.346
Edirne	MRT	0.393	0.524	0.140	-0.001	0.342	0.548	0.283	0.135
Elazığ	CMED	0.497	0.305	-0.044	-0.150	0.413	0.518	0.424	0.019
Erzincan	CEAN	0.490	0.700	-0.021	0.145	0.487	0.733	0.212	0.538
Erzurum	CEAN	0.229	0.522	0.441	-0.308	0.668	0.562	0.460	0.302
Fethiye	MED	0.395	0.590	0.282	-0.247	0.415	0.627	0.662	0.508
Florya	MRT	0.551	0.344	0.019	0.575	0.711	0.663	0.504	0.649
Gaziantep	CMED	0.463	0.776	0.295	0.437	0.351	0.813	0.083	0.322
Giresun	BLS	-0.069	0.095	0.771	0.620	0.159	0.465	0.752	0.604

Table 4.15 Continued

İğdır	CEAN	0.545	0.173	0.374	0.721	0.579	0.735	0.440	0.786
Inebolu	BLS	0.792	0.418	-0.076	0.474	0.816	0.637	0.330	0.457
Isparta	MEDT	0.674	-0.173	0.258	0.769	0.590	0.611	0.451	0.731
İskenderun	MED	0.312	0.563	0.622	-0.496	0.521	0.664	0.790	0.290
İzmir	MED	0.620	0.583	-0.011	-0.315	0.678	0.662	0.623	0.432
Kastamonu	CCAN	0.739	0.527	0.142	0.083	0.688	0.688	-0.726	0.297
Kayseri	CCAN	0.407	0.646	0.417	0.748	0.535	0.680	0.452	0.788
Kırşehir	CCAN	0.198	0.723	0.577	0.653	0.072	0.745	0.643	0.659
Kireçburnu	MRT	-0.256	0.671	0.237	0.072	0.424	0.808	0.569	0.465
Konya	CCAN	0.462	0.811	0.668	0.755	0.461	0.801	0.716	0.752
Kumköy	MRT	0.051	0.759	0.149	0.401	0.314	0.894	0.678	0.556
Kütahya	MEDT	0.649	0.388	0.267	0.659	0.670	0.450	0.609	0.668
Lüleburgaz	MRT	0.240	0.414	-0.070	0.323	0.676	0.473	0.231	0.619
Malatya	CMED	0.287	0.482	-0.037	-0.166	0.419	0.805	0.605	0.630
Manisa	MED	0.668	0.516	0.538	0.378	0.717	0.525	0.670	0.236
Mardin	CMED	0.333	-0.007	0.570	0.335	0.227	0.003	0.686	0.280
Mersin	MED	0.434	0.213	0.468	0.342	0.500	0.367	0.673	0.503
Muğla	MED	0.490	0.461	0.567	0.347	0.591	0.508	0.767	0.554
Niğde	CCAN	0.512	0.623	0.417	0.162	0.478	0.685	0.551	0.372
Rize	BLS	0.535	0.845	0.607	0.181	0.489	0.848	0.756	0.491
Sakarya	BLS	0.194	0.481	0.432	0.114	0.493	0.636	0.316	0.535
Samsun	BLS	0.669	0.517	0.305	0.699	0.671	0.761	0.590	0.803
Siirt	CMED	0.647	0.350	0.592	0.270	0.585	0.667	0.496	0.684
Sinop	BLS	0.736	0.731	0.627	0.436	0.671	0.760	0.704	0.553
Sivas	CCAN	0.551	0.556	0.456	0.431	0.647	0.655	0.521	0.584
Şanlıurfa	CMED	0.116	-0.254	0.301	0.395	0.050	-0.338	0.262	0.689
Şile	MRT	-0.051	0.638	0.397	0.448	0.541	0.874	0.570	0.752
Tekirdağ	MRT	0.567	0.588	-0.036	0.075	0.688	0.657	0.317	0.534
Uşak	MEDT	0.313	0.516	0.487	0.364	0.479	0.471	0.609	0.443
Van	CEAN	0.280	0.568	0.860	0.392	0.261	0.783	0.854	0.299
Yozgat	CCAN	0.128	0.555	0.451	0.264	0.010	0.578	0.685	0.669
Zonguldak	BLS	0.704	0.621	0.133	0.617	0.699	0.706	0.275	0.660

4.4.2.4 AO and WeMO responses

i) Multiple Linear Regression (MLR)

The significant relationship between precipitation extremes and the pair of AO and WeMO is obtained at 6 stations in summer. 2 of 6 stations are located in CEAN while the remaining are located in BLS, CCAN, MED and MEDT regions one by one. In addition, the relationship coefficient is higher than the effective sample size threshold at 5 stations in autumn. MEDT includes 2 of 5 stations. Remaining stations belong to BLS, CEAN and MED rainfall regions. Also, the extreme precipitation behavior of 3 stations, 2 from CCAN and 1 from MED, are significantly related to the AO and WeMO pair in spring according to the MLR results. Lastly, in winter, there are only 2 stations which point the significant relationship.

The distribution of the MLR coefficients is denoted on the Turkey map in Figure 4.28. In summer, CCAN, CEAN and the northern BLS are obviously under the influence of AO and WeMO pair. In addition, the values of the correlations in autumn increase regarding the single analyses of AO and WeMO. The single influence of AO on decadal extreme precipitation maintains its presence on the same areas. Additionally, correlation in small areas are also revealed. The most apparent one of these areas takes places in southeastern of Turkey. Examining the MLR results of the spring extremes, the extreme precipitation of the regions in the western Turkey and the westernmost of the BLS is related to the pair of AO and WeMO. Finally, the high relationships attract the attention in the inner parts of Turkey during winter months.

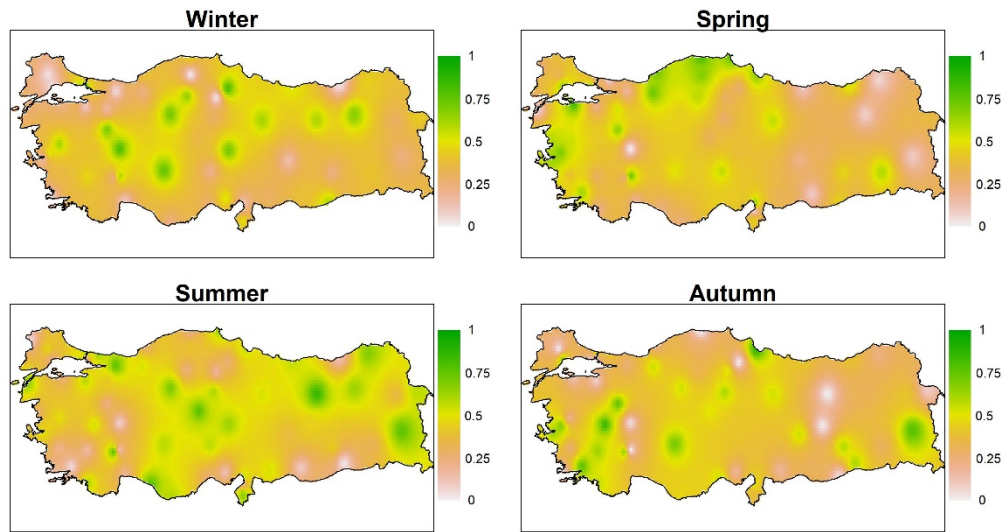


Figure 4.28 The continuous map of multiple linear regression coefficient between AO and WeMO pair and extreme precipitation with respect to seasons

In like manner to the other climate index pairs, the significance of the relationships are evaluated with respect to the actual sample size for AO and WeMO pair. In consequence of the evaluation, the MLR coefficients are found as significant at 54 stations in spring. Also, in summer, 52 stations have the significant correlation with NAO and WeMO pair. Finally, the significant relationships are caught at 50 stations for autumn and winter.

ii) Multivariate Adaptive Regression Splines (MARS)

In accordance with MARS, AO and SOI pair is a significant driver for the summer extremes at 16 stations. It has been only 6 stations considering MLR results. In addition, the relationship of the 11 stations are assigned as significant in spring and 8 stations are assigned as significant in autumn. MLR has found the significant relationships at 3 and 5 stations for spring and autumn seasons. There are also increase in the significantly related station number in winter from 2 to 5. Thus, it can be inferred that MARS expresses much stronger relationships between extreme

precipitation and the pair of AO and SOI. The number of stations with significant relationship in rainfall regions are represented in Table 4.16

Table 4.16 The number of the station with significant relationship with AO and WeMO pair based on the effective sample size threshold with respect to the rainfall regions and seasons

Rainfall Region	Total Station Number	Number of the station having the significant relationship			
		Spring	Summer	Autumn	Winter
BLS	8	2	2	0	0
CCAN	11	0	3	3	2
CEAN	6	0	2	1	0
CMED	8	0	1	0	1
MED	19	6	3	1	1
MEDT	4	1	1	2	1
MRT	9	2	4	1	0
Total	65	11	16	8	5

Figure 4.29 represents the continuous map of the MARS relationship coefficients. In keeping with this figure, it is likely to deduce that the pair of AO and WeMO is one of the main drivers on summer extremes across Turkey excluding small areas. Further, NAO and SOI pair is defined as an important driver for summer extremes in section 4.4.2.3. To measure which impact is stronger, the magnitude of the MARS coefficients for NAO and WeMO are compared with the MARS coefficients for AO and WeMO at each station. In summer, the relationship coefficients of AO and WeMO are greater at 29 stations while the relationship coefficients of NAO and WeMO are greater at 36 stations. Also, this pair shows the high relationships with extreme precipitation of some regions in other seasons. For instance, the higher relationships are found CCAN and MEDT in autumn and the west and northwestern part of the country in spring.

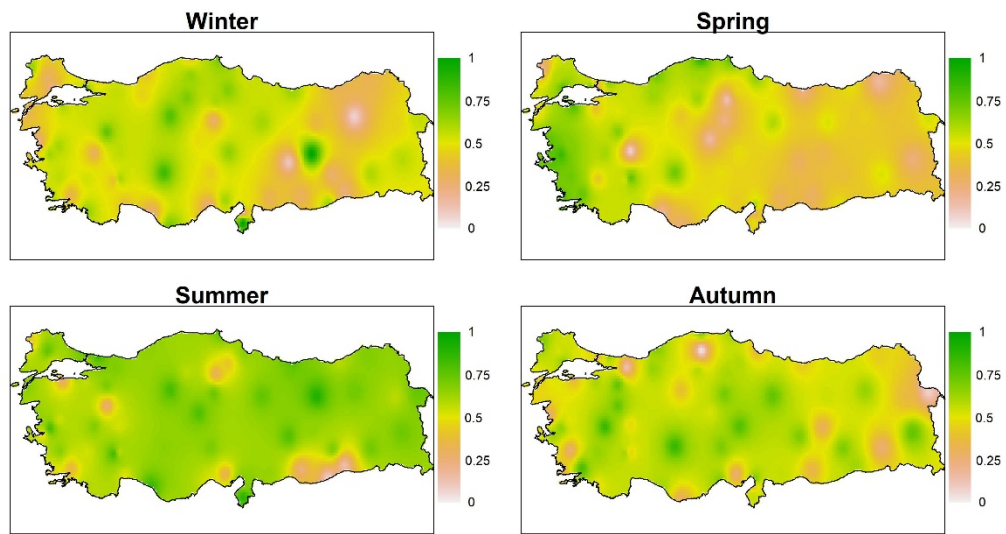


Figure 4.29 The continuous map of multivariate adaptive regression splines coefficient between AO and WeMO pair and extreme precipitation with respect to seasons

The significance of the relationships are also examined based on the actual sample size threshold. MARS results exceed this threshold at 63 stations for summer. In winter, the MARS coefficients of 62 stations are higher than the actual sample size limit of the significance measurement. Lastly, there are 61 and 59 stations having the significant relationship considering the actual sample size threshold in autumn and spring respectively.

Table 4.17 exhibits the MLR and MARS result of all stations included by this study.

Table 4.17 The relationship between anomaly of extreme precipitation and the pair of AO and WeMO anomaly (*Bold black numbers= The significant relationship for the effective sample size and the actual sample size, Red Numbers: The significant relationship for the actual sample size, Black Numbers= The insignificant relationship*)

		Multiple linear regression (MLR)				Multivariate adaptive regression splines (MARS)			
Station	Region	Spring	Summer	Autumn	Winter	Spring	Summer	Autumn	Winter
Adana	MED	0.426	0.134	-0.180	0.509	0.433	0.330	0.258	0.618
Afyon	CCAN	-0.013	0.080	0.044	-0.793	0.074	0.535	0.473	0.580
Ağrı	CEAN	-0.350	0.364	0.413	-0.298	0.410	0.585	0.365	0.453
Akhisar	MED	0.552	0.486	0.213	0.623	0.685	0.553	0.514	0.616
Alanya	MED	0.231	0.763	0.442	0.365	0.186	0.853	0.619	0.250
Anamur	MED	0.239	0.598	0.468	-0.223	0.249	0.628	0.278	0.706
Ankara	CCAN	0.444	0.693	0.538	0.709	0.417	0.812	0.394	0.781
Antakya	MED	-0.442	0.668	0.374	-0.488	-0.486	0.884	0.562	-1.000
Antalya	MED	0.217	0.194	0.358	0.110	0.568	0.508	0.567	0.407
Artvin	BLS	0.074	0.674	0.235	0.446	0.171	0.686	0.442	0.327
Aydın	MED	0.413	-0.213	0.268	-0.362	0.724	0.669	0.250	0.579
Bandırma	MED	0.814	-0.260	0.136	-0.212	0.782	0.258	0.377	0.606
Bilecik	MRT	0.539	0.425	0.379	-0.168	0.515	0.698	0.748	0.569
Bodrum	MED	0.421	0.135	-0.049	0.049	0.783	0.449	0.336	0.594
Bolu	BLS	0.716	0.525	0.546	0.231	0.630	0.644	0.642	0.455
Burdur	MEDT	0.258	0.755	0.650	-0.233	0.532	0.821	0.616	-0.400
Bursa	MRT	0.212	-0.580	-0.086	0.098	0.406	0.562	0.606	0.552
Ceylanpınar	CMED	0.452	0.244	-0.039	0.595	0.492	0.077	0.562	0.627
Çanakkale	MED	0.079	0.659	0.399	0.261	0.481	0.677	0.446	0.327
Çankırı	CCAN	0.579	0.243	0.329	0.641	0.631	0.580	0.588	0.693
Çorum	CCAN	0.285	0.182	0.511	-0.041	0.128	0.296	0.611	0.612
Denizli	MED	0.296	0.166	0.622	0.469	0.426	0.538	0.651	0.539
Dikili	MED	0.595	0.298	-0.456	0.355	0.764	0.649	-0.269	0.223
Diyarbakır	CMED	0.461	0.438	0.583	-0.229	0.385	0.687	0.691	0.262
Dörtyol	MED	0.679	0.569	0.435	0.139	0.624	0.673	0.710	0.558
Edirne	MRT	0.284	0.083	0.247	0.255	0.215	0.424	0.687	0.647
Elazığ	CMED	0.292	0.445	0.021	-0.351	0.340	0.658	0.309	-1.000
Erzincan	CEAN	0.315	0.847	-0.014	-0.601	0.525	0.901	0.549	-0.364
Erzurum	CEAN	0.089	0.632	0.312	-0.672	0.447	0.720	0.645	0.079
Fethiye	MED	0.224	0.591	0.546	-0.384	0.545	0.582	0.497	0.636
Florya	MRT	0.627	0.599	0.115	0.567	0.789	0.716	0.506	0.500
Gaziantep	CMED	0.319	0.526	-0.180	0.289	0.303	0.644	0.562	0.319
Giresun	BLS	0.107	0.555	0.415	0.521	-0.224	0.757	0.438	0.637

Table 4.17 Continued

Iğdır	CEAN	0.367	0.580	0.092	0.432	0.535	0.741	0.087	0.568
Inebolu	BLS	0.793	0.235	0.017	0.446	0.854	0.635	0.669	0.455
Isparta	MEDT	0.718	0.135	0.001	0.595	0.750	0.582	0.463	0.611
İskenderun	MED	0.018	0.225	0.493	-0.262	-0.254	0.666	0.401	-0.169
İzmir	MED	0.644	0.494	0.627	-0.158	0.782	0.483	0.637	-0.522
Kastamonu	CCAN	0.678	0.410	-0.280	0.029	0.611	0.620	-0.026	0.650
Kayseri	CCAN	0.382	0.634	0.413	0.706	0.487	0.624	0.782	0.656
Kırşehir	CCAN	0.313	0.756	0.512	0.352	0.162	0.789	0.531	0.477
Kireçburnu	MRT	-0.278	0.505	0.333	0.298	0.410	0.748	0.197	0.612
Konya	CCAN	0.502	0.580	0.708	0.738	0.716	0.671	0.849	0.825
Kumköy	MRT	0.257	0.699	0.656	0.364	0.522	0.823	0.578	0.251
Kütahya	MEDT	0.652	0.233	0.740	0.697	0.675	0.251	0.747	0.751
Lüleburgaz	MRT	0.314	0.460	-0.027	-0.038	0.590	0.749	0.531	0.291
Malatya	CMED	0.219	0.372	0.549	-0.146	-0.295	0.779	0.689	-0.108
Manisa	MED	0.691	0.453	0.680	0.511	0.840	0.809	0.656	0.622
Mardin	CMED	0.359	0.031	0.602	0.349	0.419	0.143	0.623	0.242
Mersin	MED	0.449	0.258	0.548	0.276	0.526	0.528	0.678	0.232
Muğla	MED	0.614	-0.062	0.752	0.368	0.736	0.360	0.800	0.340
Niğde	CCAN	0.561	0.573	0.423	0.209	0.485	0.700	0.695	0.444
Rize	BLS	0.528	0.125	0.407	0.027	0.495	0.580	0.531	0.314
Sakarya	BLS	0.184	0.751	0.252	0.060	0.548	0.692	0.130	0.569
Samsun	BLS	0.633	0.539	-0.861	0.468	0.649	0.668	0.388	0.541
Siirt	CMED	0.588	0.317	0.308	0.407	0.522	0.711	0.262	0.598
Sinop	BLS	0.755	0.646	0.261	0.429	0.768	0.756	0.623	0.717
Sivas	CCAN	0.564	0.524	0.542	0.610	0.594	0.749	0.752	0.619
Şanlıurfa	CMED	0.102	-0.104	0.301	0.390	0.289	-0.247	0.344	0.299
Şile	MRT	0.094	0.627	0.409	0.367	0.668	0.839	0.637	0.475
Tekirdağ	MRT	0.615	0.232	0.629	-0.036	0.755	0.567	0.648	0.221
Uşak	MEDT	0.404	0.539	0.830	0.401	0.617	0.684	0.851	0.304
Van	CEAN	0.105	0.752	0.774	0.239	0.247	0.723	0.748	0.581
Yozgat	CCAN	0.273	0.588	0.595	0.294	0.217	0.727	0.711	0.281
Zonguldak	BLS	0.704	0.298	0.258	0.400	0.722	0.660	0.677	0.413

4.4.2.5 SOI and WeMO responses

As stated before, the relationship analysis between SOI and WeMO pair and extreme precipitation is only performed for summer. Because, according to the single analysis results, both SOI and WeMo are commonly effective in summer rather than other

seasons. MLR discovers the significant relationship between this pair and summer extremes at 6 stations. MARS enhances this number to 18 stations. Table 4.18 gives the rainfall regions to which these stations belong.

Table 4.18 The number of the station having the significant relationship with SOI and WeMO pair in summer based on the effective sample size threshold with respect to the rainfall regions

Rainfall Region	Total Station Number	Number of the station having the significant relationship	
		Multiple linear regression (MLR)	Multiple adaptive regression splines (MARS)
BLS	8	2	2
CCAN	11	1	4
CEAN	6	2	4
CMED	8	0	1
MED	19	1	2
MEDT	4	0	1
MRT	9	0	4
Total	65	6	18

The continuous map of the MLR and MARS relationship coefficients are addressed in Figure 4.30. When the figure is analyzed, it is realized that MLR discover the high relationships over the northeastern of Turkey and considerable part of CCAN. However, MARS method is more successful in revealing relationships. This method determine new high relationship areas including some part of BLS, CEAN, CMED and MRT as well as it catches the relationships discovered by MLR.

The relationship results for MLR and MARS analysis are given in Table 4.19.

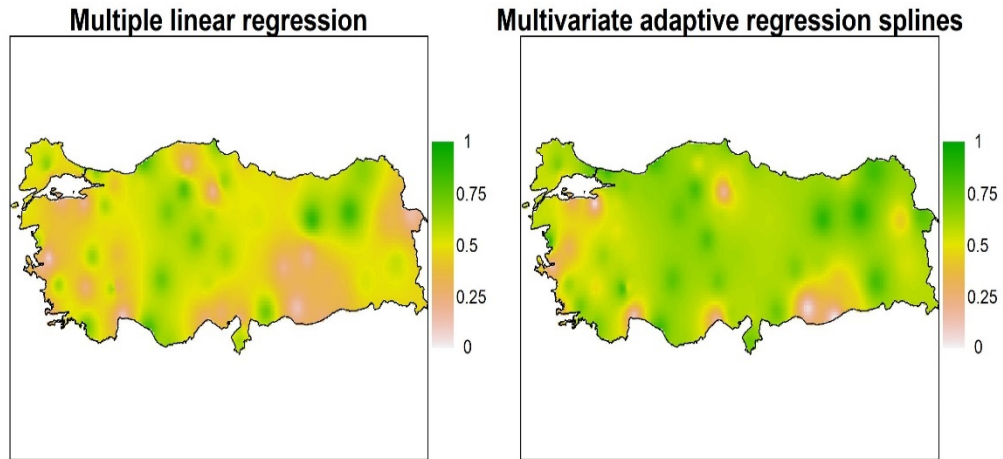


Figure 4.30 The continuous map of MLR and MARS coefficients between SOI and WeMO pair and summer extremes

Table 4.19 The relationship between anomaly of extreme precipitation and the pair of SOI and WeMO anomaly for summer (**Bold black numbers**= The significant relationship for the effective sample size and the actual sample size, **Red Numbers**: The significant relationship for the actual sample size, **Black Numbers**= The insignificant relationship)

Station	Region	Multiple linear regression (MLR)	Multivariate adaptive regression splines (MARS)
Adana	MED	0.270	0.608
Afyon	CCAN	0.379	0.550
Ağrı	CEAN	0.345	0.437
Akhisar	MED	0.385	0.310
Alanya	MED	0.811	0.831
Anamur	MED	0.641	0.643
Ankara	CCAN	0.701	0.744
Antakya	MED	0.622	0.729
Antalya	MED	0.102	-0.107
Artvin	BLS	0.670	0.822
Aydın	MED	-0.625	0.630
Bandırma	MED	-0.206	0.266
Bilecik	MRT	0.614	0.536
Bodrum	MED	0.234	0.331
Bolu	BLS	0.522	0.660
Burdur	MEDT	0.621	0.816
Bursa	MRT	0.189	0.035
Ceylanpınar	CMED	0.247	-0.017
Çanakkale	MED	0.513	0.563
Çankırı	CCAN	0.777	0.805
Çorum	CCAN	0.199	0.181
Denizli	MED	0.250	0.477

Table 4.19 Continued

Dikili	MED	0.631	0.853
Diyarbakır	CMED	0.321	0.415
Dört Yol	MED	0.193	0.539
Edirne	MRT	0.521	0.541
Elazığ	CMED	0.195	0.620
Erzincan	CEAN	0.855	0.869
Erzurum	CEAN	0.839	0.890
Fethiye	MED	0.718	0.701
Florya	MRT	0.366	0.758
Gaziantep	CMED	0.714	0.719
Giresun	BLS	0.458	0.623
İğdir	CEAN	0.146	0.773
Inebolu	BLS	0.410	0.699
Isparta	MEDT	-0.294	0.519
İskenderun	MED	0.600	0.680
İzmir	MED	0.210	0.150
Kastamonu	CCAN	0.189	0.518
Kayseri	CCAN	0.633	0.625
Kırşehir	CCAN	0.726	0.774
Kireçburnu	MRT	0.598	0.819
Konya	CCAN	0.724	0.757
Kumköy	MRT	0.690	0.869
Kütahya	MEDT	0.479	0.506
Lüleburgaz	MRT	0.666	0.688
Malatya	CMED	0.219	0.692
Manisa	MED	0.080	0.345
Mardin	CMED	0.336	0.441
Mersin	MED	0.257	0.169
Muğla	MED	0.513	0.707
Niğde	CCAN	0.558	0.716
Rize	BLS	0.534	0.546
Sakarya	BLS	0.409	0.678
Samsun	BLS	0.447	0.659
Siirt	CMED	0.531	0.806
Sinop	BLS	0.735	0.738
Sivas	CCAN	0.526	0.577
Şanlıurfa	CMED	0.128	0.048
Şile	MRT	0.690	0.847
Tekirdağ	MRT	0.377	0.482
Uşak	MEDT	0.644	0.635
Van	CEAN	0.560	0.535
Yozgat	CCAN	0.596	0.582
Zonguldak	BLS	0.812	0.830

4.5 Relationship between the teleconnection patterns and the decadal low extreme precipitation variability

The strength of climate indices on decadal dry day number variability as well as decadal high extreme precipitation variability are tested. Unlike high extreme precipitation analysis, only the individual effects of the climate indices are measured. In addition, the relationships are defined by means of Spearman's rank order correlation (SROC) method. Power law regression (PLR) method is not used since there isn't significantly difference between SROC and PLR according to the results of section 4.4.1. Finally, the significance of the results are only interpreted based on the effective sample size threshold.

4.5.1 The single relationship analysis

4.5.1.1 NAO responses

According to results, NAO is one of the most vital drivers of dry day number in winter. The correlation of the 26 stations is higher than the effective sample size threshold in this season (Table 4.20). Specifically, NAO appears as one of the essential driver on the decadal dry day number oscillation of MED. In this region, 13 of 19 stations have the greater correlation than 0.73 with NAO. In addition, NAO is also effective on the dry day number of other Mediterranean climates regions, CMED and MED. In CMED, 4 of the 8 stations and in MED, 3 of the 4 stations are significantly correlated to NAO. Finally, there are 2 and 4 stations which's correlation values are higher than the significance threshold in spring and summer while there isn't any significantly correlated station in autumn.

Table 4.20 The number of the station having the significant relationship between NAO and its dry day number in winter

Rainfall Region	Total Station Number	Number of the station having the significant relationship
BLS	8	0
CCAN	11	2
CEAN	6	0
CMED	8	4
MED	19	13
MEDT	4	3
MRT	9	4
Total	65	26

The inverse distance mapped distribution of correlations are shown in Figure 4.31. This figure ensures that NAO is a quite substantial driver for decadal dry number over very large area of Turkey in winter. To be more precise, NAO is effective on the dry day number of all regions of Turkey except for BLS and CEAN in winter season. Although these climate indices appear to have slight effects during spring and summer months they are not as powerful as for winter. In spring, the effect of NAO arises at the some parts of BLS, CCAN, CEAN and CMED. Yet, it is very hard to pinpoint the effect area of NAO in summer. Instead, it can be concluded that there are some regions in various parts of Turkey, which have partially high correlation with NAO. Last, the dominant correlations are not detected during autumn.

In Table 4.21, the correlation values for each stations can be found in respect to seasons.

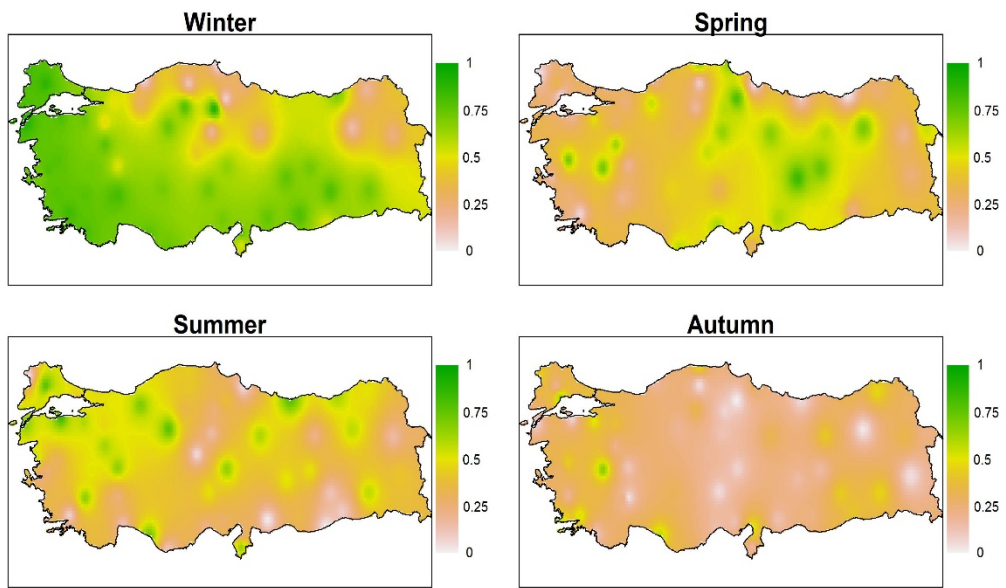


Figure 4.31 The continuous map of SROC coefficient between dry day numbers and NAO with respect to seasons

Table 4.21 The correlation between anomaly of dry day number and NAO anomaly (*Red numbers= The significant relationship for the effective sample size, Black Numbers= The insignificant relationship*)

Station	Region	Spearman's rank order correlation			
		Spring	Summer	Autumn	Winter
Adana	MED	0.502	-0.275	0.136	0.710
Afyon	CCAN	-0.195	-0.656	-0.116	0.520
Ağrı	CEAN	0.205	-0.168	-0.346	-0.242
Akhisar	MED	0.712	-0.298	0.440	0.782
Alanya	MED	0.336	-0.728	0.579	0.756
Anamur	MED	0.578	-0.114	0.346	0.741
Ankara	CCAN	0.332	-0.754	0.189	0.737
Antakya	MED	0.295	-0.643	0.173	0.529
Antalya	MED	0.387	0.130	0.316	0.731
Artvin	BLS	0.261	0.497	0.464	-0.188
Aydın	MED	0.249	-0.348	0.193	0.780
Bandırma	MED	0.187	-0.825	0.053	0.802
Bilecik	MRT	0.285	-0.469	0.396	0.470
Bodrum	MED	0.220	-0.336	0.583	0.766
Bolu	BLS	0.562	-0.690	0.263	0.296
Burdur	MEDT	0.189	0.280	0.239	0.792
Bursa	MRT	0.490	-0.600	0.515	0.739
Ceylanpınar	CMED	0.522	0.014	-0.348	0.521
Çanakkale	MED	0.347	-0.670	-0.085	0.894
Çankırı	CCAN	0.176	-0.356	0.344	0.776
Çorum	CCAN	0.585	-0.246	-0.067	0.899
Denizli	MED	0.380	-0.654	0.352	0.776
Dikili	MED	0.382	-0.558	0.348	0.764
Diyarbakır	CMED	0.513	0.123	-0.441	0.792
Dört Yol	MED	0.501	-0.277	0.516	0.664
Edirne	MRT	-0.045	-0.071	0.439	0.817
Elazığ	CMED	0.737	0.494	-0.162	0.709
Erzincan	CEAN	0.590	-0.218	0.427	0.548
Erzurum	CEAN	0.702	0.574	0.024	0.154
Fethiye	MED	0.393	-0.368	0.132	0.800
Florya	MRT	0.229	-0.410	0.446	0.687
Gaziantep	CMED	0.611	-0.020	-0.138	0.742
Giresun	BLS	-0.119	-0.767	0.060	-0.556
İğdir	CEAN	0.550	0.279	-0.225	0.421
Inebolu	BLS	-0.615	-0.441	0.470	-0.315
Isparta	MEDT	0.232	-0.238	-0.032	0.821

Table 4.21 Continued

İskenderun	MED	0.457	-0.257	0.461	0.755
İzmir	MED	0.142	-0.235	0.267	0.700
Kastamonu	CCAN	-0.093	-0.421	-0.047	-0.121
Kayseri	CCAN	0.458	-0.653	-0.077	0.656
Kırşehir	CCAN	0.559	0.062	0.187	0.432
Kireçburnu	MRT	0.076	-0.528	0.380	0.713
Konya	CCAN	0.459	-0.405	0.310	0.705
Kumköy	MRT	0.511	-0.460	0.417	0.594
Kütahya	MEDT	0.627	-0.620	0.215	0.760
Lüleburgaz	MRT	0.347	-0.762	-0.212	0.874
Malatya	CMED	0.836	-0.513	-0.163	0.750
Manisa	MED	0.345	-0.249	0.285	0.796
Mardin	CMED	0.241	-0.096	-0.414	0.649
Mersin	MED	0.608	0.220	0.132	0.668
Muğla	MED	-0.068	0.084	0.523	0.829
Niğde	CCAN	0.322	-0.492	0.051	0.719
Rize	BLS	0.019	-0.612	0.334	-0.686
Sakarya	BLS	-0.243	-0.510	0.308	0.495
Samsun	BLS	0.052	0.050	0.288	-0.249
Siirt	CMED	0.404	-0.572	-0.458	0.708
Sinop	BLS	-0.667	-0.272	0.253	-0.018
Sivas	CCAN	0.669	-0.598	0.332	0.250
Şanlıurfa	CMED	0.499	0.346	-0.229	0.790
Şile	MRT	0.248	-0.478	0.352	0.583
Tekirdağ	MRT	0.053	-0.478	0.634	0.786
Uşak	MEDT	0.715	-0.515	0.671	0.725
Van	CEAN	-0.250	-0.410	0.045	-0.516
Yozgat	CCAN	0.653	-0.160	0.122	0.184
Zonguldak	BLS	-0.237	-0.491	0.178	0.087

4.5.1.2 AO responses

In general, AO responses is quite analogous to NAO responses. Differently, the significant correlations are only detected in winter. In this season, the dry day number of 24 stations mark significant relationship with AO. Like NAO, AO is also effective in Mediterranean climate. 18 of 31 stations in CMED, MED and MEDT

have the higher correlation value than 0.73. The distribution of significantly related stations with respect to rainfall regions is remarked in Table 4.22.

Table 4.22 The number of the station having the significant relationship between AO and its dry day number in winter

Rainfall Region	Total Station Number	Number of the station having the significant relationship
BLS	8	0
CCAN	11	3
CEAN	6	0
CMED	8	1
MED	19	14
MEDT	4	3
MRT	9	3
Total	65	24

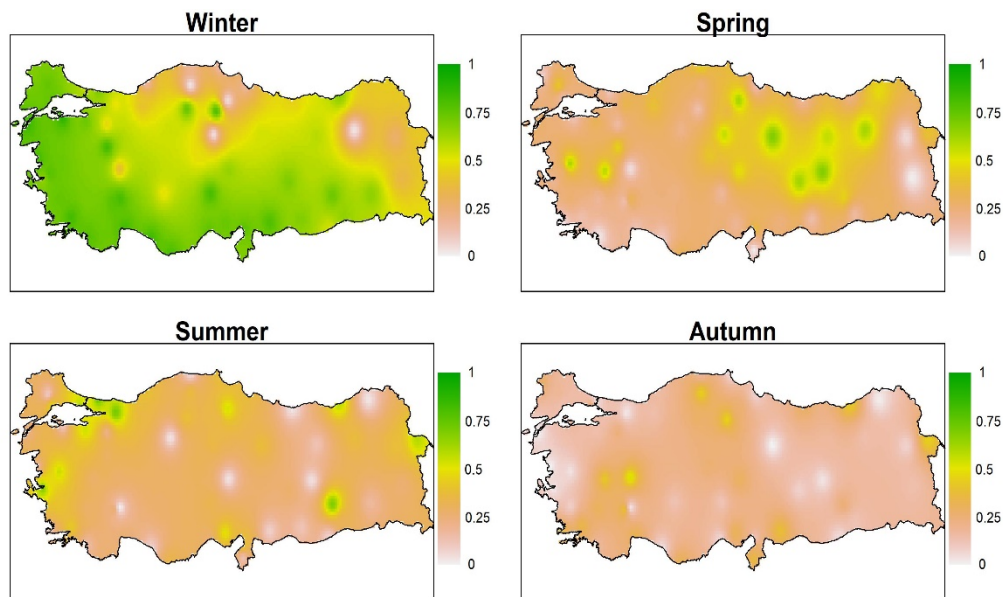


Figure 4.32 The continuous map of SROC coefficient between dry day numbers and NAO with respect to seasons

The comparatively analysis of Figure 4.31 and Figure 4.32 also reveals the similarities between the impact areas of NAO and AO on dry day number in winter. Hereby, to measure which of the NAO and AO effects are stronger, the correlations values at each station are compared. As a results, it is found out that the correlation

values with NAO is stronger at 40 stations whereas the correlation values with AO is stronger at 25 stations. The name of these stations are given in Table 4.23.

Table 4.23 The comparison of the correlation values of dry day number with NAO and AO

The stations having higher correlation with NAO	The stations having higher correlation with AO
Afyon	Adana*
Akhisar*	Ağrı
Ankara	Alanya*
Aydın*	Anamur*
Bilecik	Antakya
Bodrum*	Antalya*
Burdur*	Artvin
Bursa*	Bandırma*
Çanakkale*	Bolu
Çankırı*	Ceylanpınar*
Çorum*	Dikili*
Denizli*	Dört Yol
Diyarbakır*	Erzincan
Edirne*	Gaziantep*
Elazığ	Iğdır
Erzurum	Kırşehir
Fethiye*	Kütahya*
Florya	Mardin
Giresun	Mersin*
Inebolu	Niğde*
Isparta*	Sakarya
İskenderun*	Sinop
İzmir	Sivas
Kastamonu	Şile
Kayseri	Zonguldak
Kireçburnu	
Konya	
Kumköy	
Lüleburgaz*	
Malatya*	
Manisa*	
Muğla*	
Rize	
Samsun	
Siirt	
Şanlıurfa*	

The stations having higher correlation with NAO	The stations having higher correlation with AO
Tekirdağ*	
Uşak	
Van	
Yozgat	

*The stations having significant correlation with indicated climate indices

In previous studies (e.g. Cullen and DeMenocal, 2000; Cullen et al, 2002; Türkeş and Erlat, 2003; Türkeş and Erlat, 2005) it has been stated that NAO is one of the basic drivers of winter precipitation amount of Turkey. The results obtained during this study are in accordance with related studies in literature. Moreover, a more detailed study is conducted on some regions and stations. Consequently, in some regions where NAO is considered as the most effective driver of winter precipitation, AO is evaluated as being more effective. For instance, the driving power of two climate indices are separately significant at 21 stations. 6 of these 21 stations have higher correlation with AO. The name of those stations are Alanya, Anamur, Bandırma, Dikili, Gaziantep and Kütahya. Thus, AO may prefer at some places instead of NAO when performing analysis between precipitation and the most effective climate indices.

The SROC coefficients for each station can be comprehended by observing Table 4.24.

Table 4.24 The correlation between anomaly of dry day number and AO anomaly (*Red numbers= The significant relationship for the effective sample size, Black Numbers= The insignificant relationship*)

Station	Region	Spearman's rank order correlation			
		Spring	Summer	Autumn	Winter
Adana	MED	0.189	-0.497	-0.319	0.739
Afyon	CCAN	-0.038	-0.277	-0.528	0.390
Ağrı	CEAN	0.055	0.382	-0.079	-0.278
Akhisar	MED	0.608	0.549	0.038	0.738
Alanya	MED	0.103	0.080	-0.055	0.824
Anamur	MED	0.310	-0.350	0.318	0.796
Ankara	CCAN	0.212	-0.034	-0.226	0.551
Antakya	MED	0.018	-0.134	-0.363	0.692
Antalya	MED	0.135	-0.252	0.330	0.814
Artvin	BLS	0.474	-0.031	-0.014	-0.418
Aydın	MED	0.263	0.404	-0.090	0.747
Bandırma	MED	0.136	-0.121	-0.166	0.869
Bilecik	MRT	0.158	-0.224	0.244	0.469
Bodrum	MED	-0.018	0.175	0.387	0.709
Bolu	BLS	0.396	-0.359	-0.147	0.407
Burdur	MEDT	0.139	-0.264	0.399	0.774
Bursa	MRT	0.319	-0.544	0.142	0.731
Ceylanpınar	CMED	0.258	-0.070	0.050	0.535
Çanakkale	MED	0.266	0.236	0.014	0.834
Çankırı	CCAN	-0.146	-0.391	-0.282	0.736
Çorum	CCAN	0.364	-0.349	-0.455	0.794
Denizli	MED	0.183	-0.282	0.310	0.701
Dikili	MED	0.233	0.206	-0.001	0.808
Diyarbakır	CMED	0.452	0.687	-0.248	0.725
Dört Yol	MED	0.393	-0.386	-0.114	0.770
Edirne	MRT	0.095	-0.286	0.280	0.690
Elazığ	CMED	0.683	-0.042	-0.035	0.592
Erzincan	CEAN	0.564	-0.126	0.170	0.581
Erzurum	CEAN	0.615	0.376	0.144	0.033
Fethiye	MED	0.021	-0.164	0.179	0.779
Florya	MRT	0.256	-0.604	0.290	0.591
Gaziantep	CMED	0.239	0.083	-0.388	0.789
Giresun	BLS	0.189	-0.027	-0.285	-0.452
İğdir	CEAN	0.404	0.580	-0.450	0.422
Inebolu	BLS	-0.445	-0.053	0.186	-0.188
Isparta	MEDT	0.324	-0.001	0.026	0.813

Table 4.24 Continued

İskenderun	MED	0.185	-0.408	-0.288	0.704
İzmir	MED	0.191	0.677	0.031	0.656
Kastamonu	CCAN	-0.247	-0.372	-0.445	0.032
Kayseri	CCAN	0.488	-0.035	-0.298	0.644
Kırşehir	CCAN	0.417	-0.313	-0.262	0.482
Kireçburnu	MRT	0.095	-0.465	-0.073	0.587
Konya	CCAN	0.229	-0.279	-0.132	0.499
Kumköy	MRT	0.374	-0.547	0.041	0.494
Kütahya	MEDT	0.455	0.293	-0.243	0.819
Lüleburgaz	MRT	0.420	0.106	0.189	0.745
Malatya	CMED	0.624	-0.272	-0.081	0.692
Manisa	MED	0.262	0.472	0.065	0.774
Mardin	CMED	0.165	0.317	-0.126	0.653
Mersin	MED	0.254	-0.257	0.063	0.755
Muğla	MED	-0.144	-0.420	0.349	0.817
Niğde	CCAN	0.179	-0.332	-0.122	0.806
Rize	BLS	0.221	-0.574	-0.433	-0.662
Sakarya	BLS	-0.340	-0.711	-0.029	0.501
Samsun	BLS	0.156	-0.375	-0.079	-0.187
Siirt	CMED	0.301	-0.171	-0.174	0.659
Sinop	BLS	-0.374	-0.396	-0.049	-0.139
Sivas	CCAN	0.687	-0.382	-0.004	0.539
Şanlıurfa	CMED	0.153	-0.123	-0.183	0.685
Şile	MRT	0.107	-0.715	0.146	0.694
Tekirdağ	MRT	0.157	-0.469	0.134	0.741
Uşak	MEDT	0.583	-0.273	0.420	0.686
Van	CEAN	-0.009	0.258	0.142	-0.355
Yozgat	CCAN	0.561	-0.358	-0.253	0.041
Zonguldak	BLS	-0.368	-0.395	-0.153	0.176

4.5.1.3 SOI responses

The SOI effect on decadal dry day number oscillation in Turkey is quite less in proportion to AO and NAO. In winter, the only significant relationship between SOI anomaly and dry day number anomaly is detected at Ağrı station. Besides, the significant relationships are determined at 6 stations in summer. In fact, the summer

correlations seems relatively higher than other season's correlations in respect to spread of coefficients over Turkey (Figure 4.33). In summer, the western part of Turkey have great correlations with SOI . The dry day number of the significantly correlated stations in summer have the negative correlation with SOI without exception. In a word, the summer precipitation amount of these stations are directly proportional to SOI. To have more detailed idea, the significantly correlated stations can be seen in Table 4.25.

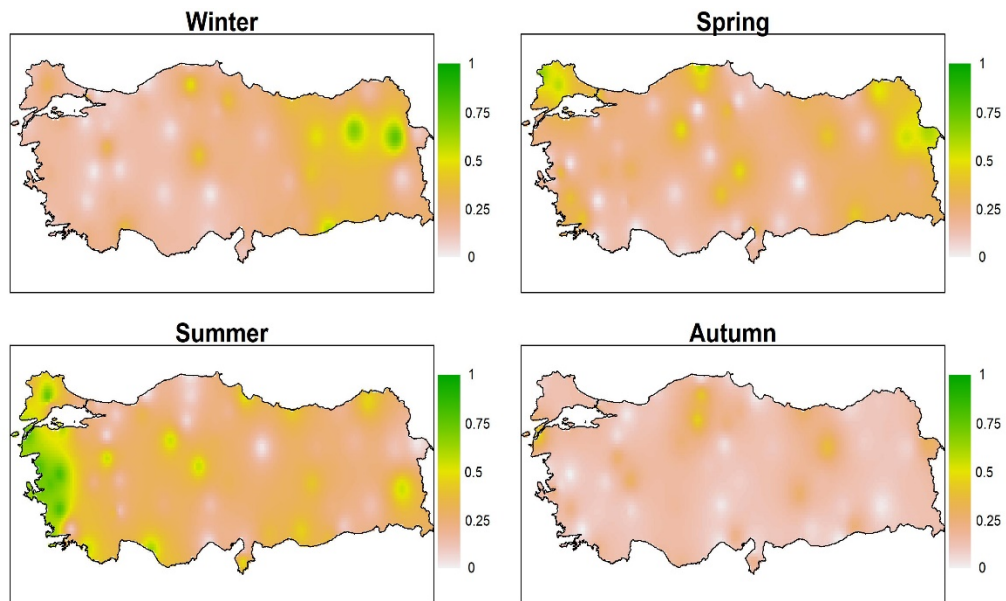


Figure 4.33 The continuous map of SROC coefficient between dry day numbers and SOI with respect to seasons

Table 4.25 The number of the station having the significant relationship between SOI and its dry day number in winter

Station	Region	Spearman's rank order correlation			
		Spring	Summer	Autumn	Winter
Adana	MED	0.072	0.201	-0.220	0.142
Afyon	CCAN	0.308	-0.162	-0.299	0.042
Ağrı	CEAN	0.548	-0.127	-0.081	0.757
Akhisar	MED	0.014	-0.813	-0.001	0.167
Alanya	MED	0.153	-0.628	-0.165	0.169
Anamur	MED	0.014	0.38	-0.196	0.153
Ankara	CCAN	0.495	-0.554	-0.248	0.043
Antakya	MED	0.166	-0.489	-0.208	0.106
Antalya	MED	0.010	0.332	0.112	0.371
Artvin	BLS	-0.511	0.462	-0.108	0.159
Aydın	MED	0.394	-0.799	-0.217	0.166
Bandırma	MED	0.329	-0.59	0.192	0.225
Bilecik	MRT	0.218	0.055	0.042	-0.090
Bodrum	MED	0.359	-0.689	0.124	0.096
Bolu	BLS	0.102	-0.343	0.122	-0.194
Burdur	MEDT	0.128	0.37	0.111	0.207
Bursa	MRT	-0.051	-0.256	0.162	-0.030
Ceylanpınar	CMED	0.267	0.375	0.008	0.595
Çanakkale	MED	0.227	-0.752	-0.465	0.100
Çankırı	CCAN	-0.005	0.065	-0.453	-0.180
Çorum	CCAN	0.381	0.235	-0.241	0.163
Denizli	MED	0.010	-0.371	0.096	0.049
Dikili	MED	0.068	-0.812	0.052	0.193
Diyarbakır	CMED	0.296	-0.235	0.093	0.302
Dört Yol	MED	0.382	0.131	-0.077	0.214
Edirne	MRT	0.654	-0.365	-0.092	-0.126
Elazığ	CMED	0.248	0.412	-0.155	0.418
Erzincan	CEAN	-0.417	-0.231	-0.375	0.494
Erzurum	CEAN	0.087	0.179	-0.096	0.688
Fethiye	MED	-0.008	-0.55	0.197	0.230
Florya	MRT	0.374	-0.172	0.134	-0.049
Gaziantep	CMED	0.066	-0.374	0.118	0.243
Giresun	BLS	0.321	-0.429	-0.282	0.395
İğdir	CEAN	-0.607	0.022	-0.301	0.090
Inebolu	BLS	0.620	0.023	-0.016	0.120
Isparta	MEDT	0.234	-0.122	-0.051	0.180
İskenderun	MED	0.052	-0.109	0.014	0.161
İzmir	MED	0.081	-0.716	0.233	0.182

Table 4.25 Continued

Kastamonu	CCAN	0.460	0.06	-0.422	0.497
Kayseri	CCAN	0.476	-0.312	0.091	0.224
Kırşehir	CCAN	-0.049	0.564	-0.116	0.424
Kireçburnu	MRT	0.467	-0.274	-0.034	0.026
Konya	CCAN	-0.061	-0.25	-0.179	0.064
Kumköy	MRT	0.232	-0.244	-0.045	-0.008
Kütahya	MEDT	0.140	-0.561	-0.274	0.346
Lüleburgaz	MRT	0.582	-0.757	-0.138	0.327
Malatya	CMED	-0.013	-0.297	-0.274	0.159
Manisa	MED	0.382	-0.766	-0.047	0.208
Mardin	CMED	0.430	-0.105	-0.245	0.386
Mersin	MED	0.099	0.042	-0.019	0.073
Muğla	MED	0.417	-0.107	0.008	0.186
Niğde	CCAN	0.419	-0.144	-0.028	0.018
Rize	BLS	-0.117	-0.191	-0.057	-0.231
Sakarya	BLS	0.221	0.095	-0.023	0.083
Samsun	BLS	0.064	0.497	-0.017	-0.209
Siirt	CMED	0.289	-0.139	0.022	0.355
Sinop	BLS	0.064	0.252	-0.040	-0.105
Sivas	CCAN	-0.196	-0.03	-0.112	-0.136
Şanlıurfa	CMED	0.152	0.45	-0.059	0.228
Şile	MRT	0.187	-0.085	0.168	-0.001
Tekirdağ	MRT	0.511	-0.226	-0.114	0.222
Uşak	MEDT	-0.274	-0.227	0.056	-0.016
Van	CEAN	0.251	-0.544	-0.134	0.075
Yozgat	CCAN	0.294	0.322	-0.040	0.194
Zonguldak	BLS	0.266	0.016	0.086	-0.023

4.5.1.4 WeMO responses

According to results, WeMO is the least operative driver for the decadal dry day number variation between 4 climate indices. There isn't any stations which's correlation coefficient is higher than 0.73 in other seasons while there is 3 stations which's correlation coefficient is higher than 0.73 in summer. These stations are Erzurum, Siirt and Sinop. Erzurum and Siirt are located in CEAN while Sinop is located in BLS. Actually, it is seen in Figure 4.34 that the green areas are clustered

around these cities. The high correlations, the green areas, in those regions are most probably due to the stated cities. Apart from summer, the distinct green areas don't draw the attention in other season. Finally, WeMO responses with respect to stations and seasons are specified in Table 4.26.

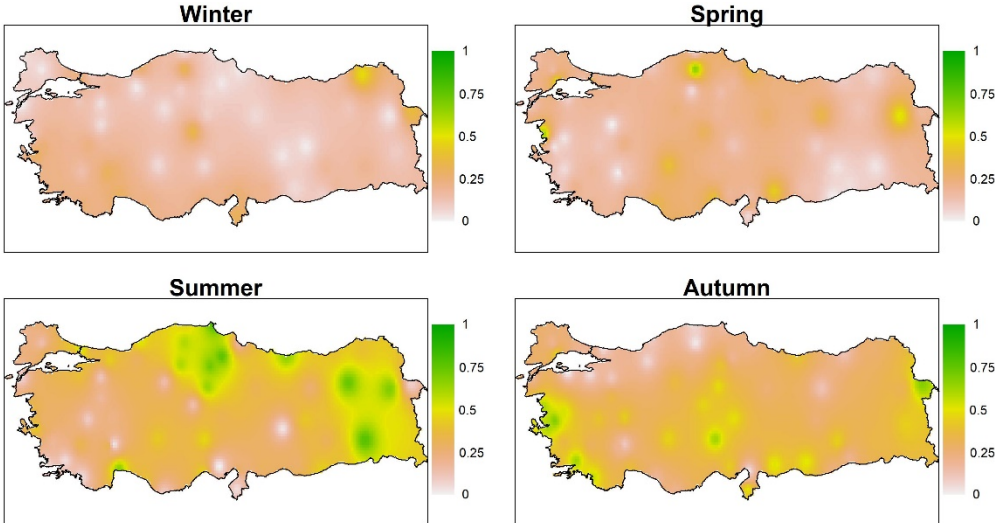


Figure 4.34 The continuous map of SROC coefficient between dry day numbers and SOI with respect to seasons

Table 4.26 The number of the station having the significant relationship between WeMO and its dry day number in winter

Station	Region	Spearman's rank order correlation			
		Spring	Summer	Autumn	Winter
Adana	MED	0.184	0.004	0.437	-0.205
Afyon	CCAN	-0.224	0.218	0.445	-0.180
Ağrı	CEAN	0.511	0.684	0.323	0.027
Akhisar	MED	-0.031	-0.281	-0.531	-0.208
Alanya	MED	0.360	0.386	0.175	-0.240
Anamur	MED	0.285	0.104	0.203	-0.203
Ankara	CCAN	0.242	0.148	0.369	-0.042
Antakya	MED	-0.051	-0.041	0.510	-0.314
Antalya	MED	-0.216	-0.676	-0.389	-0.300
Artvin	BLS	-0.078	-0.397	0.266	0.480
Aydın	MED	-0.052	-0.185	-0.357	-0.218
Bandırma	MED	-0.088	0.342	-0.003	-0.168
Bilecik	MRT	-0.191	0.107	-0.107	0.041
Bodrum	MED	0.063	0.015	-0.324	-0.239
Bolu	BLS	-0.200	0.298	0.071	-0.021
Burdur	MEDT	0.005	-0.34	0.200	-0.312
Bursa	MRT	-0.181	0.391	-0.046	-0.115
Ceylanpınar	CMED	0.007	0.45	0.235	-0.084
Çanakkale	MED	0.137	0.077	-0.201	-0.014
Çankırı	CCAN	-0.059	0.603	-0.236	0.090
Çorum	CCAN	0.146	0.714	0.405	-0.064
Denizli	MED	-0.182	0.332	-0.298	-0.143
Dikili	MED	0.653	0.348	-0.612	-0.106
Diyarbakır	CMED	-0.036	-0.312	0.451	-0.184
Dört Yol	MED	-0.134	-0.318	-0.026	-0.271
Edirne	MRT	0.162	-0.205	-0.267	0.051
Elazığ	CMED	0.099	-0.419	0.255	0.016
Erzincan	CEAN	-0.344	-0.266	0.127	0.109
Erzurum	CEAN	-0.124	-0.74	0.298	-0.117
Fethiye	MED	-0.187	0.054	-0.558	-0.248
Florya	MRT	-0.083	0.334	0.167	-0.203
Gaziantep	CMED	0.437	-0.294	0.522	-0.206
Giresun	BLS	0.244	0.664	0.405	-0.165
İğdir	CEAN	-0.170	0.08	0.673	0.378
İnebolu	BLS	0.106	0.469	0.059	0.069
İsparta	MEDT	-0.128	-0.021	0.099	-0.272
İskenderun	MED	-0.283	-0.108	0.166	-0.269
İzmir	MED	-0.162	-0.441	-0.611	-0.299

Table 4.26 Continued

Kastamonu	CCAN	0.663	0.596	0.020	-0.325
Kayseri	CCAN	0.122	0.321	0.490	-0.132
Kırşehir	CCAN	0.309	0.143	0.461	-0.350
Kireçburnu	MRT	0.091	0.614	0.231	-0.205
Konya	CCAN	0.390	-0.425	0.460	-0.059
Kumköy	MRT	0.220	0.494	0.159	-0.213
Kütahya	MEDT	0.004	-0.176	-0.352	-0.046
Lüleburgaz	MRT	0.160	0.14	-0.193	-0.022
Malatya	CMED	0.192	0.033	0.336	-0.029
Manisa	MED	-0.027	-0.277	-0.682	-0.256
Mardin	CMED	-0.047	0.391	0.209	0.177
Mersin	MED	0.400	-0.446	0.311	-0.237
Muğla	MED	-0.208	-0.055	-0.620	-0.217
Niğde	CCAN	0.197	0.47	0.617	-0.067
Rize	BLS	0.099	0.405	0.128	0.146
Sakarya	BLS	-0.196	0.444	0.196	-0.176
Samsun	BLS	-0.362	0.168	0.192	0.026
Siirt	CMED	0.033	0.774	0.348	0.195
Sinop	BLS	-0.283	0.817	-0.148	-0.052
Sivas	CCAN	0.272	0.327	0.257	0.058
Şanlıurfa	CMED	0.135	0.268	0.509	-0.057
Şile	MRT	0.191	0.329	0.045	-0.111
Tekirdağ	MRT	0.468	0.324	-0.457	-0.076
Uşak	MEDT	-0.116	-0.099	-0.414	-0.239
Van	CEAN	0.187	0.491	0.444	0.100
Yozgat	CCAN	0.180	0.636	0.482	-0.084
Zonguldak	BLS	0.109	0.52	0.105	-0.277

4.6 5-years block responses

Entire analysis in section 4 have been clarified based on 10-years block responses until this point. Nonetheless, the 5-years block responses are mentioned in this section. In fact, all of the tests performed for 10-years block anomalies (i.e. section 4.2, 4.3, 4.4, 4.5) are also performed for 5-years block anomalies. However, 5-years block responses aren't explained in detail as it is in the 10-years block responses. There are two reasons for this situation. First, the main intent of this study is to focus

and elaborate on 10 years of oscillations. Second, if the block length gets smaller, the oscillations increase thanks to the nature of the QPM since it is encountered with more exclusive events at small block lengths (Taye and Willems, 2012). This may prevent the possible perturbation tendencies on the decadal scale from being seen. Instead, the smaller scale variations are seen. Meanwhile, the blocks longer than 10 years may miss the variations by smoothing the outputs because the total data length is only 60 years. Therefore, it is thought that the most optimum block length is 10 years for this study due to the main purpose, the nature of the method and the data length. Nevertheless, 5-years block analysis are also conducted to see the differences between 5-years oscillations and 10-years oscillations. In Figure 4.35, the responses of winter anomalies for different block lengths can be found for each region. By analyzing this figure, it can be easily seen that the variances of the 5-years block responses are higher than the variances of the 10-years block responses. In addition, Table 4.27 shows the amount of increment in standard deviations for each region. According to Tabari and Willems (2016), the anomalies in humid regions are less sensitive to the block length than arid regions. This claim is supported by some regions within the scope of the study area. For instance, BLS, the wettest in region in Turkey, have the least increment in terms of standard deviation while CCAN that is one of the regions receiving the least precipitation have the most increment. However, the wettest region in winter, MED, also have a quite high standard deviation increment. Although the main cause of this condition is not precisely investigated in the scope of this study, the vulnerability of the MED region to climate change (Giorgi and Lionello, 2008) may be the driver of the inconsistent precipitation behavior.

Table 4.27 The standard deviation increment for different block lengths

	Total yearly precipitation (mm)	Total winter precipitation (mm)	Standard deviation of winter anomalies (10- years block)	Standard deviation of winter anomalies (5- years block)	Increment of standard deviation (%)
BLS	1062.81	316.69	0.060	0.072	20
CCAN	415.56	123.17	0.049	0.099	103
CEAN	437.07	110.93	0.068	0.090	32
CMED	486.25	211.10	0.033	0.063	87
MED	778.21	397.63	0.040	0.070	78
MEDT	514.47	200.27	0.071	0.095	33
MRT	661.57	234.48	0.067	0.098	45

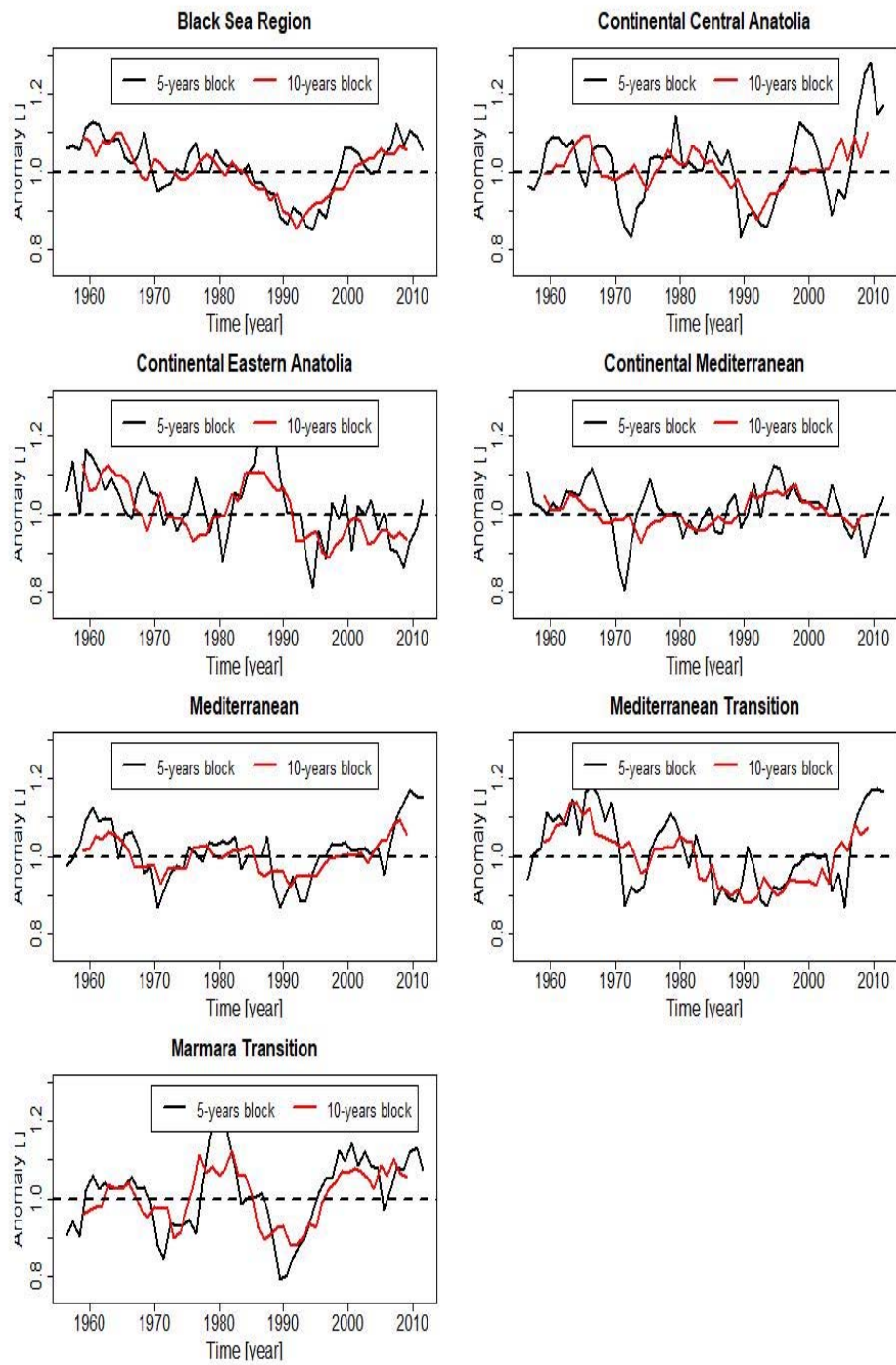


Figure 4.35 Winter anomalies of the regions for block lengths of 5 and 10 years

CHAPTER 5

CONCLUSION, SUMMARY AND RECOMMENDATIONS

In the first part of study, the statistical analysis are performed by means of QPM to discover high and low anomaly oscillations over Turkey in decadal period. The analyses are done for seven different rainfall regions of Turkey. These regions are BLS, CCAN, CEAN, CMED, MED, MDT and MRT. Moreover, 60-years data period which covers the years between 1955-2014 are used. Daily precipitation data are obtained from 65 stations across Turkey. Secondly, the relationship analysis are accomplished between the anomaly of extreme precipitation and 4 climate indices arising from sea level pressure alterations. The relationships are measured by the aid of both the single and multiple relationship methods separately. Further, the non-linear relationship methods are utilized along with the linear relationship methods to explore whether defined relationships changes in respect to linearity of the methods.

Based on the QPM results, in general, the amount of the winter anomalies keep increasing from starting the second half of 2000s to the present. Such high levels in positive anomalies have not been observed since the early 1960s. Besides, the lowest winter anomalies are detected at the early 1990s. The winter anomalies are very low in this time period compared to the rest of study period. In spring, high anomaly values are obtained for most of the stations in the first half of 2000. In contrast to this situation, the spring anomalies are quite low along 1970s except for CMED. In autumn, the lowest amount of the extreme precipitation is determined during 1960s while the highest is determined in the late 2000s. Lastly, summer anomalies are generally highly variable. Still, corresponding to the results summer extremes are prone to being positive.

As it is mentioned above, in the second half of the 2000s, high-level of extreme precipitation anomalies are observed in winter, summer and autumn. However, an

increase in the amount of total precipitation is not detected. On the contrary, there is an obvious uprising in dry day number anomalies, especially for winter and summer months. The positive anomalies are detected in the dry day number of all regions in winter. They are also determined in the extreme precipitation of BLS, CCAN, MED, MEDT and MRT. Especially in the regions with Mediterranean climate, the increment of region anomaly reaches %10 higher than baseline level. In summer, MRT, CCAN and BLS bear an increase in dry day number and the increase in extreme precipitation of all regions are observed except for CCAN and CEAN. In short, the amount of the extreme precipitation and the number of dry days rises for the majority of regions whereas the total amount of precipitation does not change. This means that individual precipitation events generate higher amount of precipitation compared to before. Correspondingly, it may be claimed that the probability of the devastating showers to occur, grows. Hence, it is obvious that Turkey may be going to face more flood events unless the necessary precautions are taken.

According to the relationship analyses with single driver, NAO is the most effective driver of Turkey's extreme precipitation among 4 climate indices. Still, it can not be said that NAO is a very strong driver of decadal extreme precipitation variability as much as it is in total precipitation and dry day number. It is only partially effective in the interior and western parts of Turkey. Also, AO has spatially similar effect to NAO on extreme precipitation. Besides, it can be claimed that there is not an explicit difference between the output of the SROC and PLR method. However, the situation is different for the relationship analysis with multiple drivers. MARS obviously defines higher relationships than MLR. Moreover, in relationship analysis with multiple drivers, the most effective climate indices pair is the combination of NAO and SOI. This pair seems to be one of the essential drivers of the winter extremes in Turkey. Even though it is known that the precipitation in summer commonly originates due to convective reasons, it can be stated that SOI and WeMO pair has important influence on oscillation of decadal summer extremes.

NAO has a great impact on the decadal dry day number oscillations of the country. Like the results of the extreme precipitation analysis, the influence of AO on dry day number is quite parallel to NAO. In winter, these two indices are influential drivers of the country's dry day number except for the northeastern and eastern part. The indices are quite operative especially in the western areas. Albeit NAO shows higher relationship in more stations, AO is superior when analyzing precipitation behavior in some regions. In addition, if the effect of climate indices on the precipitation extremes and the dry days numbers are compared, it can be concluded that climate indices have more effects on the dry days numbers.

All analyses included in this study are performed by using decadal-scale data. Decadal oscillations of precipitation extremes are represented and decadal relationships between precipitation extremes and climate indices are investigated. Explaining the connection between hydrological extremes and climate indices that show (multi)decadal oscillations in (multi)decadal-scale provides two fundamental advantages. First, the anomalies in hydrological extremes originated by the natural variability can be distinguished from long-term trends that result from climate change (Taye and Willems, 2012). The relationship between extremes and climate indices clarify the naturally occurred periods of high and low precipitation. Secondly, the relationship can be utilized to predict forthcoming decadal persistence in precipitation. Indisputably, predicting the possible forthcoming precipitation periods contribute greatly to water management; one of the most important and vital problems of our time.

REFERENCES

- Afshar, M. H., & Yilmaz, M. T. (2017). Remote Sensing of Environment The added utility of nonlinear methods compared to linear methods in rescaling soil moisture products. *Remote Sensing of Environment*, 196, 224–237.
- Baltacı, H., Göktürk, O. M., Kindap, T., Ünal, A., & Karaca, M. (2014). Atmospheric circulation types in Marmara Region (NW Turkey) and their influence on precipitation. *International Journal of Climatology*, 1820 (September 2014), 1810–1820.
- Bulut, B., & Yılmaz, M. T. (2016). Türkiye ' deki 2007 ve 2013 Yılı Kuraklıklarının. *İMO Teknik Dergi*, 7619–7634.
- Cullen, H. M., & DeMenocal, P. B. (2000). NORTH ATLANTIC INFLUENCE ON TIGRIS – EUPHRATES. *International Journal of Climatology*, 20.8, 853–863.
- Cullen, H. M., Kaplan, A., Arkin, P. A., & DeMenocal, P. B. (2002). Impact of the North Atlantic Oscillation on Middle Eastern climate and streamflow. *Climatic Change*, 55(3), 315–338.
- Feliciísimo, Á. M., Cuartero, A., Remondo, J., & Quirós, E. (2013). Mapping landslide susceptibility with logistic regression, multiple adaptive regression splines, classification and regression trees, and maximum entropy methods: A comparative study. *Landslides*, 10(2), 175–189.
- Friedman, J. H. (1991). Multivariate Adaptive Regression Splines Author (s): Jerome H . Friedman Source : The Annals of Statistics , Vol . 19 , No . 1 (Mar . , 1991), pp . 1-67 Published by : Institute of Mathematical Statistics Stable URL : <http://www.jstor.org/stable/224183>. *The Annals of Statistics*, 19(1), 1–67.
- Giorgi, F., & Lionello, P. (2008). Climate change projections for the Mediterranean

region. *Global and Planetary Change*, 63(2), 90–104.

Gotway, C. A., Ferguson, R. B., Hergert, G. W., & Peterson, T. A. (1996). Comparison of Kriging and Inverse-Distance Methods for Mapping Soil Parameters. *Soil Science Society of America Journal*, 60(4), 1237–1247.

Hurrell W. James. (1995). Decadal Trends in the North Atlantic Oscillation : Regional Temperatures and Precipitation, 269(5224), 676–679.

James, H. W., Latif, M., Visbeck, M., Delworth, T. L., Danabasoglu, G., Dommenget, D., ... Tribbia, J. (2010). Decadal Climate Variability, Predictability and Prediction: Opportunities and Challenges. *Proceedings of OceanObs'09: Sustained Ocean Observations and Information for Society*, (1), 279–295.

Maktav, D., Erbek, F. S., & Jürgens, C. (2005). Remote sensing of urban areas. *International Journal of Remote Sensing*, 26(4), 655–659.

Mathbout, S., López-bustins, J. A., Vide, J. M., & Rodrigo, F. S. (2016, April). On the Relationship between Atmospheric Circulation Indices and Precipitation in the Eastern Mediterranean. In EGU General Assembly Conference Abstracts (Vol. 18, p. 7224).

MGM. (2010). Retrieved April 17, 2017, from <https://www.mgm.gov.tr/arastirma/dogal-afetler.aspx?s=taskinlar>

Ntegeka, V., & Willems, P. (2008). Trends and multidecadal oscillations in rainfall extremes, based on a more than 100-year time series of 10 min rainfall intensities at Uccle, Belgium. *Water Resources Research*, 44(7).

Raja, N. B., Aydın, O., Türkoğlu, N., & Çiçek, I. (2017). Space-time kriging of precipitation variability in Turkey for the period 1976–2010. *Theoretical and Applied Climatology*, 129(1-2), 293-304.

Smakhtin, V. U. (2001). Low flow hydrology: A review. *Journal of Hydrology*, 240(3–4), 147–186.

Sönmez, F. K., Kömüşçü, A. Ü., Erkan, A., & Turgu, E. (2005). An Analysis of

Spatial and Temporal Dimension of Drought Vulnerability in Turkey Using the Standardized ... An Analysis of Spatial and Temporal Dimension of Drought Vulnerability in Turkey Using the Standardized Precipitation Index. *Natural Hazards*, 35.2(June), 243–264.

SU PEK Proje ve Müşavirlik A.Ş. (2016). *Sakarya Havzası Taşkın Yönetim Planının Hazırlanma İşi*.

T.C. Orman ve Su İşleri Bakanlığı. (2015). *Yeşilirmak havzası taşkın yönetim planı*.

T.C. Orman ve Su İşleri Bakanlığı. (2016). *Antalya Havzası Taşkın Yönetim Planı*.

Tabari, H., & Willems, P. (2016). Daily Precipitation Extremes in Iran: Decadal Anomalies and Possible Drivers. *Journal of the American Water Resources Association*, 52(2), 541–559.

Taye, M. T., & Willems, P. (2011). Influence of climate variability on representative QDF predictions of the upper Blue Nile basin. *Journal of Hydrology*, 411(3–4), 355–365.

Taye, M. T., & Willems, P. (2012). Temporal variability of hydroclimatic extremes in the Blue Nile basin. *Water Resources Research*, 48(3), 1–13.

Türkeş, M., & Erlat, E. (2008). Influence of the arctic oscillation on the variability of winter mean temperatures in Turkey. *Theoretical and Applied Climatology*, 92(1), 75–85.

Türkeş, M. (1996). Spatial and temporal analysis of annual rainfall variations in Turkey. *International Journal of Climatology*, 16.9, 1057–1076.

Türkeş, M., & Erlat, E. (2003). Precipitation changes and variability in Turkey linked to the North Atlantic oscillation during the period 1930-2000. *International Journal of Climatology*, 23(14), 1771–1796.

Türkeş, M., & Erlat, E. (2005). Climatological responses of winter precipitation in Turkey to variability of the North Atlantic Oscillation during the period 1930 – 2001. *Theoretical and Applied Climatology*, 81.1, 45–69.

Vaes, G., Willems, P., & Berlamont, J. (2002). 100 years of Belgian rainfall: Are there trends? *Water Science and Technology*, 45(2), 55–61.

Yucel, I., & Onen, A. (2013). Evaluating the extreme precipitation events using a mesoscale atmosphere model and satellite based precipitation product. *Natural Hazards and Earth System Sciences Discussions*, 1(6), 6979–7014.